NATIONAL TRANSPORTATION SAFETY BOARD

Office of Research and Engineering
Materials Laboratory Division
Washington, D.C. 20594

February 19, 2013

MATERIALS LABORATORY FACTUAL REPORT Report No. 13-013

A. ACCIDENT INFORMATION

Place	:	Boston, Massachusetts
Date	:	January 7, 2013
Vehicle	:	Boeing 787, Registration JA829J
NTSB No.	:	DCA13IA037
Investigator-in-Charge	:	David Helson

B. GROUP MEMBERS

Company	Name	Function
NTSB (National Transportation Safety Board)	• Joseph Panagiotou	Group Chairman, Fire and Explosion Investigator
	• Erik Mueller	Materials Research Engineer, Ph. D, PE
FAA (Federal Aviation Administration)	• Philip J. Sheridan	Aerospace Electrical Engineer Aircraft Certification Service Transport Airplane Directorate – (Renton, Washington, USA)
	• Steven Summer	Project Engineer, Fire Safety Branch, (Atlantic City, New Jersey, USA)
	• Harry Webster	Senior Project Engineer, Fire Safety Branch, (Atlantic City, New Jersey, USA)
Naval Surface Warfare Center Carderock Division	• Clinton Winchester	Senior subject matter technical expert lithium-ion batteries, Systems Safety and Integration
	• Daphne Fuentevilla	Chemical Engineer, Ph. D
The Boeing Company	• Glen Brown	Manager, Ph. D, Battery operations, Boeing S & IS - California (USA)
	• Dwaine Coates	Technical Fellow, Battery Technology, Boeing Phantom Works
JAL (Japan Airlines)	• Hajime Okada	Manager, Flight Avionics Control Section, (Narita, Japan)
Thales	• Arezki Bouzourene	Engineer, Ph. D, Engineering Department - (Paris, France)

GS Yuasa	• Yoshitaka Ishida	Battery and cell engineer, Development Department - (Kyoto, Japan)
	• Takahiro Shizuki	Battery expert, Development Department - (Kyoto, Japan)

C. COMPONENTS EXAMINED

Auxiliary power unit (APU) battery.

D. DETAILS OF THE EXAMINATION

On January 7, 2013, about 1021 eastern standard time, smoke was discovered by cleaning personnel in the aft cabin of a Japan Airlines (JAL) Boeing 787, JA829J, that was parked at a gate at Logan International Airport, Boston, Massachusetts. About the same time, a maintenance manager in the cockpit observed that the auxiliary power unit (APU) had automatically shut down. Shortly afterward, a mechanic opened the aft electronic equipment bay and found smoke and flames coming from the APU battery. No passengers or crewmembers were aboard the airplane at the time, and none of the maintenance or cleaning personnel aboard the airplane were injured. Aircraft rescue and firefighting personnel responded to the battery fire, and one firefighter received minor injuries. The airplane had arrived from Narita International Airport, Narita, Japan, as a regularly scheduled passenger flight operated as JAL flight 008 and conducted under the provisions of 14 *Code of Federal Regulations* Part 129.

E. EXTERNAL DOCUMENTATION OF THE AS-RECEIVED ACCIDENT BATTERY

1. History of the aircraft and battery

Line 84 (JA829J) was delivered to JAL on December 20, 2012.[1] The aircraft accumulated 22 flight cycles and 169 flight hours at the time of the incident. The on-scene fire factual report (Fire Investigation Factual Report 13-014) identified the APU battery as the source of the incident.

2. Description of the battery

Figure 1 and Figure 2 show the APU battery as it was received at NTSB headquarters on January 11, 2013. In addition to the information contained in this report, further documentation of the APU battery can be found in the Computed Tomography Specialist's Factual Report.

a. Battery design

The APU battery is a LVP65-8-402 battery pack, manufactured by GS Yuasa, nominally providing 75 Ampere-hours (Ah) and 29.6 Volts (V). The battery pack is comprised of eight GS Yuasa LVP65 lithium-ion (Li-ion) cells (Attachment 1) connected

[1] Line 84 refers to the eighty-fourth B-787 built.

in series and arranged in two rows of four cells. The cell chemistry is based on a Lithium cobalt oxide compound. Fixation trays, BPA[2] thermoplastic polyester (BPA-TP) and chlorinated rigid aliphatic thermoplastic (CRAT) insulation sheets, and polyimide tape provide electrical insulation and physical separation between the cells and between the cells and the electrically grounded battery case. Battery monitoring and control is performed by four battery monitoring units (BMU) located inside the battery case.

b. Battery specifications

Specifications for the incident battery are listed in Table 1.

Table 1. Battery specifications.

Model	LVP65-8-402
Type	lithium-ion, eight LVP65 (GS Yuasa P/N) lithium-ion cells connected in series
Manufacturer	GS Yuasa Corporation, Kyoto, Japan
Manufactured Date	The battery cells were manufactured in a lot that was produced between May and September 2012
Rated Watt Hour (Wh) (EOL)	1440 Wh
Case	Two-piece assembly (top lid and pre-assembled “box” structure) constructed of 6061 aluminum alloy that is 0.063 inch thick, lid is 0.032 inch thick
Nominal capacity	75 Ah
Nominal voltage	29.6 V
Operational voltage range	20–32.2 V

	Measurement of APU battery **before failure event** (acceptance test report information)	Measurement of APU battery **after failure event** (approximate)[a]
Weight:	61.8 lbs (28.06 kg)	56.0 lbs (25.4 kg)
Dimensions:	A: 14.25 inch (362 mm) B: 10.9 inch (277 mm) C: 8.46 inch (215 mm)	A: 14.25 inch (362 mm) B: 10.7 inch (273 mm) C: 8.54 inch (217 mm)

a. Battery mounting brackets remained in the aircraft.

c. Top down documentation of the open battery, numbering of cells, and identification of key components and features

The battery box contains eight battery cells electrically connected in series, two physical circuit boards containing the four battery monitoring units (BMUs), a Hall effect current sensor (HECS) for current monitoring, a contactor, busbars for the main current pathways between the cells and for the main current pathway to the “J3” connector leading outside of the battery box, and the sense wires leading back to the BMU and

[2] Bisphenol A (IUPAC designation 4,4'-(propane-2,2-diyl)diphenol).

"J1" connector leading outside of the battery box. An electrical circuit diagram for the battery is shown in Figure 3.

The battery is operated to a maximum voltage of 32.2 V, which equates to approximately 4.025 V per cell, and is rated at 65 Ah at the beginning of its design life based on a 70 A discharge rate. The nominal design capacity of the cell is 75 Ah. The battery is rated at 50 Ahr at end of life when subjected to a 75 A discharge. The battery design incorporates a contactor rated to 400 A, and four BMU circuits located on two physical circuit boards. The four BMU circuits contain three independent levels of cell-level over-voltage protection, one of which activates the contactor. The BMUs inhibit charging when an over-discharge condition is detected within the battery. A negative thermal coefficient (NTC) and a positive thermal coefficient (PTC) thermistor monitor temperature on two centermost cell-to-cell busbars (Figure 4). The NTC, which is covered in epoxy, inhibits charging at the BMU level on over- or under-temperature conditions. The NTC temperature is reported to the BMU. The PTC temperature is reported to the battery charging unit (BCU). The BMU performs cell balancing on cells over 4.00 V and monitors overall battery voltage for under-voltage conditions. BIT circuits on BMU 1 and BMU 2 provide independent evaluation of battery failure conditions. Voltage and temperature measurements are taken with sense wires positioned across the top of the battery (Figure 2 and Figure 4).

The main battery positive terminal on the power connector for the battery (designated "J3") (Figure 6) connects directly to the contactor and then to the positive cell connection on Cell 8. The main battery negative terminal from the power connector for the battery passes through the Hall effect current sensor and connects to the negative terminal on Cell 1. External to the battery box, the negative terminal is connected directly to airplane ground. The battery box itself is electrically isolated from the individual cells and the J3 power connector but is connected to airplane ground exterior to the battery box via the ground stud visible in Figure 5 and Figure 6. Nickel electroplated copper busbars provide the main electrical connections between the series-connected cells.

3. Documentation of the top, bottom, and four sides of the battery

The battery is housed in an aluminum case comprised of a single sheet of AA 6061 aluminum alloy approximately 0.063 inch thick folded up on the sides to form the case body. The battery box lid is comprised of the same aluminum alloy material of 0.032 inch thickness with edges folded to form a lip and eight mounting tabs used to affix the battery box to the lid with two screws on each side. Figure 6, Figure 7, and Figure 4 show views of an exemplar battery, the main battery from the JA829J Boeing 787 aircraft.

Figure 1 shows the battery box as it was received at NTSB headquarters. Observations were documented using a numbering system designating the front of the battery (forward) facing the external power connectors as Side 1 (S1), the left hand side as Side 2 (S2), the rear of the battery closest to the back wall of the electronics cabinet when installed in the airplane (aft) as Side 3 (S3), and the right hand side as Side 4

(S4). The top (consisting of the removable lid or the view into the battery from the face with the lid) is referred to as “top” and the floor of the battery is referred to as “bottom.” The same nomenclature (S1 through S4, top, and bottom) is used to refer to the as-designed orientation of the sides of the cells and other components of the battery.

The battery arrived at NTSB headquarters with the lid affixed to the battery box by two of the eight original screws. The mounting tab eyelets on S2, S3, and S4 of the battery box lid were torn open (Figure 8). The screws from the torn mounting tabs remained affixed to the battery box with detached remnants of the eyelets still secured under the screw heads. A detailed description of the condition of the mounting tabs is provided in Section E5.

The battery box lid was deformed with the back right corner adjoining S3 and S4 pushed up away from the battery box. S3 and S4 of the battery box lid had brown and black residue on the exterior and interior of the lid, concentrated at the S3/S4 corner (Figure 1). Two tamper-proof seals, spanning the lid and battery box on S2 and S4, were present (Figure 8). The seal of S4 was torn in half and the seal on S2 remained intact with the lid, leaving adhesive residue on S2. The blue paint on the battery box lid exterior appeared intact. A five-inch section of silicone sponge rubber remained of the gasket that fits into the interior of the battery lid lip to seal the box.

Part of a synthetic webbing carrying strap remained attached to the exterior of the battery box case with two brackets on S2. The strap consists of two lengths of synthetic webbing doubled up, which appeared melted through and torn at the midpoint (Figure 9). Melted synthetic webbing residue was found in one of the two brackets used to secure the strap on S4 (Figure 10).

The interior of the battery is visibly more damaged than the exterior of the battery case. The eight cells are arranged in two rows of four cells each. When viewed from the top of the battery, the cells are numbered as cells 1 through 8 (C1 through C8), starting with the cell closest to the BMU on S2 (left side when viewed from S1) and ending with the cell closest to the BMU on S3. With this numbering system, C1 and C8 are closest to the BMU and C4 and C5 are closest to S3 of the battery box (Figure 2 and Figure 11). C1 through C4 are located on the left side of the battery box and C5 through C8 are located on the right hand side of the battery box using this convention.

The exterior of S1 of the battery box (Figure 5), accessible from the front of the equipment rack in the aft electronics and equipment (EE) bay, exhibited black residue and white powdery material on the exterior surface, consistent with the report of flames seen at the J3 and J1 connector during the incident and the JAL mechanic’s firefighting efforts. Witness marks of clean paint were left where adhesive labels identifying the J1 and J3 connectors would have been. Residue from the caution label and danger label remained on the right side of the connectors. Most of the name plates remained intact but were not legible. The condition of the connectors and ground wires are documented in the Airworthiness Group Chairman Factual Report.

The exterior of S2 of the battery box appeared to have sustained the least visible damage (Figure 12). The right angle mounting bracket on the exterior of the battery case was detached from the battery case during removal from the aircraft by firefighting personnel, there were minor gouges in the S2 wall just above the bracket location, and there was some sooty residue. The two brackets securing the synthetic webbing carrying strap remained and the portion of the synthetic webbing strap on this side of the case as well as the two black plastic buckles appeared dirty but undamaged.

The exterior of S3 of the battery box, the rear of the battery box when it is installed in the EE bay cabinet, appeared minimally damaged on the side closest to S2 but appeared heavily damaged on the side closest to S4 (Figure 13). Two labels were still attached to the center of the S3 face but had partially disbonded on the S4 edge of the battery box. A gouge in the aluminum was present just above the label location. Vertical black streaks consistent with tracks from dripping liquid (now solidified) covered the S4 side and corresponded to the location of the damaged and elevated corner of the battery box lid. A roughly oval deposit of black residue covered the upper portion of the S3 face near the S4 edge. The most notable feature of S3 was a roughly circular distortion near the lower S3/S4 corner. This distortion was a paint discoloration approximately one-inch in diameter with a nodular protrusion in the middle. The center protrusion appeared metallic and extended horizontally out from the case a quarter-inch from the vertical plane. The distortion is further documented in Section F8.

The exterior of S4 of the battery box appeared to have the most severe visible damage of the battery box sides (Figure 14). The exterior is heavily coated with black residue, concentrated closer to S3 of the battery. Thicker black deposits, consistent with melted synthetic webbing, were visible on the brackets that would have secured the straps and on the right side of the face closer to the battery box lid. However, remains of the torn tamper-proof seal are still present on the relatively less damaged forward portion of S4. The exterior mounting bracket for S4 of the battery box remained with the aircraft after removal of the battery from the aircraft by firefighting personnel, and a gouge in the aluminum is present half way up on the right hand side. S4 of the battery box also sustained damage to the paint and aluminum. Large, roughly circular areas of thermal damage to the paint were located at the same elevation as the cell vent discs are visible from the exterior. A distortion characterized by a deformation to the battery case was adjacent and opposite to the C7 vent. An area of thermal damage to the paint on the case was adjacent and opposite to the C6 vent. In both the C7 and C6 vent disc locations, the black residue on the case took on a different appearance from the surrounding residue and the aluminum appeared rounded outward. In the case of the C7 vent disc location, the paint and soot had flaked away leaving a relatively concentric appearance. Discolorations of the exterior paint on the box were also visible for the locations of C5 and C8, although these are partially obscured by the strap attachment brackets on the box.

The exterior of the bottom of the battery box had scratches and surface residue on the side closest to S4 but was otherwise undamaged upon visual inspection (Figure 15). A dent in the edge along S1, the front face of the battery box, was consistent with reported attempts by firefighting personnel to remove the battery from the EE bay cabinet by force.

4. Serial number (S/N) of each cell and battery assembly

APU battery S/N 394 (manufactured by GS Yuasa in September 2012) was installed in the aircraft on October 15, 2012. On approximately October 19, 2012, the battery charged on the airplane for the first time. S/N 394 was delivered with the airplane. According to Boeing records from GS Yuasa, S/N 394 was a new battery and had not been refurbished. Table 2 lists information on the manufacturing of the individual cells.

Table 2. Manufacturing of S/N 394.

Battery S/N 394	**Manufacturing Number: H5378**	**Assembled Battery Manufacturing Month and Date: 2012/9**
	S/N[a]	Manufacturing Cell Date
Cell 1	53780052	7/11/2012
Cell 2	53780040	7/12/2012
Cell 3	53780041	7/10/2012
Cell 4	53780112	7/19/2012
Cell 5	53780049	7/10/2012
Cell 6	53780113	7/19/2012
Cell 7	53780042	7/10/2012
Cell 8	53780108	7/19/2012

a. The first four digits of the S/N are the lot number, the last four digits are the specific cell. For example, 53780052 is the 52nd cell from the 5378 lot. Lot 5378 was manufactured at GS Yuasa in July 2012. There were approximately 350 cells in the lot.

5. Documentation of the damage to the bolt tabs of the battery box lid

Eight mounting tabs were used to attach the lid on the battery box, as identified in Figure 16 by the letter A and B on each edge of the lid. Phillips-type pan-washer head M4 x 0.7 screws are used to fasten the mounting tabs to the lower battery box. Examination of the as-received battery box at the incident scene revealed that mounting tabs A and B on S1 remained engaged with the screws. The other six mounting tabs separated from their respective fasteners as indicated in Figure 17. Examination of the mounting tabs using a 5X to 50X zoom stereo microscope revealed that the mounting tabs on S2, S3, and S4 tore from the fastening screws by gross deformation and overstress.

In general, the fractured and separated mounting tabs exhibited deposits consistent with exposure to a fire. The deposits covered the inner surfaces of the tabs that would normally form faying surfaces with the external surfaces of the battery box during normal installation. Some deposits were also noted on the exterior tab surfaces, including the surfaces covered by the bolt head during normal lid installation. A closer view of the fractured S3A mounting tab reveals the presence of fire-related deposits on the fracture surface and the inner wall of the remaining bolt hole (Figure 18).

6. Cell design

In the battery's configuration, the orientation of each cell was such that the vent discs were oriented toward the exterior walls of the battery box. This arrangement requires that two different configurations of cells are manufactured, referred to as type A and type B. Such a configuration accommodates the designated busbar routing internal to the battery pack (in order to minimize bussing) and maintains orientation of the vent discs toward the outside of the pack (versus facing inside, toward each other).

Each cell is comprised of internal cell elements consisting of three 10-meter-long foils, totaling 30 m. These internal cell windings can be described as "jelly rolls." The edges of each roll are not coated with active material, enabling current collectors for the anode and cathode to be welded by ultrasonic welding on the side of the rolls accordingly. The cell case closure weld is performed by tungsten inert gas (TIG) arc welding, with hermeticity checks, and electrical internal resistance performed during cell processing. The separator material between the anode and cathode layers is polyolefin.

Notionally, the cell case is floating with respect to the cell terminals. For cells charged to 4.025 V, cell case to positive terminal has a voltage of approximately 1.0 V to 1.4 V, and negative terminal to cell case has a voltage of approximately 2.6 V to 3.0 V.

Finally, acceptance test data for cells and battery assembly were reviewed and appeared nominal for all cells used in the incident battery assembly. Battery data were also reviewed as nominal, though voltage-time curves were not examined by the group. Capacity and open circuit stand measurements provided were all nominal and consistent with specification requirements. The cells used in this battery assembly completed manufacturing in July 2012.

7. Cell specifications

Based on information from the battery manufacturer, nominal specifications for the individual battery cells are listed in Table 3.

Table 3. Cell specifications.

Nominal capacity	75 Ah
Nominal voltage	3.7 V
Operational voltage range	2.5 V–4.025 V
Maximum discharge capacity	approximately 1000 A (though typically 450 A for ~45 seconds, when being used for APU start-up, and no greater than three attempts at start up)
Case	stainless steel (0.8 mm thick, deep-drawn case) with nickel vent disc (20 mm in diameter, minimum burst pressure 0.6 MPa) on one side of each cell, the header wall thickness is thinner than the case wall
Weight	6 lbs (2.7 kg)
Dimensions	
Width	5.2 inch (132 mm)
Depth	2.0 inch (50 mm)
Height	7.7 inch (195.6 cm)

F. OBSERVATIONS MADE DURING BATTERY DISASSEMBLY TO INDIVIDUAL CELL LEVEL

1. Documentation of removal of the debris on top of the battery

The examination of the battery box internal components began with an examination of the top surface of the battery's eight cells (Figure 19). Charred material debris that had accumulated on the battery cell headers (the top portion of the cell with the terminal stud connectors) was carefully removed in all areas where it was possible, until enough was removed to expose all the terminal studs, busbars, and portions of the BMUs' voltage sensing wiring harness. Additionally, the charred debris was also removed from areas where it was desired to determine the presence of fixation hardware.[3] This was accomplished by direct one-to-one comparison with the exemplar, main battery. The charred debris on the battery cell headers likely consisted of portions of the BPA-TP top insulation cover, portions of the upper battery cell fixation tray, battery cell terminal stud plate insulation, and wiring harness insulation. The largest continuous portions of charred debris were portions of the BPA-TP top insulation cover that were removed from the S2/S3 corner of the battery over the C3 and C4 positions and over the S3/S4 corner over the C5 position. The rest of the debris was pried away in small pieces. All of the fixation hardware, the busbars, terminal nuts, and sensing wiring harness screws were accounted for. No instance of missing, misplaced, or extra components was observed.

[3] Describes inclusively all the materials and hardware used to hold and maintain the cells and other components in the battery assembly.

2. Examination of the sensing wire harness

After sufficient removal of the charred debris from the top portion of the battery, the physical condition of the BMUs' cell voltage sensing wiring harness was evaluated (Figure 20). The overall appearance of the wiring harness was consistent with exposure to a high-temperature environment with areas of varying severity. The insulation on the wires was mostly intact but exhibited varying degrees of thermal discoloration and staining from the expelled battery cell contents (carbonaceous material, electrolyte, and cathode material). The area of most severe damage to the wiring harness was located above C5 and C6 and in the region left half (C1 to C4) side of the battery to the right half (C5 to C8) side of the battery. Over the left half, the insulation exhibited some thermal discoloration but remained intact, including cable ties securing the wiring harness to the upper fixation tray. In the area of the transition from the left side of the battery toward the area of the right side of the battery, the condition of the wire insulation progressively degraded from thermally discolored to charred and then altogether missing. The insulation over C5 and C6 was thermally damaged to the point where the insulation was missing, mostly in the position of C5, leaving the wires bare. A gradient of progressive improvement in the condition of the wiring insulation was observed going from the position of C6 forward, toward C8. At the position of C7, the insulation was charred; at the position of C8, it was thermally discolored. Four wires in the area of the transition between the left side of the battery to the right side of the battery were severed and found to be brittle. All of the screws attaching the wiring harness to the cell terminal plates and busbars were present and securely connected.

3. Documentation and photographing of the removal of the sensing wire harness

Upon removal of the wiring harness attachment hardware, it was necessary to gently pry on portions of the wiring harness to dislodge it from the remaining charred debris stuck to the top surface of the battery. Once all of the wiring harness was dislodged from the battery top, it was removed as a single unit, with the exception of one of the fractured pieces. The wiring harness was photo documented with the fractured pieces placed near their original position (Figure 21).

4. Peeling of the sides of the battery case

The battery case consisted of two principal assemblies, the battery box lid and a rectangular open top box portion containing the battery internals. The bottom portion consisted of a folded sheet of AA 6061 material approximately 0.063 inch in thickness with a blue paint exterior finish. The folded sheet comprising the bottom portion was fastened with overlapping riveted seams. The process of disassembly, working from the exterior of the battery case, consisted of grinding small flats on the rivet heads so that heads could be carefully drilled out and separated from their shanks using a center drill bit. The process began with the S2 side of the battery case then the S4 side followed by S3. The rivets securing the center brace and brace between the cell and BMU portion of the battery case were also drilled out to facilitate the disassembly. Once all the rivet heads were drilled out, a small prying tool was used to free the overlapping battery case sides, after which the dislodged portion was folded downward and away from the battery case interior.

Folding down S2 revealed the position of C1 through C4 (Figure 22). The cells cases were obscured by the black-colored CRAT sheet of insulation remaining in place adjacent to the battery cells. Behind the CRAT insulation, through the oval cutouts along its top, a portion of the BPA-TP insulation was visible (Figure 23). The appearance of the BPA-TP insulation was white with brown hues and a flakey consistency with some missing sections. After removal of the BPA-TP, the cell cases were revealed (Figure 24). The interior surface of the folded down battery case S2 had a clean area identical in outline to the black CRAT insulation sheet (Figure 25). The remainder of the interior of the S2 side was coated with residue.

Folding down S4 revealed the position of C5 through C8 (Figure 26). The cells exhibited a darkened charred appearance with portions of the charred insulation materials adhering to them. Both of the layers of insulation, the black CRAT sheet, and BPA-TP were charred and indistinguishable from each other. The interior surface of the folded down battery case S4 had portions of the charred insulation materials adhering to it in areas where the insulation was in contact with it (Figure 27). The remainder of the interior of S4 was coated with residue.

Folding down S3 of the battery case revealed the S3 side of C4 and C5 (Figure 28). The BPA-TP insulation along this side was thermally degraded and fragmented. The S3 side of C4 had staining resembling a flowing residue. The S3 side of C5 had similar staining but also exhibited a clean area on the cell case. A corresponding area was visible on the interior of the folded down S3 of the battery case (Figure 29). This area is adjacent to the fire-damaged resin found on the interior of S4 (Figure 30). The S3 area on the interior of the battery case corresponding to C5 had large portions of BPA-TP insulation adhering to it. The BPA-TP insulation appeared to have been pressed against the battery case and exhibited some thinning. The adhering BPA-TP also exhibited some blue staining. A higher-temperature spot was observed on the battery case with a corresponding spot on the C5 cell case (Figure 31), documented in detail in Section F8.

5. BMU boards, HECS, and contactor removal and documentation

The battery assembly contained two BMU boards, a HECS, and a contactor that were located in the forward portion of the battery box (Figure 32). The contactor was removed first to provide clearance for the removal of the BMU boards. The two BMU boards were then removed from the battery case after disconnecting them from the sensing wiring harness and then unscrewing them from the stand offs which held them fixed to S1 of the battery case (Figure 33). Following the removal of the BMU boards, the HECS was removed.

The main BMU board was thermally damaged and covered with residue (Figure 34). There was evidence of reflowed solder present on the board and some instances of separated semiconductor chips. The sub-BMU board had sustained similar thermal damage (Figure 35). Overall, the thermal damage appeared more severe on the sides of the BMU boards that were closer to the S4 side of the battery box.

The contactor and HECS were thermally damaged and coated with residue (Figure 36, Figure 37, and Figure 38). No faults with these components other than the thermal damage were visually identified. Evaluation of these components were performed by the Airworthiness Group.

6. Terminal stud nut torque documentation

The terminal stud nuts on each of the eight cells were examined for tightness. Initially, they were checked by hand and found to be at least hand tight. Then the stud nuts were loosened using an indicating torque wrench.[4] Table 4 summarizes the torque measurements that were made. The torque specification per the manufacturer is 133 inch-pounds (15 N-m). Some of the terminal stud nuts had been removed in prior steps of the disassembly process (removal of the sensing and voltage balance wires) and torque measurements had not been taken, but all were sufficiently tight to require removal with a socket wrench. These are labeled as N/A in Table 4.

Table 4. Terminal stud nut peak removal torque (inch-lb).

	Cell 1	Cell 2	Cell 3	Cell 4	Cell 5[a]	Cell 6	Cell 7	Cell 8
NEG terminal	N/A	150	N/A	100	60	30	25	45
POS terminal	125	N/A	150	60	45	45	45	N/A

a. The studs on C5 began to rotate at some point while removing the nuts; therefore, the torque measurements may not accurately reflect the breaking torque.

7. Busbar removal documentation and evaluation of the contact surfaces of the busbar

During the battery disassembly process, the busbars were removed from each cell and were labeled according to the cells they connected. Photographs of both sides of the busbars connecting the batteries are shown in Figure 39. Overall, photographs of the busbars connecting C1 to the power connector (called C1-J3 busbar) and C8 to the contactor (called C8-contactor busbar) are shown in Figure 40. Closer views of the connection surfaces to the contactor for the C8-contactor busbar are shown in Figure 41. Figure 41 (a-b) shows the contact surfaces between the busbar and the contactor and Figure 41 (c-d) shows the faying contact surfaces[5] for C8-contactor busbar at the C8 positive terminal. Closer views of the connection surfaces for the C1-HECS busbar are show in Figure 42. Figure 42 (a-b) shows the faying surfaces between the busbar and the J3 power connector. The faying contact surfaces for C1-J3 busbar at the C1 negative terminal are shown in Figure 42 (c-d). The contactor-J3 busbar is shown in Figure 43. For each bolted connection, the condition of the faying contact surfaces were

[4] CDI Torque Products model 3002LDIN.
[5] Either of a pair of surfaces that are in contact in a joint.

visually evaluated using a 5X to 50X zoom stereo microscope. Key observations and attributes are indicated in Table 5 and Table 6.

The elastomeric insulators on the C1-J3 and C8-contactor busbars were removed to expose the surfaces of the busbars underneath, as demonstrated in Figure 44. In a number of places, the insulation adhered to the busbar surface, leaving a film of elastomer on the surface of the busbar. The surfaces under the insulation were stained, consistent with exposure to heat inside the battery box during the fire. No dark oxides or interference colors associated with high-temperature resistive heating were observed on surfaces of the C1-J3, C8-contactor, or contactor-J3 busbars.

Metallurgical cross sections of some of the busbars were prepared in order to facilitate microhardness testing and microstructural evaluation. Figure 45 (a) shows the sections taken of the 90° bends closest to the battery terminals for the C1-J3 and C8-contactor busbars. Figure 45 (b) shows the section of the C4-C5 busbar. The cross sections were mounted, polished, and microhardness tested in accordance with ASTM E384 - 11e1.[6] The locations of the microhardness indentations are displayed on Figure 46 and Figure 47. The mounted samples were then microetched in accordance with ASTM E407 - 07e1.[7] No microstructural changes, such as grain growth associated with localized heating, were observed.

[6] ASTM E384 - 11e1 “Standard Test Method for Knoop and Vickers Hardness of Materials,” ASTM International, West Conshohocken, PA.
[7] ASTM E407 - 07e1 “Standard Practice for Microetching Metals and Alloys,” ASTM International, West Conshohocken, PA.

Table 5. Busbar and battery terminal observations and attributes.

		Faying surface condition											
		Nut side				Battery side				Sensing wire connections			
Busbar	**Battery terminal**	Arcing damage	High heat tint	Fretting wear	Corrosion/ oxidation/ staining	Arcing damage	High heat tint	Fretting wear	Corrosion/ oxidation/ staining	Arcing damage	High heat tint	Fretting wear	Corrosion/ oxidation/ staining
C1-C2	C1 pos	N	N	N	1	N	N	N	1	N	N	N	1
	C2 neg	N	N	N	1	N	N	N	1	N	N	N	1
C2-C3	C2 pos	N	N	N	1	N	N	N	1	N	N	N	1
	C3 neg	N	N	N	1	N	N	N	1	N	N	N	1
C3-C4	C3 pos	N	N	N	1	N	N	N	1	N	N	N	1
	C4 neg	N	N	N	1	N	N	N	1	N	N	N	1
C4-C5	C4 pos	N	N	N*	1	N	N	N	1	N	N	N	1
	C5 neg	N	N	N*	1	N	N	N	1	N	N	N	1
C5-C6	C5 pos	N	N	N	2	N	N	N	2	N	N	N	1
	C6 neg	N	N	N	2	N	N	N	2	N	N	N	1
C6-C7	C6 pos	N	N	N	2	N	N	N	2	N	N	N	1
	C7 neg	N	N	N	3	N	N	N	2	N	N	N	1
C7-C8	C7 pos	N	N	N*	2	N	N	N	2	N	N	N	1
	C8 neg	N	N	N	2	N	N	N	2	N	N	N	1

N = no evidence of indicated condition when viewed under a 5X to 50X zoom stereo microscope.
* = scoring/adhesive wear consistent with rotation sliding motion.
1 = dull matte appearance with faint interference colors consistent with minor oxidation or staining.
2 = dull matte appearance with darker interference colors consistent with minor oxidation or staining.
3 = ring of dark staining on the faying surfaces.

Table 6. Busbar and connection observations and attributes.

Busbar	Connection	Faying surface condition											
		Nut side				Battery side/contactor/power connector side				Sensing wire connections			
		Arcing damage	High heat tint	Fretting wear	Corrosion/ oxidation/ staining	Arcing damage	High heat tint	Fretting wear	Corrosion/ oxidation/ staining	Arcing damage	High heat tint	Fretting wear	Corrosion/ oxidation/ staining
C1-J3	C1 negative post	N	N	N	1	N	N	N	1	N	N	N	1
	J3 power connector	N	N	N	1	N	N	N	1	N	N	N	1
C8-contactor	C8 positive post	N	N	N	1	N	N	N	1	N	N	N	1
	Contactor	N	N	N	1	N	N	N	1	N	N	N	1
Contactor-J3	Contactor	N	N	N	1	N	N	N	1	N	N	N	1
	J3 power connector	N	N	N	1	N	N	N	1	N	N	N	1

N = no evidence of indicated condition when viewed under a 5X to 50X zoom stereo microscope.
* = scoring/adhesive wear consistent with rotation sliding motion.
1 = dull matte appearance with faint interference colors consistent with minor oxidation or staining.
2 = dull matte appearance with darker interference colors consistent with minor oxidation or staining.
3 = ring of dark staining on the faying surfaces.

8. Battery case S3 defect

S3 of the battery case exhibited a protrusion on the lower left side (see Figure 48). This protrusion corresponded with one of four defects on the battery cell case of C5, which rests adjacent to the defect on S3 of the battery case. The laboratory analysis of the defect on both the battery and C5 cell case are described below.

a. S3 battery case

Figure 49 shows the nodular protrusion from the exterior of S3 of the battery case, as received. There were two concentric rings surrounding the protrusion, corresponding with discoloration of the exterior paint. The protrusion itself was absent of paint. Deposits consistent with combustion products were prevalent on and near the defect. The protrusion was approximately 0.25 inch in girth and extended approximately 0.12 inch from the case surface.

An area surrounding the defect was sectioned and removed for closer inspection. Figure 50 and Figure 51 show the protrusion from both the exterior and interior of the battery, respectively. The defect consisted of a variety of non-metallic decomposition compounds, including dull gray flaky material consistent with ignition spatter and shiny black material consistent with combusted plastics and tars. Much of the interior side of the protrusion contained these materials.

In order to better facilitate analysis of the defect, the protrusion was cleaned using a combination of light brushing in ethanol and ultrasonic cleaning in acetone immersion. Figure 52 and Figure 53 show the exterior and Figure 54 and Figure 55 show the interior of the defect after this cleaning procedure. From the exterior, the paint adjacent to the defect had volatilized. The paint outside of this area showed evidence of bubbling and combustion. The protrusion itself exhibited a dull metallic luster with facets and wrinkles.

At least three holes on the periphery of the protrusion could be identified (the largest two are highlighted in Figure 53). These holes were also visible from the interior (Figure 54). A variety of brown and black compounds consistent with decomposition products encircled the interior circumference of the defect. Discoloration consistent with heat tinting is evident near the defect (below on Figure 55). The top of the defect shows multiple particles embedded in a flat, dark section protruding downward—this feature is consistent with melting and resolidification of metal incorporating adjacent material.

The defect was inspected using a scanning electron microscope (SEM). Figure 56 is a micrograph that illustrates the exterior of the protrusion. The surface of the defect exhibited a fractured, reticulated structure (Figure 57). This morphology is consistent with thin oxide layers that form on the surface of molten alloys while in contact with air. This thin surface oxide typically crumples and cracks as the alloy solidifies and contracts during cooling. Larger folds of the protrusion at the base are illustrated in Figure 58. The chemical composition of the defect was inspected using energy dispersive X-ray spectroscopy (EDS) and was consistent with the specified aluminum alloy (AA 6061). The dark-colored compounds on the exterior contained elevated levels of carbon, oxygen, sulfur, and other non-metallic elements typically comprising decomposition products.

The interior of the defect is illustrated in Figure 59. Similar to the exterior, a reticulated pattern on the metallic regions was observed. The interior of the protrusion exhibited extensive oxidation and large carbon-rich areas. In addition to the aluminum alloy, several particles of an iron-based alloy, enriched with chromium and nickel, were embedded in the combustion products of the interior of the defect (Figure 60). These particles also exhibited a wrinkled reticulated surface morphology consistent with thin surface oxidation that typically accumulates during melting in a non-protective environment. The chemical composition was consistent with type 304 stainless steel, which is the specified material for the battery cell cases. In addition to these particles, there were areas on the interior of the defect with high concentrations of fluorine and phosphorus. These elements comprise lithium-based electrolyte salt ($LiPF_6$). In addition, cobalt-based oxide spherical particles were frequently found (Figure 61). These particles are consistent with the cathode material (lithium cobalt oxide compound) that is used to coat the aluminum foil wrapping in the battery cells. It should be noted that the EDS technique used in this investigation is unable to detect lithium.

b. C5 case—facing S3 of the battery case

Figure 62 shows the battery cell case of C5 adjacent to S3 of the battery case. This cell had been damaged during the failure event, particularly on its periphery. On the lower portions of this side of the cell case, four holes were identified (labeled 1 through 4 in Figure 62). All of the holes exhibited dark, rough compounds consistent with decomposition products. Hole 1, as designated in Figure 62, which corresponds with the location of the protrusion on the battery case, is the largest in terms of size and decomposition compounds. The lower portion of the C5 cell case was excised and cleaned in order to facilitate inspection in the SEM.

Figure 63 illustrates hole 1, as viewed from the exterior of the cell case. The hole exhibited a variety of compounds and alloys that were not part of the cell case material, type 304 stainless steel. Within the field of view, large, dark non-metallic areas were present with high concentrations of carbon, oxygen, sulfur, and alkali elements consistent with decomposition products. Within the field of view, large amounts of reticulated aluminum were found in and around the hole (Figure 64). Inspection by EDS showed this aluminum to be consistent with the battery case material. Elevated levels of cobalt, phosphorus, and fluorine were found in and near the hole, consistent with elements found in the cathode and electrolyte materials.

Figure 65 shows an area of hole 1 with rounded protuberances (or lumps) of the cell case material. Many of these rounded lumps that were examined were covered with aluminum. Both the lumps and aluminum alloy outer layer exhibited the reticulated morphology typical of surface oxidation effects during solidification and contraction during cooling. There were a variety of spherical particles found embedded in the combustion compounds in hole 1 (see Figure 66). The composition of the spheres was consistent with the cell case material (stainless steel). Spherical particles on or near resolidified areas is consistent with the melting, separation, and solidification processes typical of electric arc damage. For reference, the temperatures that would be required to melt aluminum alloys are in excess of 1250° F, while those required to completely melt this stainless steel alloy are typically in excess of 2700° F.

Examination of the three other holes on the C5 cell case revealed similar results. Figure 67 and Figure 68 display holes 2 and 3, respectively, from the interior of the case. Of note was the spherical globule located near hole 3 on the exterior of the case. The globule was consistent with type 304 stainless steel, and it exhibited a reticulated surface pattern. The case material was wrinkled near hole 3. There were also indications of metallization "splats" of aluminum alloy near the hole (Figure 69). The flattened shape of this metallization is consistent with the case material being near the molten aluminum temperature during deposition. Near hole 4, a depressed lamellar structure was observed in the case material (Figure 70). This surface morphology is consistent with incipient melting of the material, which occurs at temperatures high enough to cause some of the alloy constituents to liquefy.[8]

9. Cell removal documentation

After the removal of the busbars, the portions of the upper fixation tray along with the center and forward brace were removed (Figure 71). The battery cell removal began with the cells exhibiting the least amount of damage. These cells were located along the left (S2) side of the battery assembly and all but one had vented through the vent disc (Figure 72). The first cell to be removed was C1 (Figure 73). The insulation material between C1 and C2 remained attached to the S3 side of C1 during its removal from the battery box. The next cell to be removed was C2 (Figure 74). The insulation between C2 and C3 remained attached to the S3 side of C2 when it was removed from the battery box. C3 and C4 were removed together as a unit from the battery box (Figure 75). The insulation between C3 and C4 was firmly adhering to both cells and when moderate force was applied, the insulation disbonded from C4 and remained attached to S3 of C3. With C1 through C4 removed, the cell removal process began on the side containing C5 through C8, starting with C5 (Figure 76). After C5 was removed, C6, C7, and C8 were removed along with the lower fixation tray as a unit and then separated (Figure 77). C6, C7, and C8 were then separated from each other. The insulation material between C5 through C8 was completely charred and portions of it remained attached to all of the cells. At this point, all of the components had been removed from the battery box (Figure 78, Figure 79, and Figure 80).

10. Documentation of the insulators (sides, top, and bottom), including fixation trays

The battery design incorporates various layers of insulators to isolate cell cases from each other and from the battery box. An upper BPA-TP insulation cover laid over

[8] Type 304 stainless steel has an approximate fusion temperature of 2670° F.

the top of the cell terminals under the battery box lid, as seen in the exemplar, main battery in Figure 7, isolates the cell terminals and headers from the aluminum battery case. An upper and lower fixation tray, molded from thermoplastic polyester, fixes the position and orientation of the cells in the battery box (Figure 81 and Figure 82). One sheath of folded BPA-TP wraps around C1 through C4 and another around C5 through C8 (Figure 83). Two additional pieces of BPA-TP insulation sheets[9] and a resin spacer made from CRAT cover S2 and S4 of the battery box. Two one-inch tall CRAT resin spacers fit inside the BPA-TP sheath along the S2 face of C6 through C8 and along the S4 face of C1 through C3. In between C1 and C2, C3 and C4, C5 and C6, and C7 and C8 are three pieces of CRAT. Two of the pieces are black upside down U-shaped insulators that sandwiches a third solid white insulating sheet. In between C2 and C3 and C6 and C7 are two pieces of white CRAT. All CRAT sheets are textured on one side and untextured on the other.

The upper insulation cover sheet was not found intact in the incident battery (Figure 2). However, portions of melted insulation consistent with the cover sheet material were found adhering to areas of the cell tops.

Figure 84 shows the appearance of the insulation on S2 of the battery pack after the side was peeled down. The outermost insulation layer, consisting of a black sheet of CRAT with oval cutouts for the C1 and C2 and the C3 and C4 vents, remained structurally intact. Fragments of white BPA-TP insulation sheath surrounding C1 to C4 can be seen through the cutouts in the CRAT and along the bottom edge of the battery case. The S2 edge of the upper thermoplastic polyester fixation tray appeared structurally intact.

Figure 85 shows the condition of the single BPA-TP insulation layer between the cell cases and S3 of the battery box case. Darkened BPA-TP fragments are visible on the bottom of C4. It appeared that C5 sealed itself to the battery box case, but there is no evidence of electrical shorting between the cell and the battery box except at the protrusion in the lower corner, documented in Section F8. The upper fixation tray appears intact along C4 but is no longer present along the S3 edge of C5.

Figure 86 shows the condition of the insulation on S4 of the battery pack. The layers of insulation on the side, as well as the majority of the upper and lower fixation trays, were heavily damaged and no longer distinguishable.

Figure 33 shows the condition of the insulation on S1 of the battery pack between the BMU space and the S1 faces of C1 and C8. Some insulation remains on the S1 face of C1, however there is no visible presence of insulation remaining on the S1 face of C8.

[9] It was noted that the battery assembly and design documentation provided to the NTSB indicates only one sheet of BPA-TP insulation, in addition to the CRAT and the BPA-TP sheath, along sides 2 and 4 of the battery pack, which is not consistent with the two sheets found in the JAL exemplar, main battery box.

Figure 87 and Figure 88 show the condition of the insulation between the row of C1 through C4 and the row of C5 through C8. Little of the insulation is distinguishable.

Figure 89 and Figure 90 show the condition of the lower fixation tray. Debris and discoloration consistent with thermal damage was present on the C1 through C4 footprints. The footprints of C5 through C8 were pyrolyzed. Portions of the tray were not readily removed or distinguishable from other debris in the battery box.

Figure 91 and Figure 92 show the condition of the upper fixation tray. The portions of the tray in contact with C1 through C4 sustained less damage than the portions of the tray in contact with C5 through C8. Debris and discoloration of the tray can be seen on S2. The C4 imprint remained mostly intact, but C1, C2, and C3 showed progressively more damage. Minimal material remained from the C5 through C8 side of the upper fixation tray. Figure 93 documents a damage assessment of the upper fixation tray with a qualitative sliding scale where 10 represents the least damaged and 1 represents the most damaged cell imprints. An assessment of each side of the aluminum brace spanning the middle of the battery is also included.

Figure 94 shows the condition of the insulation between the cells. The insulation between C1 through C4 was damaged but distinguishable from general debris in the battery box. Figure 95 shows the CRAT insulation between C2 and C3 and between C3 and C4. The insulation for C5 through C8 could not be identified. An example of the remnants of this insulation is shown in Figure 96.

G. DOCUMENTATION OF THE J3 POWER RECEPTACLE AND CONNECTOR

Views of the J3 power connector and receptacle are shown in Figure 97 and Figure 98. As indicated in Figure 98, Figure 99, and Figure 100, the power receptacle exhibited thermally-induced deformation on one corner. Additionally, the polymer housing exhibited cracks, as identified in Figure 100. When viewed with a 5X to 50X zoom stereo microscope, the J3 power connector exhibited dark deposits on one of the blades of the positive junction (terminal) (Figure 101). The other blades appeared clean and free from deposits, stains, or discoloration (Figure 102). Samples of the dark deposit were removed from the terminal and analyzed by Fourier transform infrared spectroscopy (FTIR), using the attenuated total reflectance (ATR) method. Spectra indicate that the deposits are consistent with a straight chain hydrocarbon, such as polyolefin. The blades on the negative junction of the J3 power connector appeared clean and free from deposits, stains, or discoloration. The terminals on the J3 receptacle were examined with a 5X to 50X zoom stereo microscope. No indication of deposits, stains, or discoloration was observed.

H. EXTERNAL DOCUMENTATION OF INDIVIDUAL BATTERY CELLS

As the cell cases were removed from the battery box, they were individually photo documented on all sides and observations were made about their physical condition.

C1 had areas of black staining and charred materials adhering to some surfaces (Figure 103). The thermoplastic polyester film that was covering the vent disc was still intact and secured in place by the polyimide tape. The thermoplastic polyester film was cloudy and exhibited some thermal deformation (Figure 104). The C1 vent disc had opened. The amber-colored polyimide tape was still intact and firmly adhered to the cell case. On S4 of the cell case, the polyimide tape had a wrinkled appearance consistent with thermal distortion and appeared darker than the polyimide tape on S2. The sulfide crystalline thermoplastic stud insulator material on the cell header was intact and did not exhibit signs of thermal degradation. The CRAT insulation material that would have been between C1 and C2 adhered to S3 of C1. After removal of the insulation, S3 of the case was exposed (Figure 105). S3 was relatively clean but exhibited some staining in a pattern consistent with a liquid having flowed down its surface. S4 of the cell had some charred BPA-TP insulation adhering to its surface. The cell's weight after the insulation was removed was 2669.6 grams. The cell's deformation appeared to be slightly convex on S1 and S3 with no appreciable deformation on S2 and S4. The cell header and cell bottom had convex deformation. There was no evidence of electrical arcing anywhere on the exterior of this cell.

C2 had areas of black staining and charred materials adhering to some surfaces (Figure 106). The thermoplastic polyester film that was covering the vent disc was still intact and secured in place by the polyimide tape. The thermoplastic polyester film was cloudy and exhibited some thermal deformation (Figure 104). The vent disc on this cell had opened. The amber-colored polyimide tape was still intact and firmly adhering to the cell case on all sides except at the upper S3/S4 corner. On S4 of the cell case, the polyimide tape had a wrinkled appearance consistent with thermal distortion and a darker appearance than on S2. The sulfide crystalline thermoplastic stud insulator material on the cell header was intact and did not exhibit signs of thermal degradation. The CRAT insulation material that would have been between C2 and C3 had adhered to S3 of C2. After removal of the insulation, S3 of the case was exposed (Figure 107). S3 of the cell case exhibited staining on its entire surface with a pattern similar to a liquid having flowed down its surface. S4 of the cell had some charred BPA-TP insulation adhering to its surface. The cell's weight after the insulation was removed was 2532.6 grams. The cell's deformation appeared to be slightly convex on S1 and S3 with no appreciable deformation on S2 and S4. The cell header and cell bottom had some convex deformation. There was no evidence of electrical arcing anywhere on the exterior of this cell.

C3 had areas of black staining and charred materials adhering to some surfaces (Figure 108). The thermoplastic polyester film that was covering the vent disc was still intact and secured in place by the polyimide tape. The thermoplastic polyester film was cloudy and exhibited some thermal deformation (Figure 104). The vent disc on this cell had opened. The amber-colored polyimide tape was still intact and firmly adhering to the cell case on all sides. On S4 of the cell case, the polyimide tape had a wrinkled appearance consistent with thermal distortion and a darker appearance than on S2. The sulfide crystalline thermoplastic stud insulator material on the cell header was intact and did not exhibit signs of thermal degradation. The CRAT insulation material that would have been between C3 and C4 adhered to the S3 side of C3. After removal of the insulation, the S3 side of the case was exposed (Figure 109). S3 of the cell case exhibited some dark staining on the bottom portion. S4 of the cell had some charred BPA-TP insulation adhering to its surface. The cell's weight after the insulation was removed was 2529.0 grams. The cell's deformation appeared to be slightly convex on S1 and S3 with no appreciable deformation on S2 and S4. The cell header and cell bottom had convex deformation. There was no evidence of electrical arcing anywhere on the exterior of this cell.

C4 had areas of black staining and charred materials adhering to some surfaces (Figure 110). The thermoplastic polyester film that was covering the vent disc was still intact and secured in place by the polyimide tape. The thermoplastic polyester film was cloudy but did not exhibit signs of decomposition or thermal deformation (Figure 104). The vent disc on this cell had not opened. The amber-colored polyimide tape was still intact and firmly adhered to the cell case on all sides. On S4 of the cell case, the polyimide tape, on the bottom portion, had a wrinkled area in its center consistent with thermal distortion. Additionally, portions of charred BPA-TP insulation had adhered to the polyimide tape on the top of S4 of C4. The sulfide crystalline thermoplastic stud insulator material on the cell header was intact and did not exhibit signs of thermal degradation. Part of the BPA-TP insulation that would have been between S3 of the cell and the battery box case was charred and adhered to the S3 side of the cell case, primarily along the edge closer to the cell's S4 side. S4 of the cell had some charred BPA-TP insulation adhering to its surface. The cell's weight after removing the debris stuck to it was 2645.5 grams. The cell's deformation appeared to be slightly convex on S1 and S3 with no appreciable deformation on S2 and S4 or the header and bottom. The deformation to this cell was less than that of C1 through C3. There was no evidence of electrical arcing anywhere on the exterior of this cell.

C5 had staining and charred materials adhering to its surfaces (Figure 111). The thermoplastic polyester film that was covering the vent disc was consumed (Figure 104). The vent disc on this cell had opened. The amber-colored polyimide tape was still present only on S2 where it exhibited thermal damage. On S4 of the cell case, the polyimide tape was indistinguishable from the rest of the charred materials adhering to the case. Part of the BPA-TP insulation that would have been between S3 of the cell and the battery box case was charred and adhered to S3 of the cell case. Additionally, on S3 of the cell case, there was an area of clean cell case material with no evidence of staining or residue. S4 of the cell case was completely covered in charred material. The sulfide crystalline thermoplastic stud insulator material on the cell header was charred. The cell's weight after removing some of the more loosely adhering debris that was stuck to it was 2217.9 grams. The cell's deformation appeared to be convex on S1 with a concave to flat area approximately mid-height along this side. On S3, it exhibited a convex appearance. S2 and S4, as well as the bottom and cell header, exhibited a convex appearance (Figure 112). On the exterior of this cell facing S3, there was evidence of electrical arcing between the cell case and battery box case.

C6 appeared to have charred materials adhering to all of its surfaces (Figure 113). The thermoplastic polyester film that was covering the vent disc was consumed (Figure 104). The vent disc on this cell had opened and all four of its quadrants were spread out.[10] The amber-colored polyimide tape was still present only on S2, where it exhibited a blackened and wrinkled appearance consistent with thermal damage. On S4 of the cell case, the polyimide tape was indistinguishable from the rest of the charred materials adhering to the case. The sulfide crystalline thermoplastic stud insulator material on the cell header was charred. Parts of the CRAT insulation that would have been between this cell and C5 and C7 were charred and adhered to the cell case. The cell's bottom also had charred material adhering to its surface. The cell's weight after removing some of the more loosely adhering debris that was stuck to it was 2160.7 grams. The cell's deformation appeared to be concave on S1 and slightly convex with a flat area in the middle on S3 (Figure 114). S2 and S4, as well as the bottom and cell header, exhibited a convex appearance. The exterior of this cell did not exhibit any evidence of electrical arcing.

C7 appeared to have charred materials adhering to all of its surfaces (Figure 115). The thermoplastic polyester film that was covering the vent disc was consumed (Figure 104). The vent disc on this cell had opened, spreading out into four quadrants. The amber-colored polyimide tape was still present only on S2 where it exhibited a blackened and wrinkled appearance consistent with thermal damage. On S4 of the cell case, the polyimide tape was indistinguishable from the rest of the charred materials adhering to the case. The sulfide crystalline thermoplastic stud insulator material on the cell header was charred. Parts of the CRAT insulation that would have been between this cell and C6 and C8 were charred and adhered to the cell case. The cell's bottom also had charred material adhering to its surface. The cell's weight after removing some of the more loosely adhering debris that was stuck to it was 2124.0 grams. The cell's deformation appeared to be concave on S1 and convex on S3 (Figure 116). S2 and S4, as well as the bottom and cell header, exhibited a convex appearance. The exterior of this cell did not exhibit any evidence of electrical arcing.

C8 appeared to have charred materials adhering to all of its surfaces (Figure 117). The thermoplastic polyester film that was covering the vent disc was consumed and indistinguishable (Figure 104). The vent disc on this cell had opened and all four of its quadrants were spread out. The amber-colored polyimide tape was still present on S2, where it exhibited a blackened and wrinkled appearance consistent with thermal damage. On S4 of the cell case, the polyimide tape was more thermally damaged than on S2. The sulfide crystalline thermoplastic stud insulator material on the cell header was charred. Parts of the CRAT insulation that would have been between this cell and C7 were charred and adhering to the cell case. The cell's weight after removing some of the more loosely adhering debris that was stuck to it was 2156.1 grams. The cell's deformation appeared to be convex on S1 and convex on S3. S2 and S4, as well as the bottom and cell header, exhibited a convex appearance. The exterior of this cell did not exhibit any evidence of electrical arcing.

Table 7 summarizes the individual cell information for comparison.

Joseph Panagiotou
Fire and Explosion Investigator

[10] The vent disc is scored to facilitate rupture. This leaves the vent disc comprised of four quadrants.

Table 7. Individual cell information.

	Battery Cell Number							
	C1	**C2**	**C3**	**C4**	**C5**	**C6**	**C7**	**C8**
Serial number	53780052	53780040	53780041	53780112	53780049	53780113	53780042	53780108
Cell weight (g) (nominal 2700 g)	2669.6	2532.6	2529.0	2645.5	2217.9	2160.7	2124.0	2156.1
Cell voltage (V)	0	0	0	0	0	0	0	0
Cells shorted (less than 1 Ohm between terminals as measured by a digital voltmeter)	yes	yes	yes	yes	yes	yes	yes	no (112 Ohm)
Vent disc (Figure 104)	open	open	open	closed	partial rupture	complete rupture	complete rupture	complete rupture
Thermoplastic polyester film over vent disc (melting point > 250° C)	intact	intact	intact	intact	melted	melted	melted	melted
Polyimide tape	intact	intact	intact	intact	degraded	degraded	degraded	degraded
Upper fixation tray (scale of 1–10, with 10 being best condition)	intact (9)	intact (7)	intact (6–7)	intact (8)	consumed (1)	consumed (1)	consumed (1)	consumed (1)
Lower fixation tray (scale of 1–10, with 10 being best condition)	intact (9.5)	intact (9)	intact (8.5)	intact (9)	consumed/ missing (4)	consumed/ missing (2)	partially charred and consumed (2.5)	intact (5)
Stud insulators	both intact	both intact	both intact	both intact	both consumed	both consumed	both consumed	both charred

(continued)

	Battery Cell Number							
	C1	**C2**	**C3**	**C4**	**C5**	**C6**	**C7**	**C8**
Stud torque (nominal torque 133 inch-lb)	POS terminal 125 inch-lb	NEG terminal 150 inch-lb	POS terminal 150 inch-lb	NEG terminal 100 inch-lb, POS terminal 60 inch-lb	NEG terminal 60 inch-lb, POS terminal 45 inch-lb (these studs began to rotate after a few turns)	NEG terminal 30 inch-lb, POS terminal 45 in-lb	NEG terminal 25 inch-lb, POS terminal 45 inch-lb	NEG terminal 45 inch-lb
Cell deformation (S1 is side facing forward, S3 is side facing aft)	S1 convex, S3 convex	S1 convex, S3 convex	S1 convex, S3 convex	S1 convex (minimal), S3 convex (minimal)	S1 convex (with a concave area), S3 convex	S1 concave, S3 convex	S1 concave, S3 convex	convex in both S1 and S3
Arcing evidence on cell case exterior	no	no	no	no	yes (arcing between cell case and battery case)	no	no	no
CT scan	yes	no	yes	yes	yes	yes	yes	no

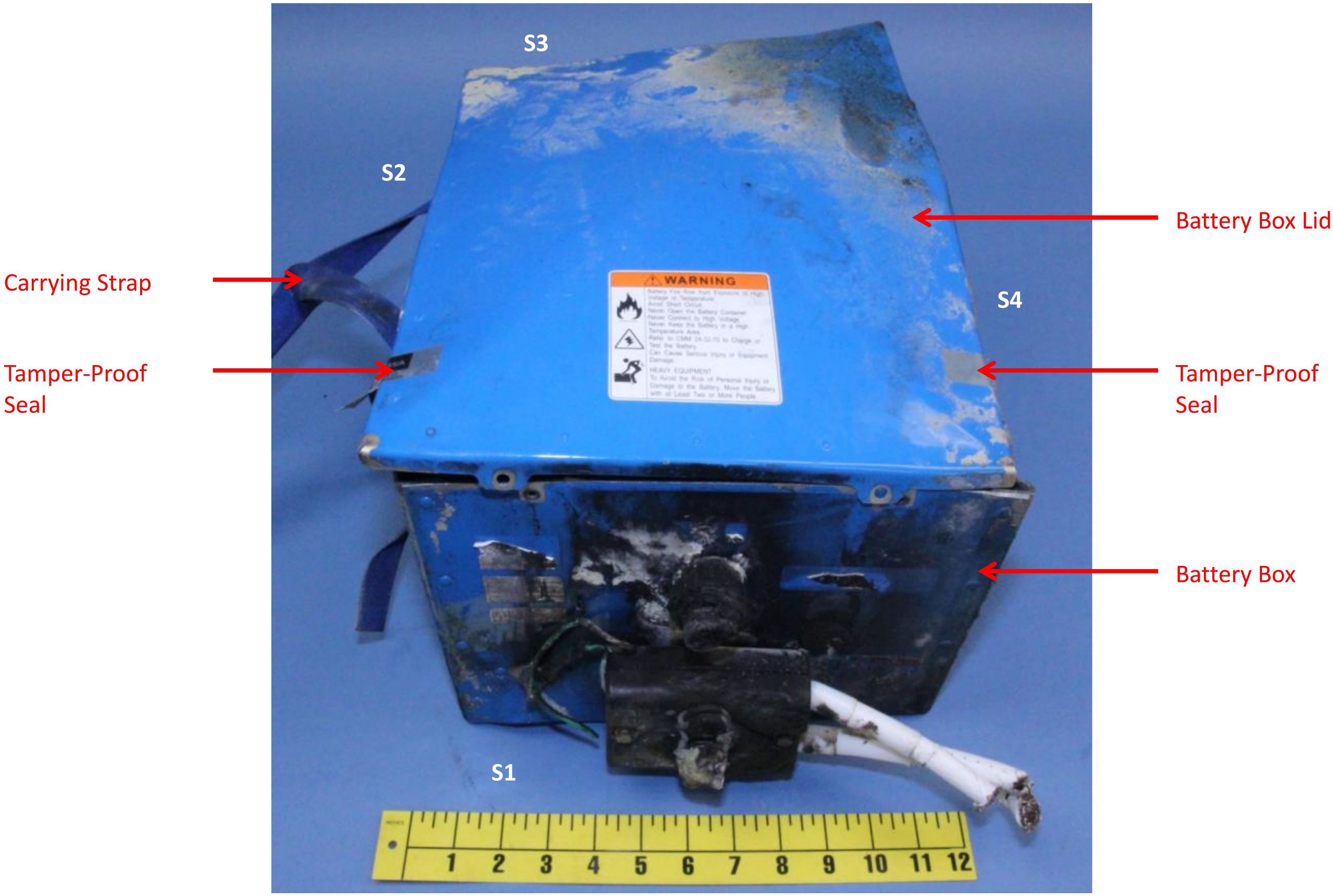

Figure 1. Accident battery as received by the NTSB laboratories.

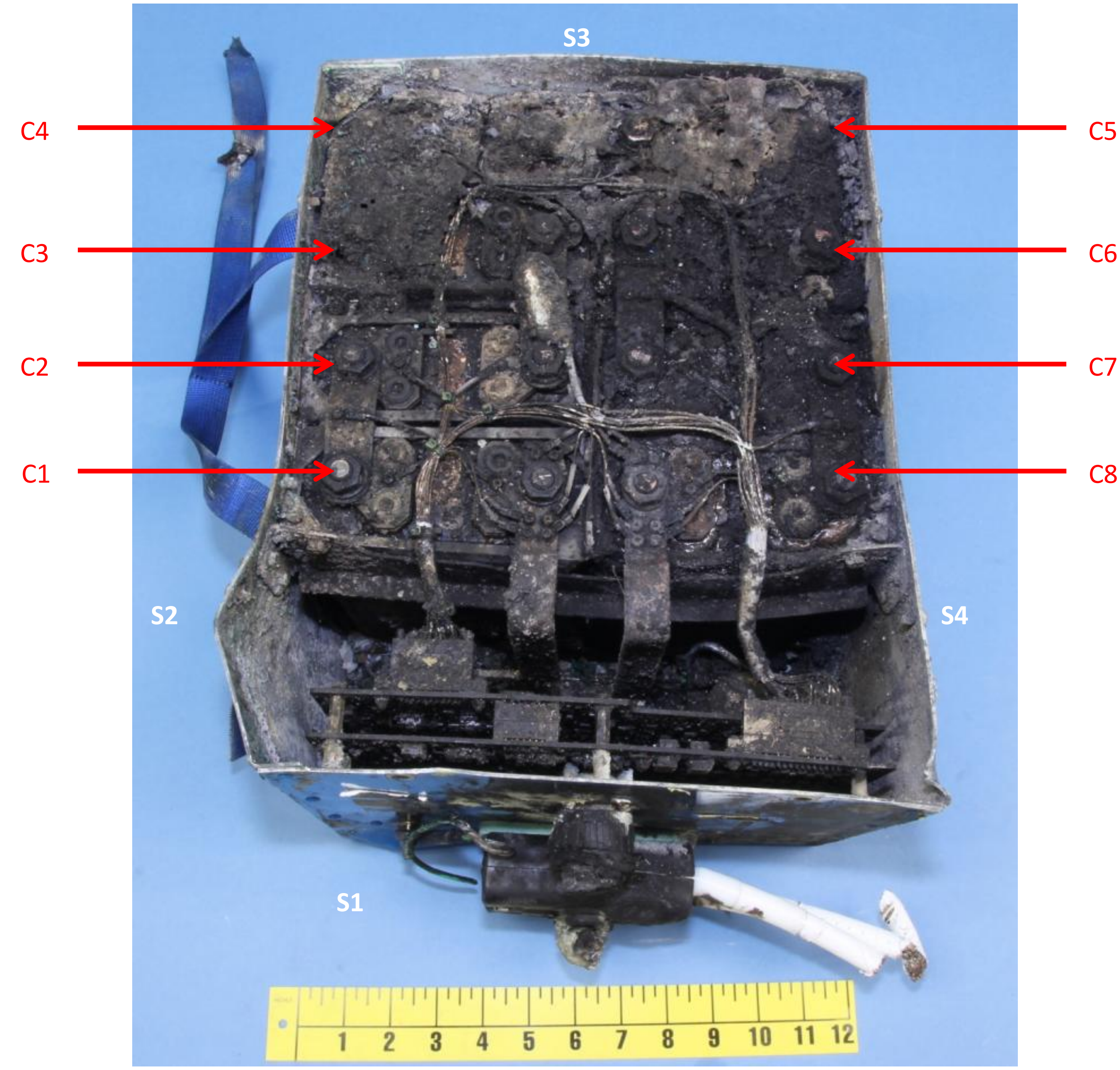

Figure 2. Opened battery box with approximate cell locations.

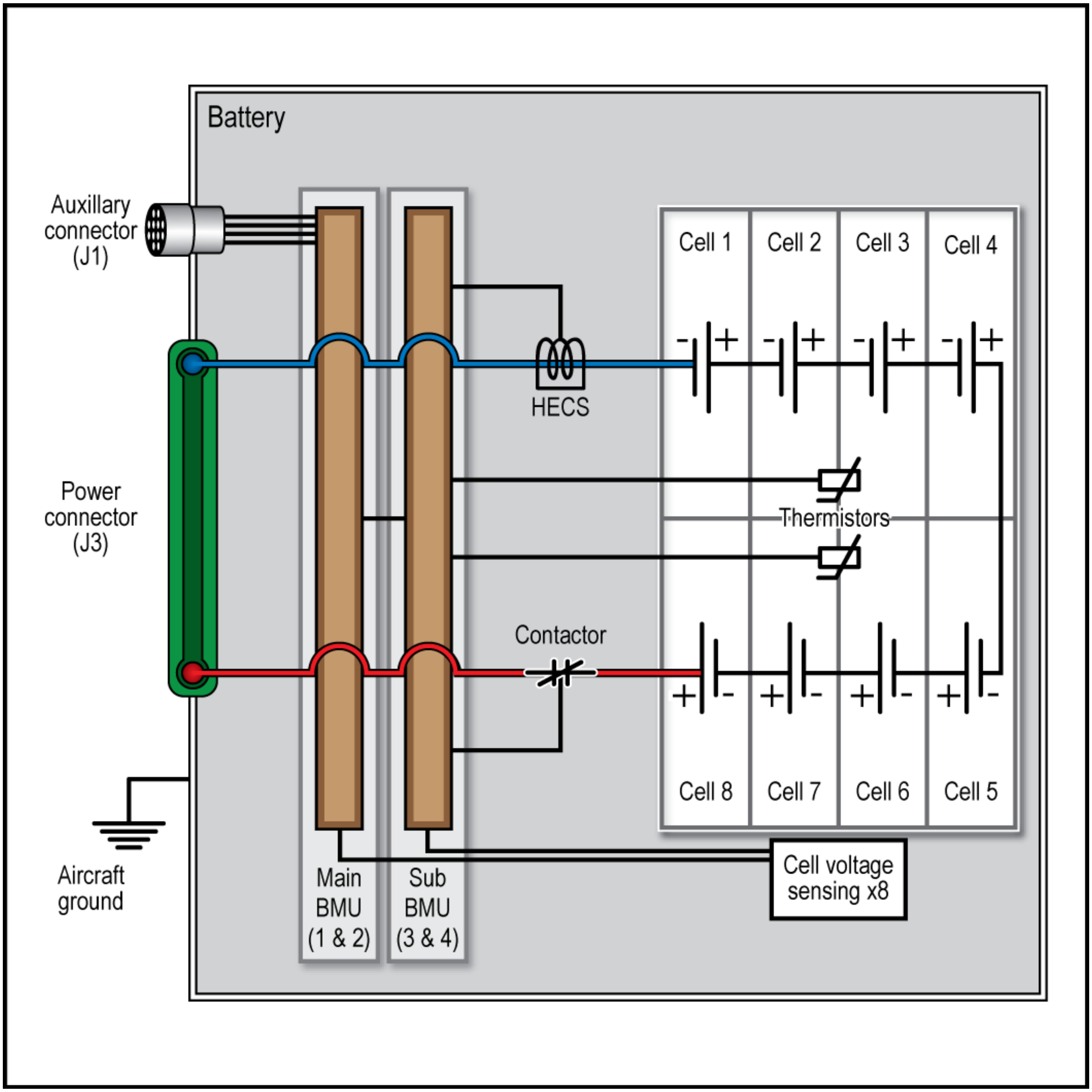

Figure 3. Electrical schematic of the LVP65-8-402 battery.

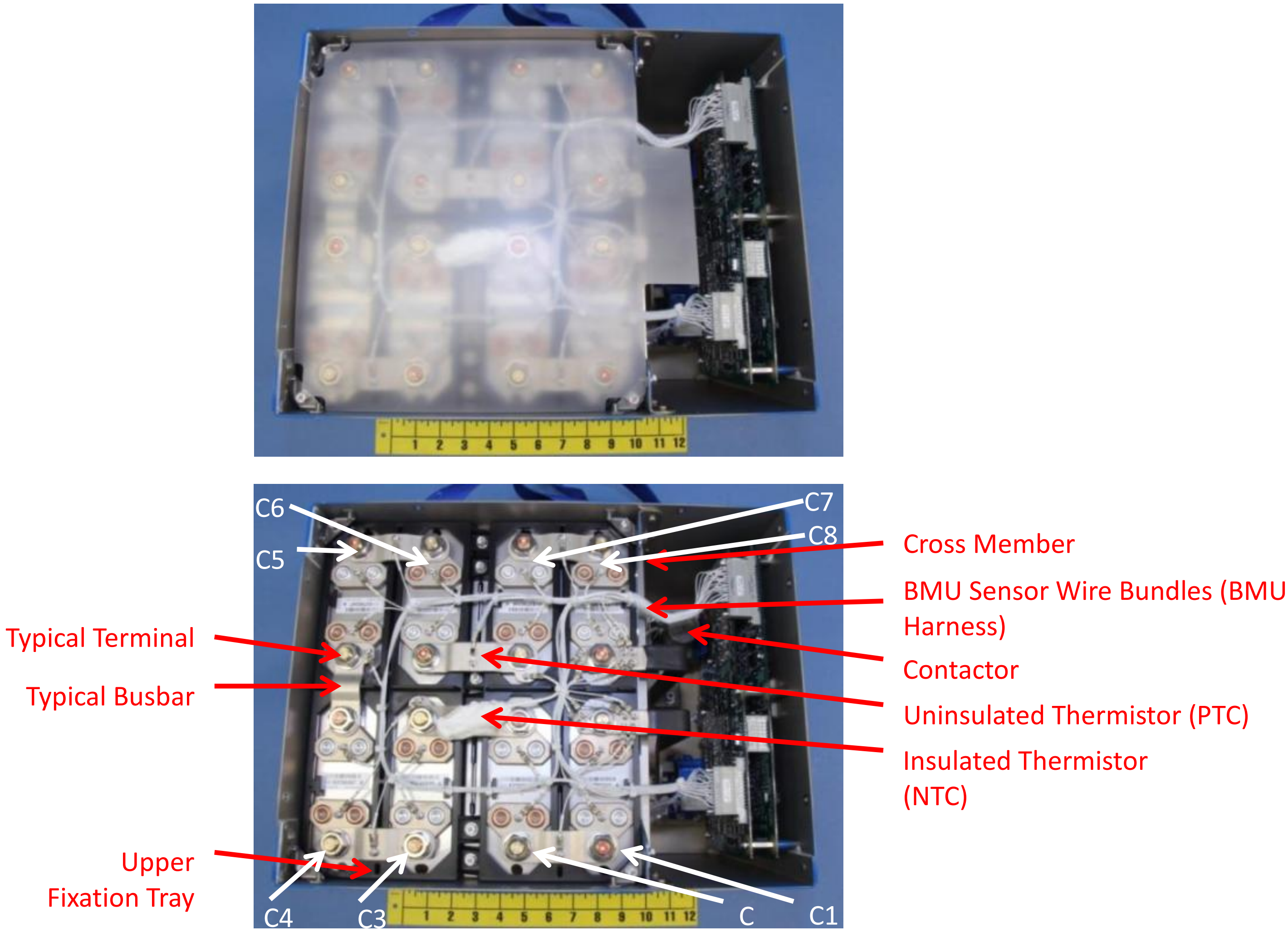

Figure 4. Photos of the exemplar, main battery top insulator sheet in place and removed from the battery box.

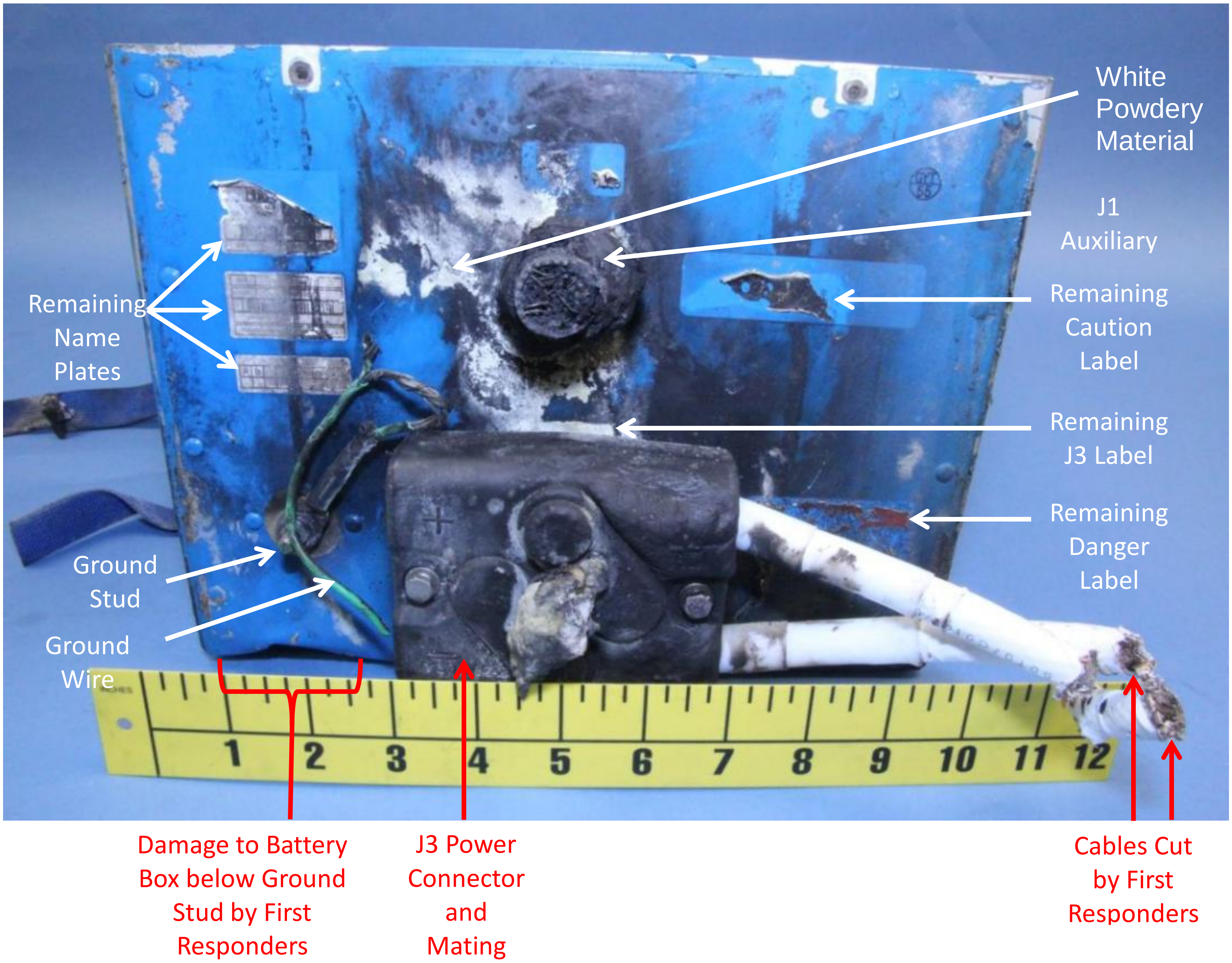

Figure 5. View of S1 exterior damage.

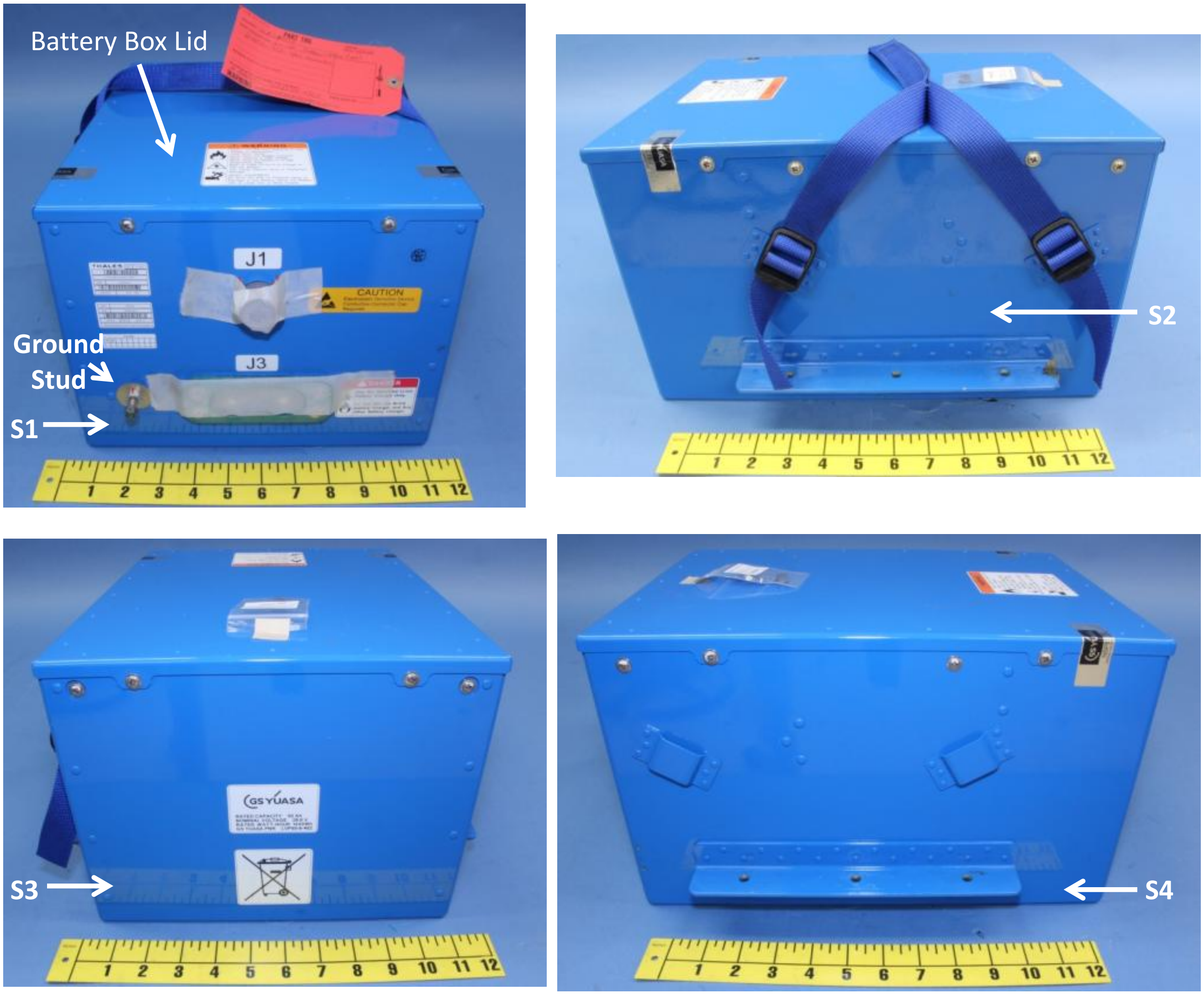

Figure 6. Four views of an exemplar, main battery showing S1, S2, S3, and S4.

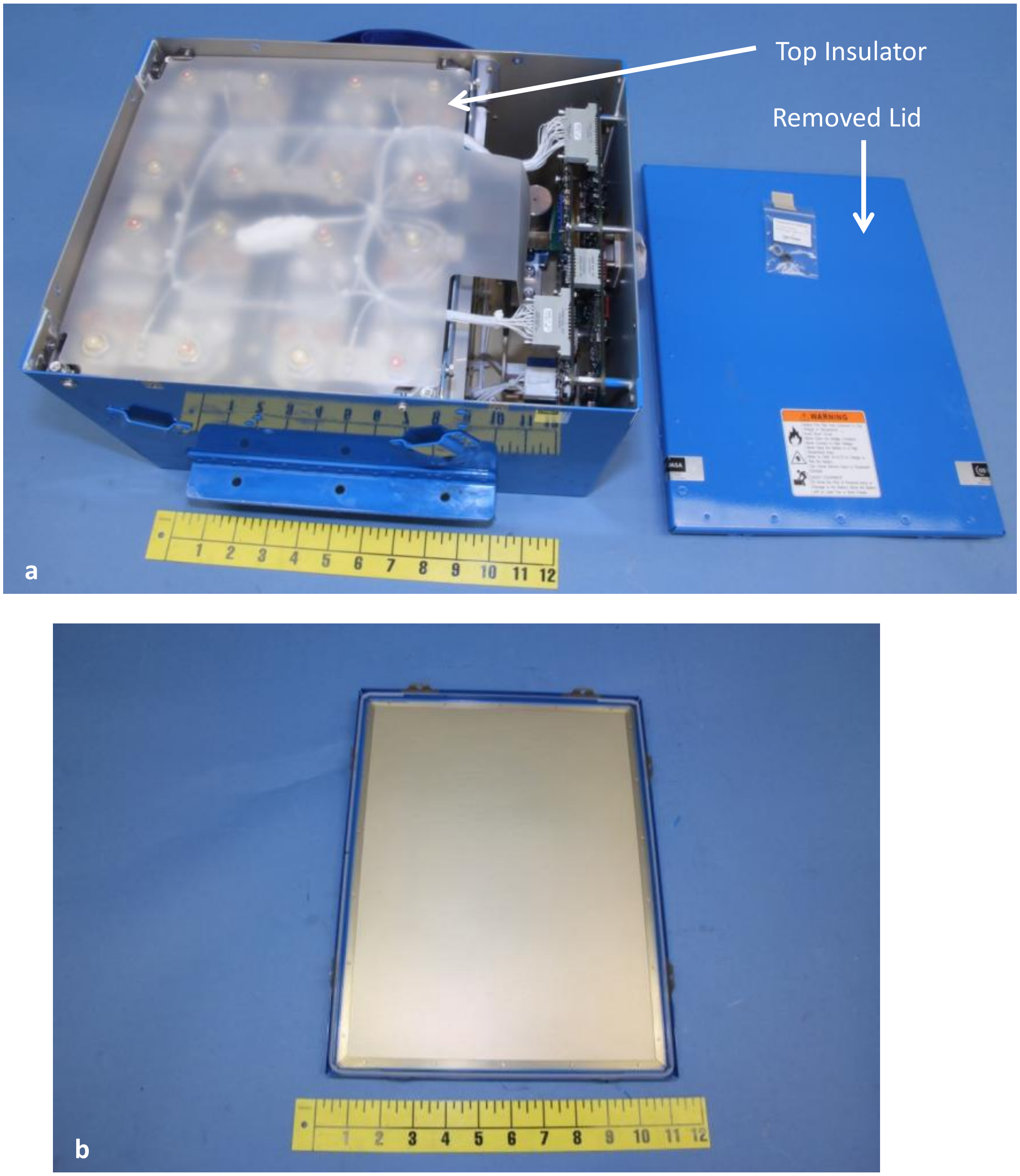

Figure 7. Exemplar, main battery with the battery box lid removed. Photo (a) is a view with the battery box lid removed. Photo (b) is a view of the inside of the battery box lid surface.

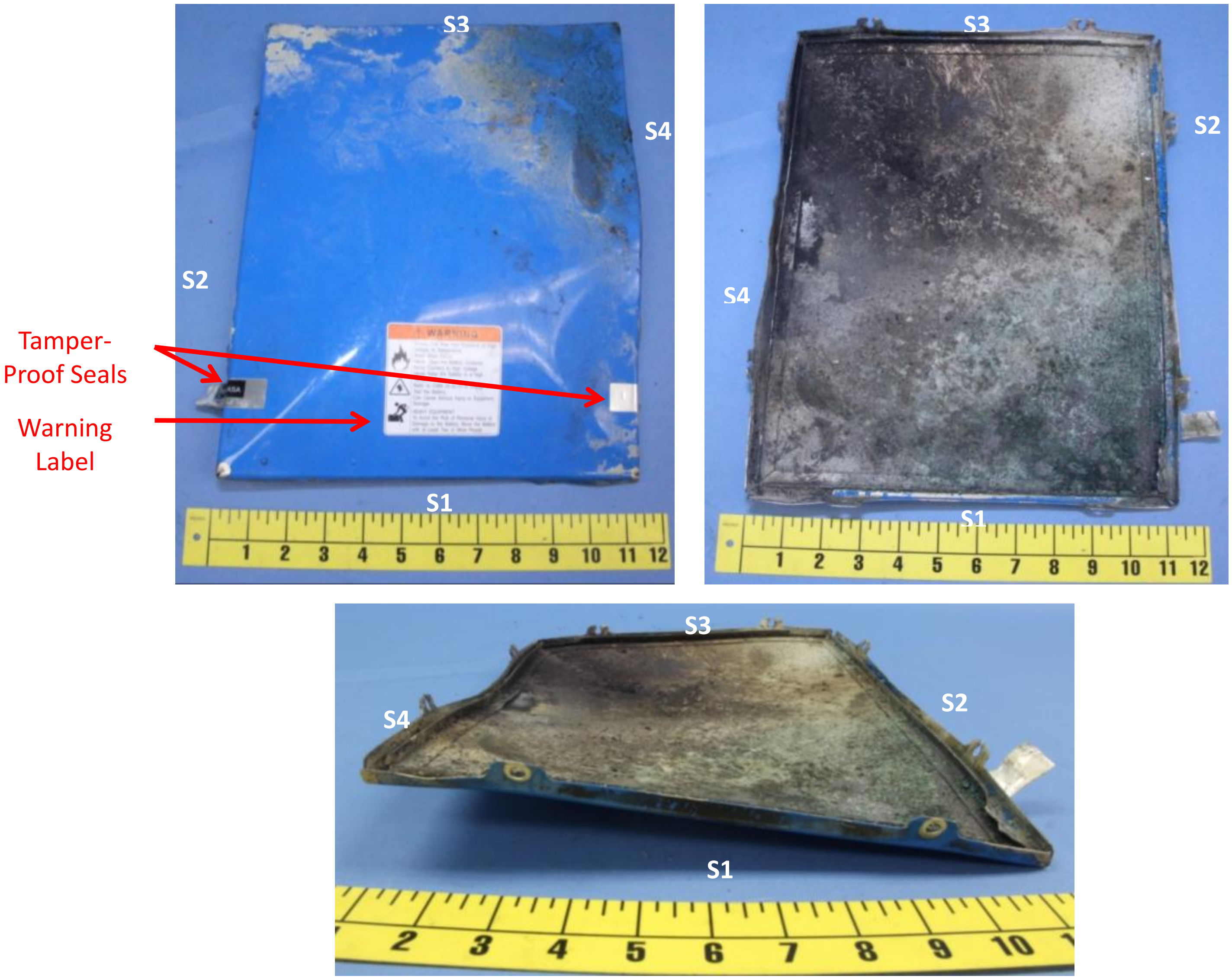

Figure 8. Top and bottom views of the battery box lid showing warning label and seals.

Figure 9. Battery box carrying strap.

Figure 10. S4 end of the battery box carrying strap.

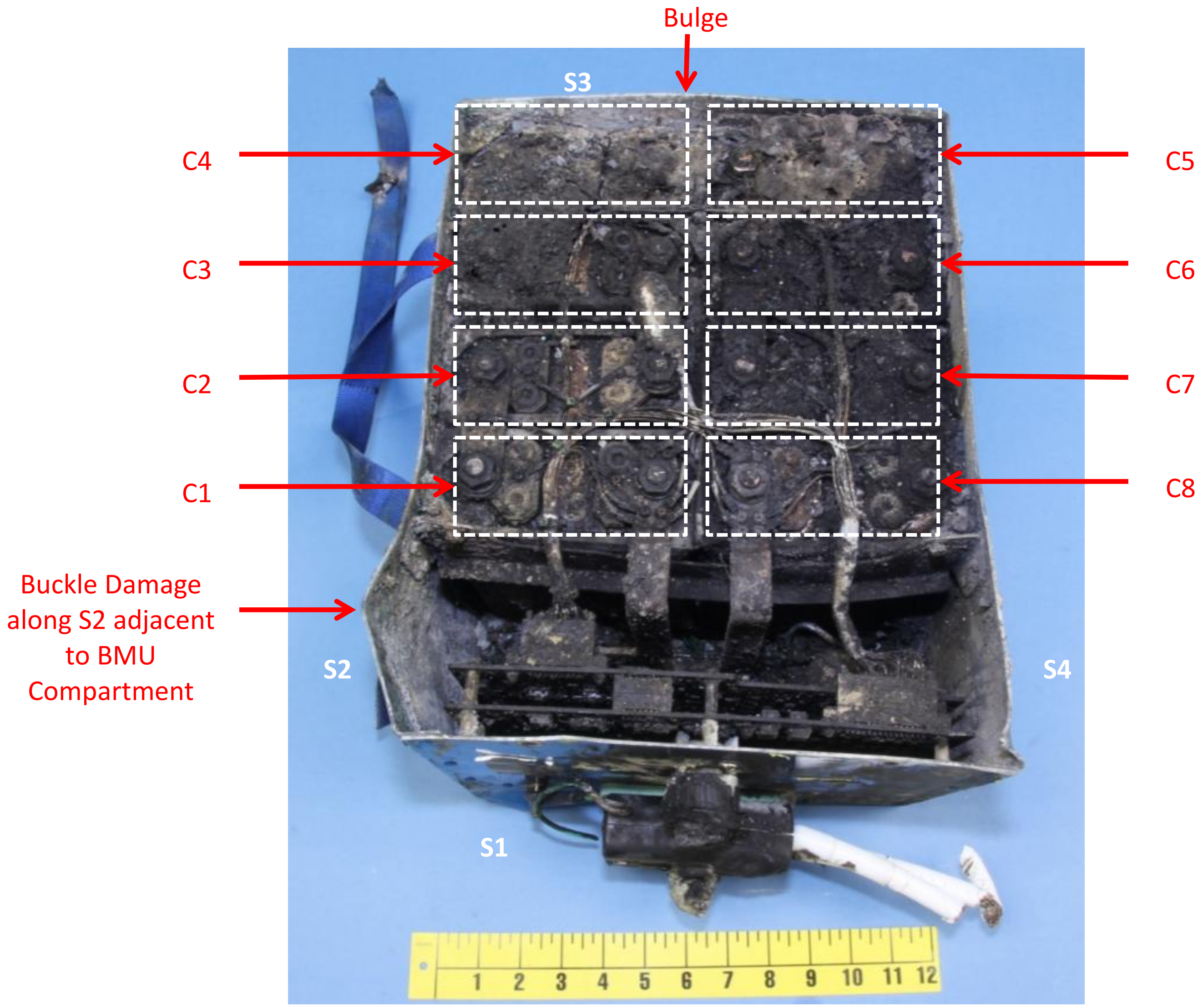

Figure 11. Opened battery box showing buckling and bulging.

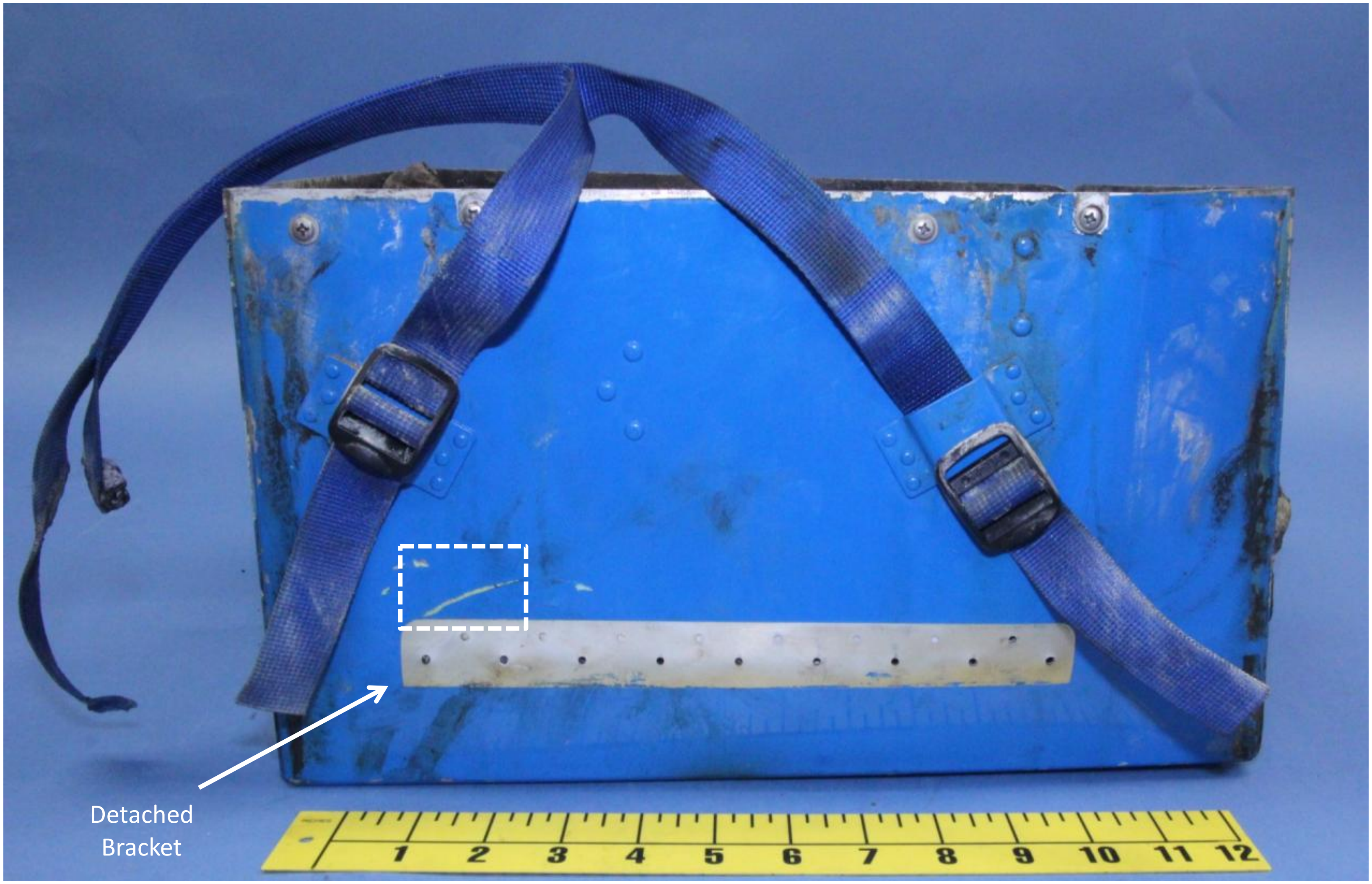

Figure 12. View of S2 exterior damage showing the carrying strap and detached bracket. The white highlighted area shows a gouge.

Figure 13. View of S3 exterior damage. The white highlighted area is a nodular protrusion. The yellow highlighted area shows a gouge.

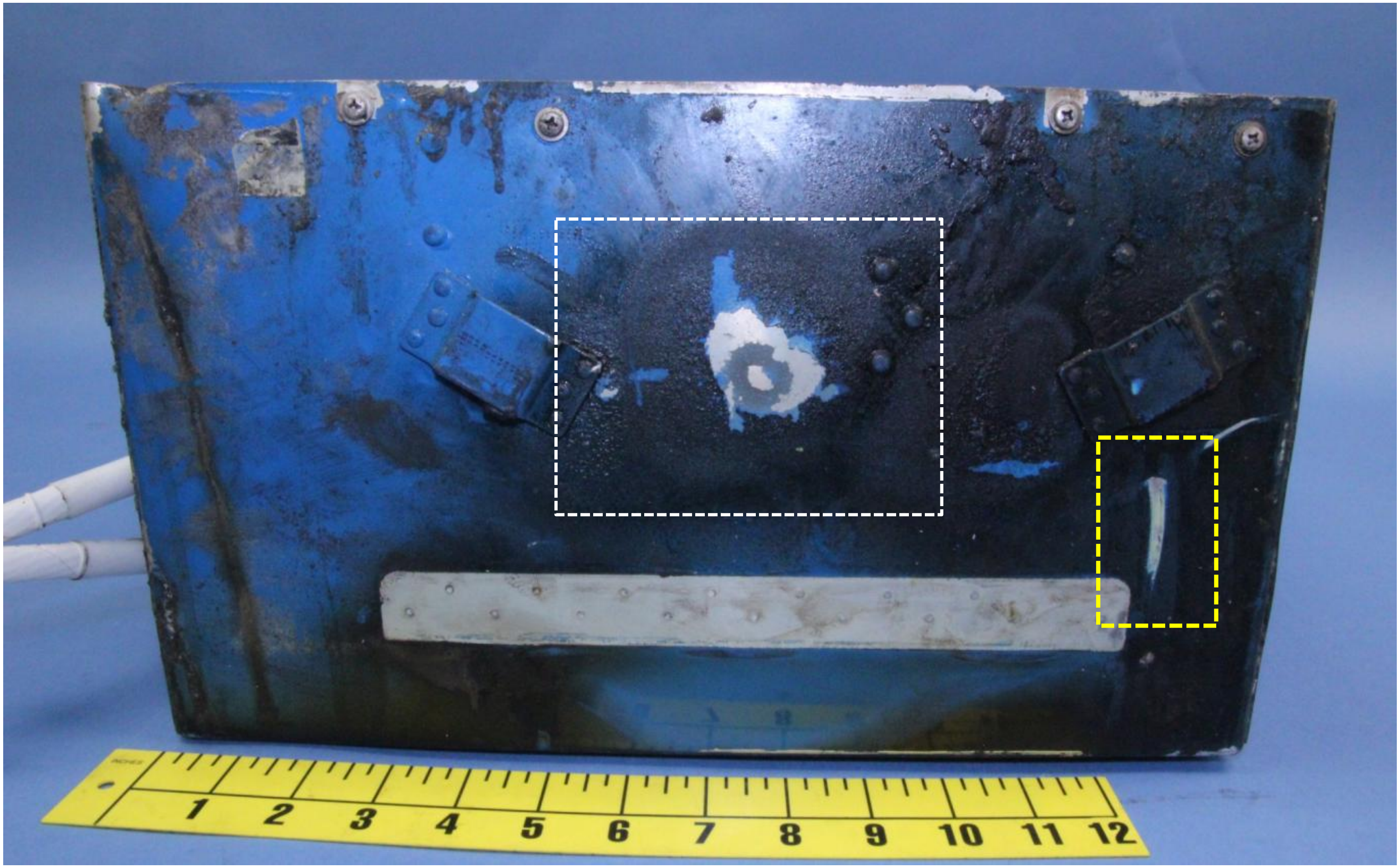

Figure 14. View of S4 exterior damage. The white highlighted area corresponds with the location of the C7 vent. The yellow highlighted area shows a gouge.

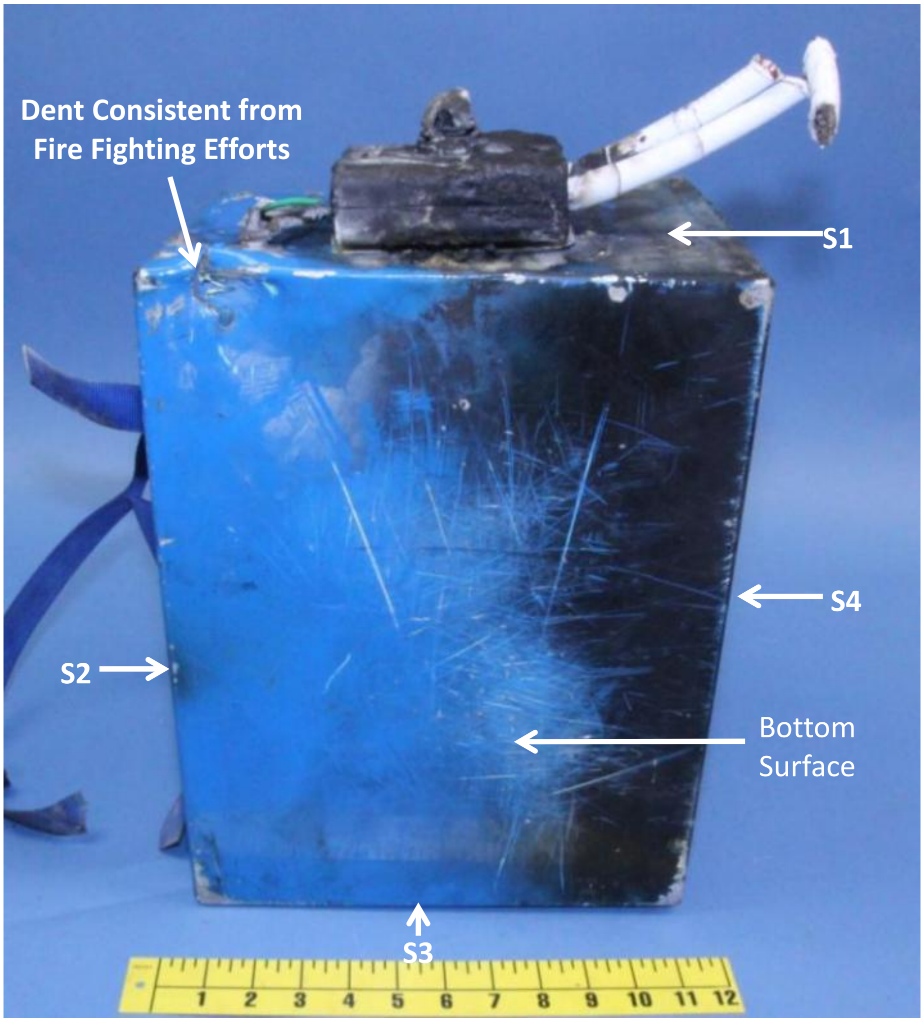

Figure 15. View of the bottom surface of the battery box.

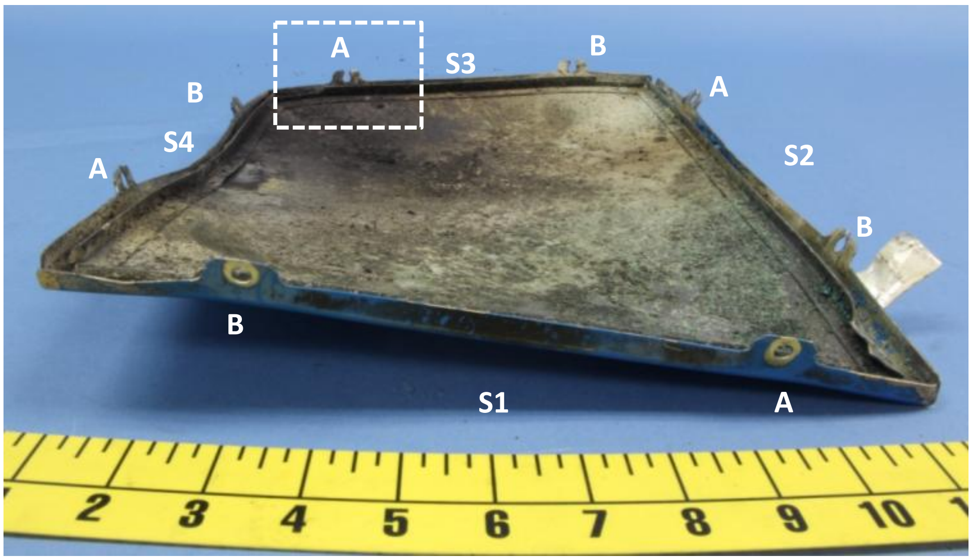

Figure 16. View of the underside of the battery box lid showing the positions of the tabs. The tabs are labeled A and B on each edge of the lid. The highlighted area shows the fractured S3A tab (a close-up view is shown in Figure 18).

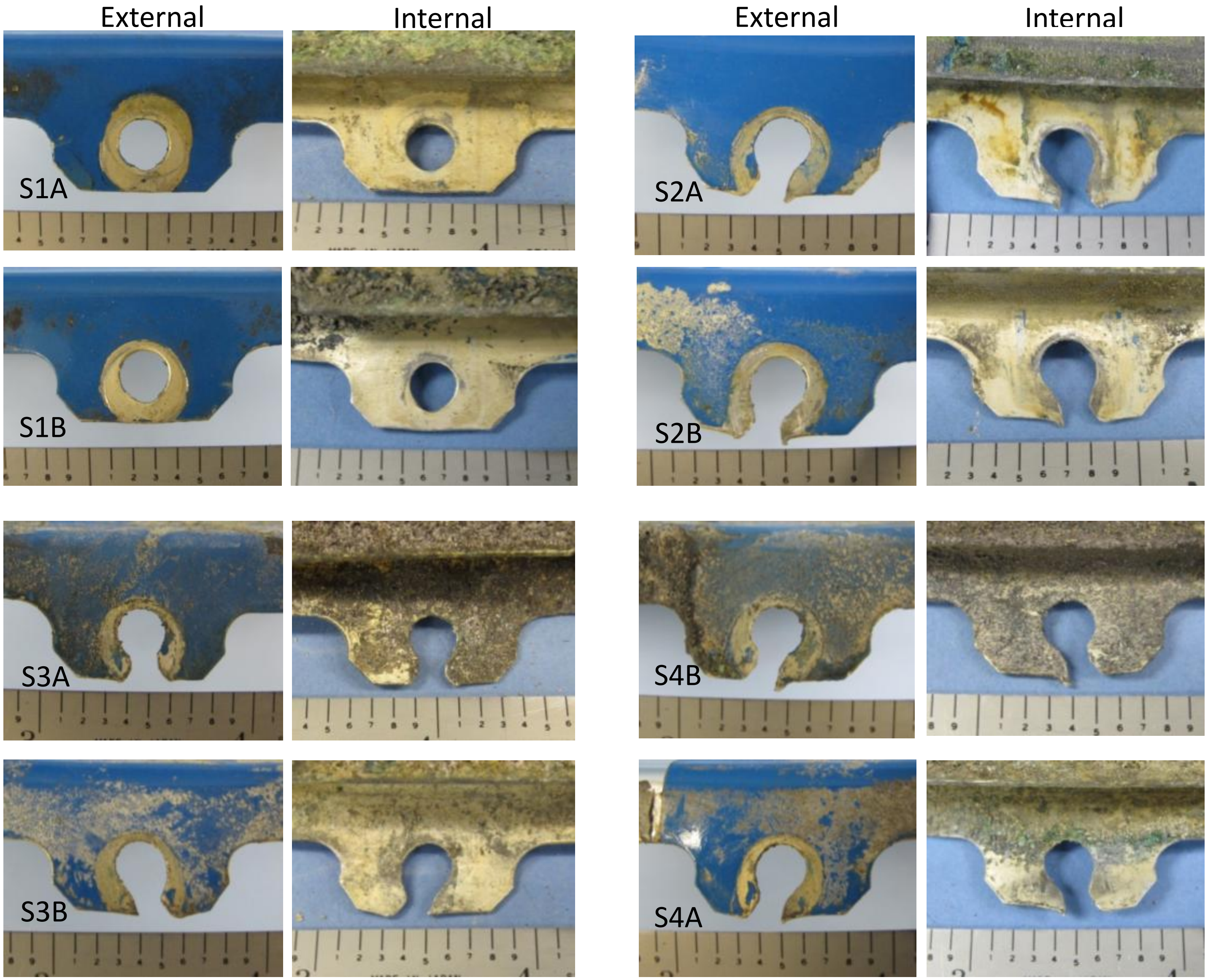

Figure 17. Close-up views of the battery box lid tabs.

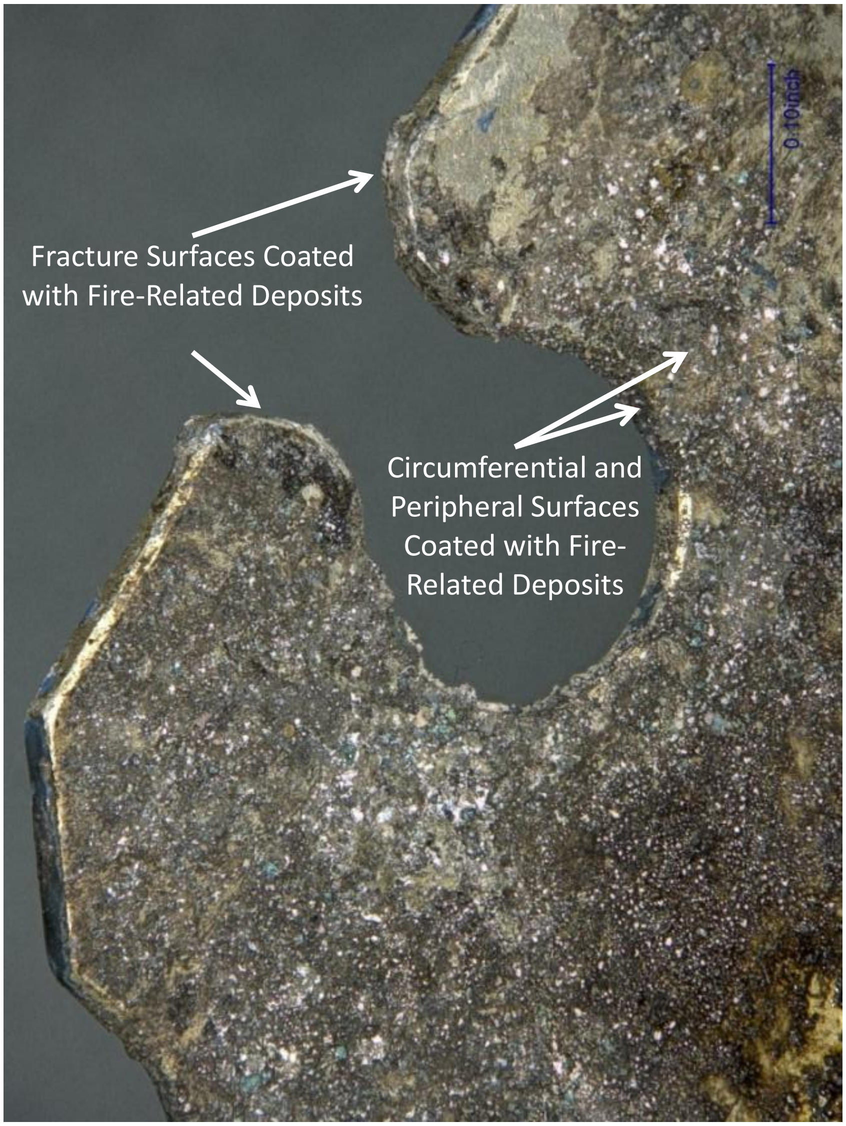

Figure 18. Close-up view of the fractured S3A mounting tab.

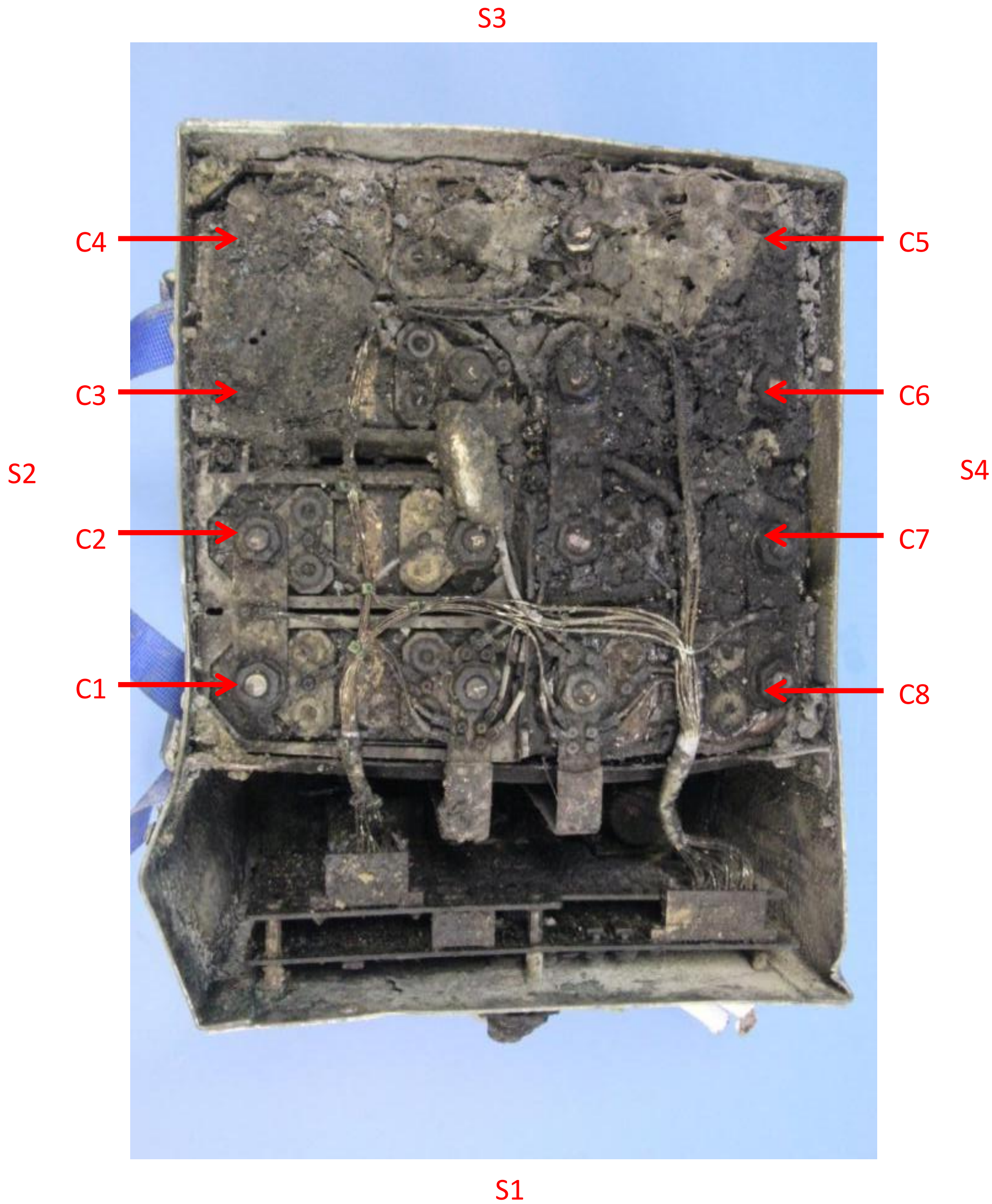

Figure 19. Battery top with debris.

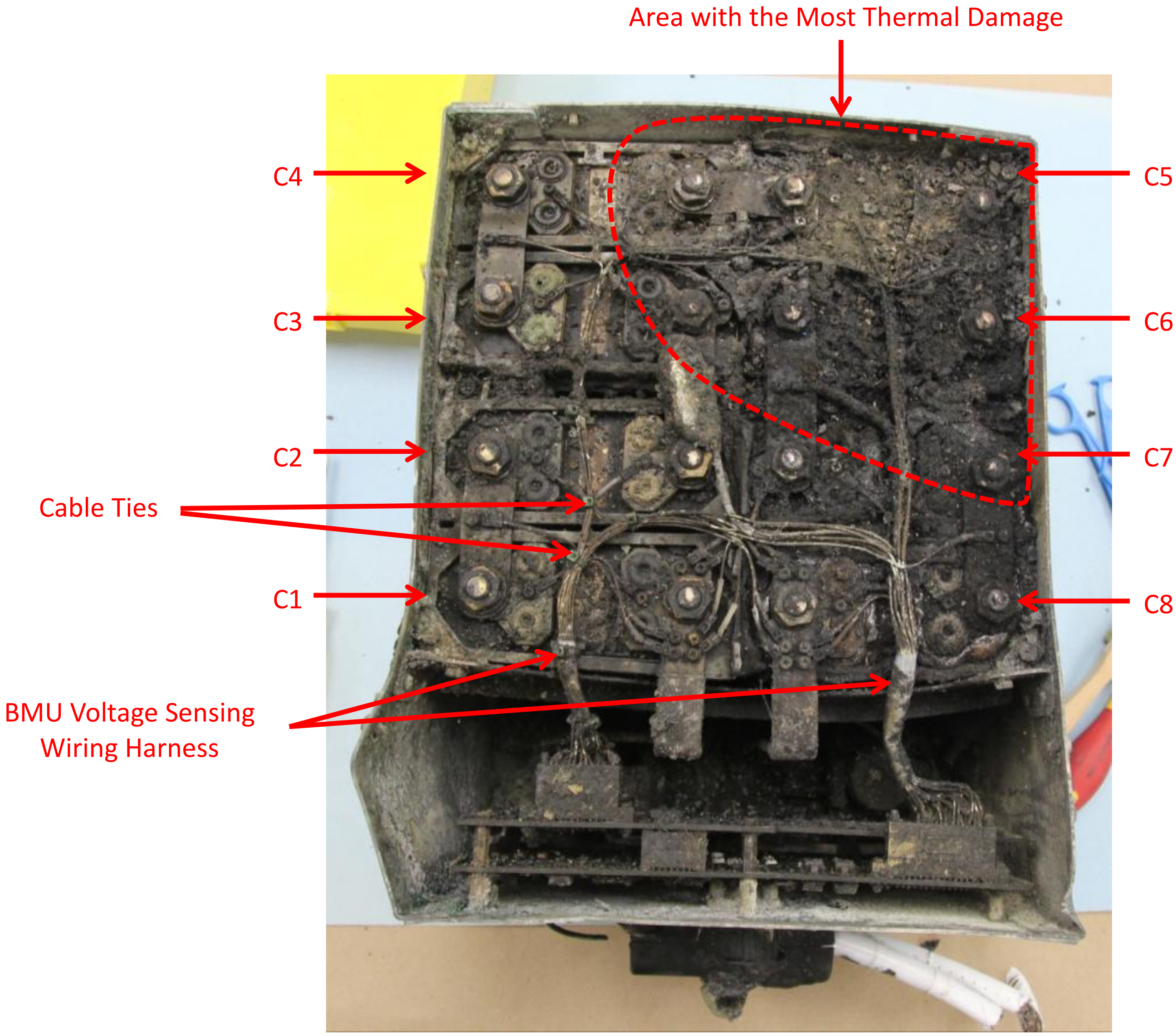

Figure 20. Battery top with debris removed.

Figure 21. Wiring harness, as removed. The photo on the left is a view from the bottom. The photo on the right is a view from the top.

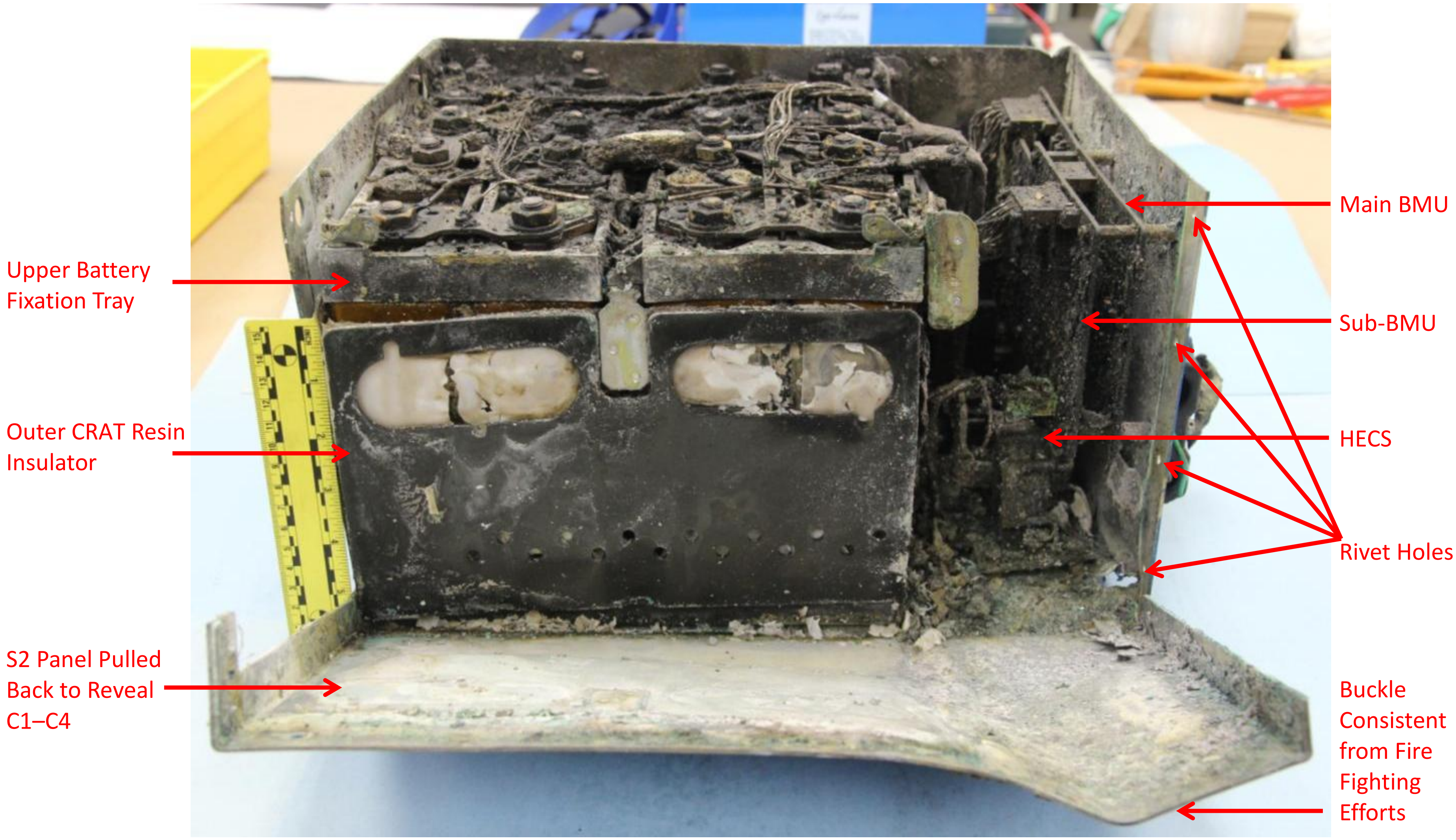

Figure 22. S2 view with battery box panel pulled back to reveal C1 through C4 and the BMU cavity.

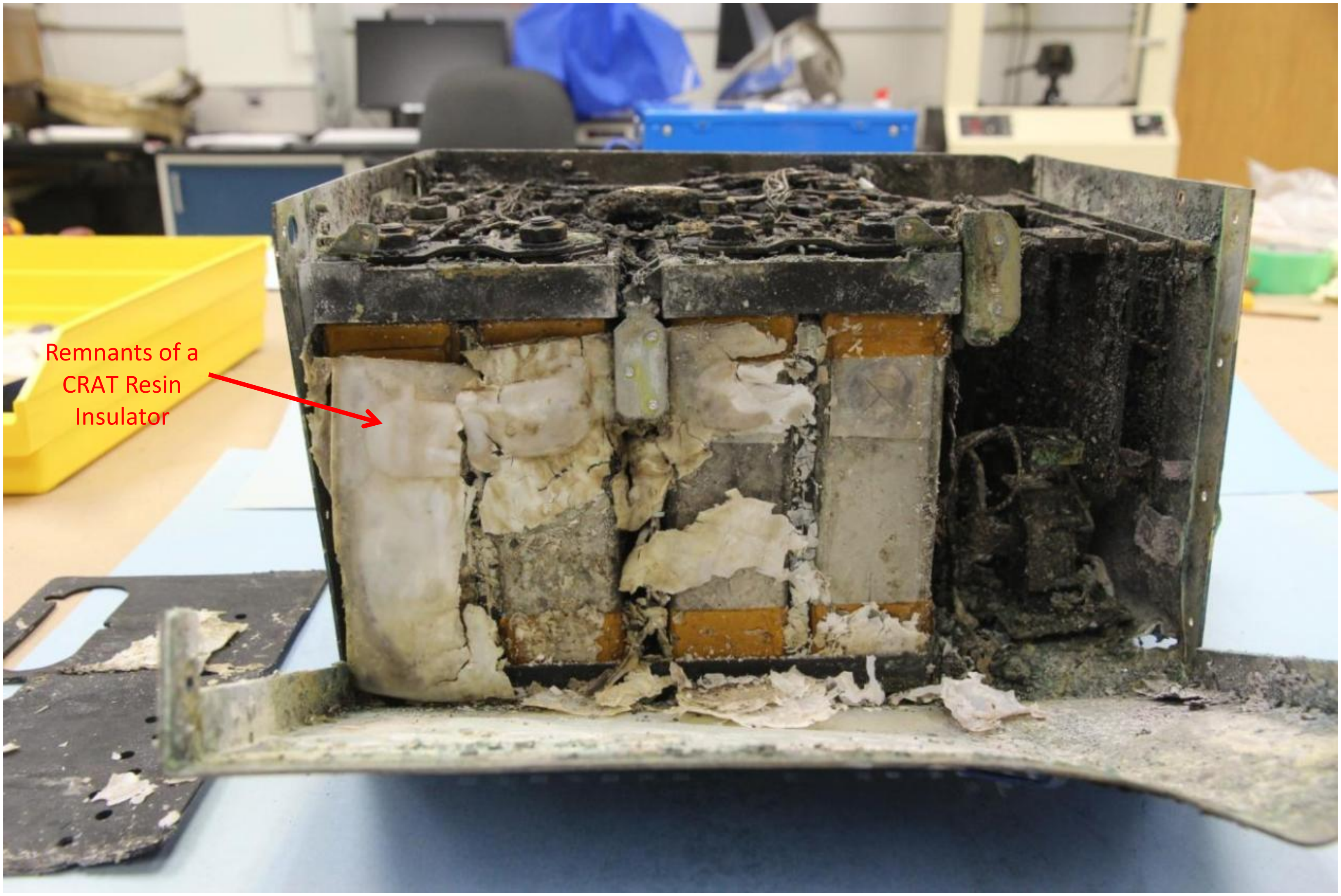

Figure 23. S2 with the outer CRAT resin insulator removed to reveal the inner BPA-TP resin insulator.

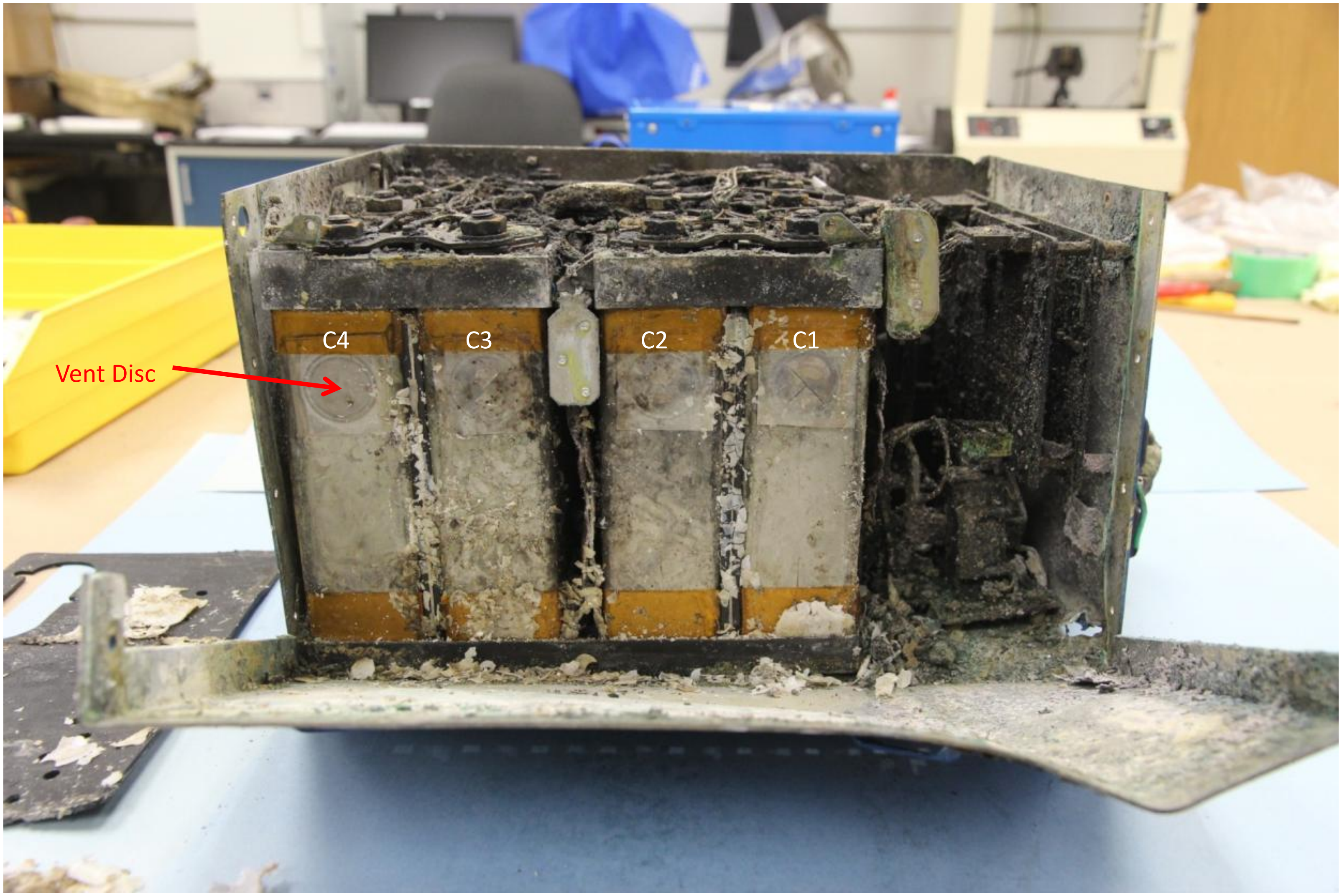

Figure 24. S2 with the remnants of the inner BPA-TP resin insulator removed to reveal the vent disc side of C1 through C4.

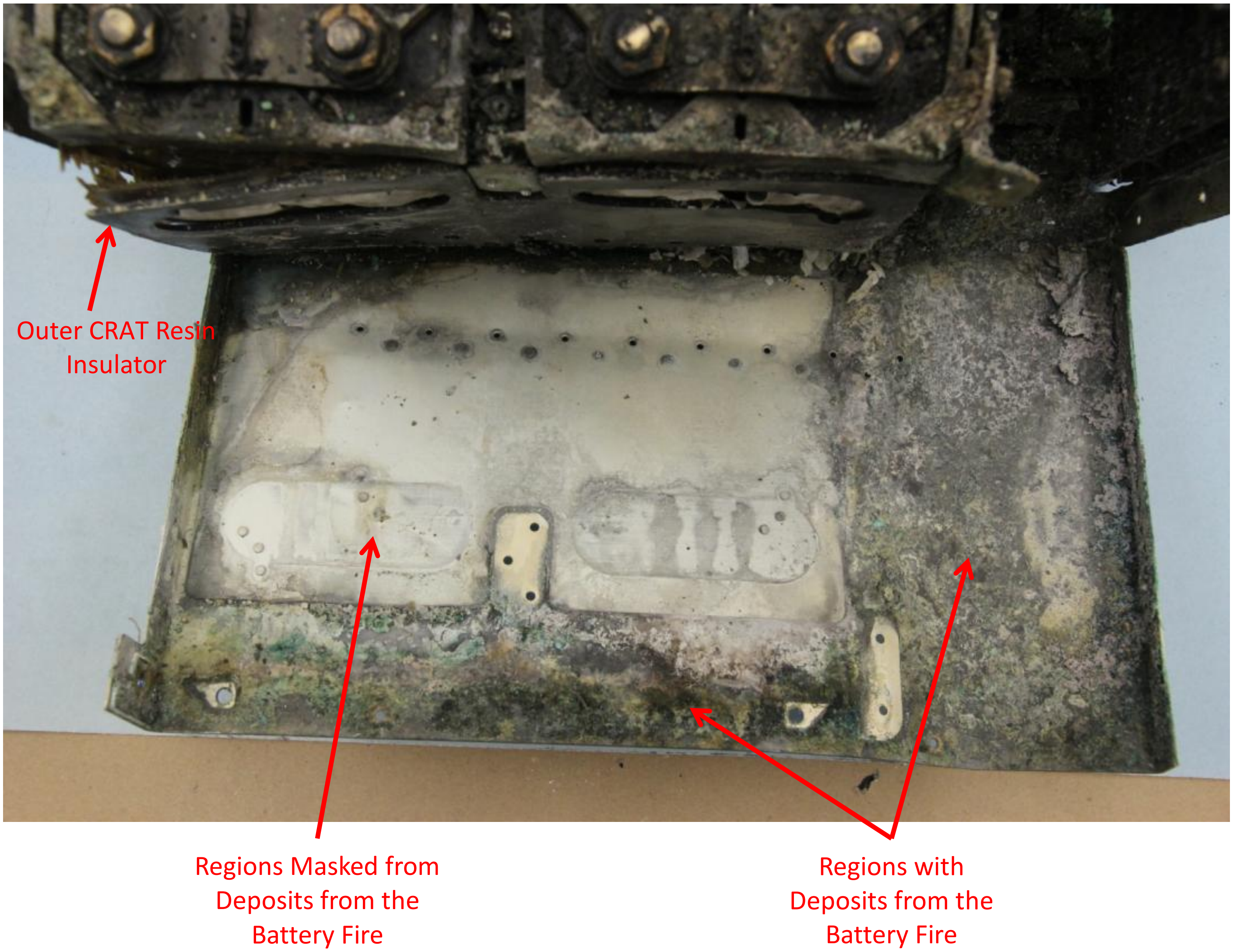

Figure 25. Top view of S2 (battery box interior).

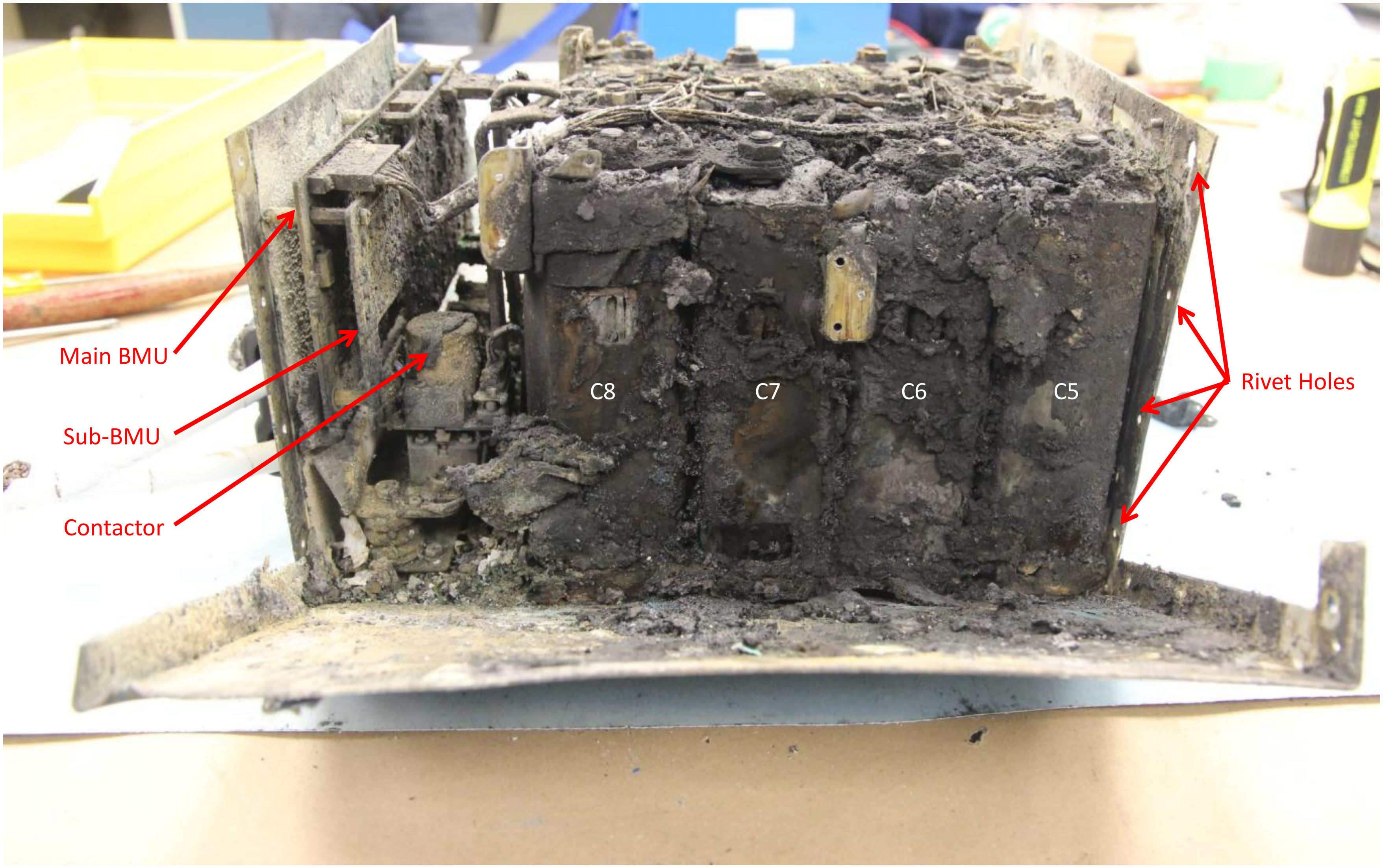

Figure 26. View of S4 with battery box panel pulled back to reveal C5 through C8.

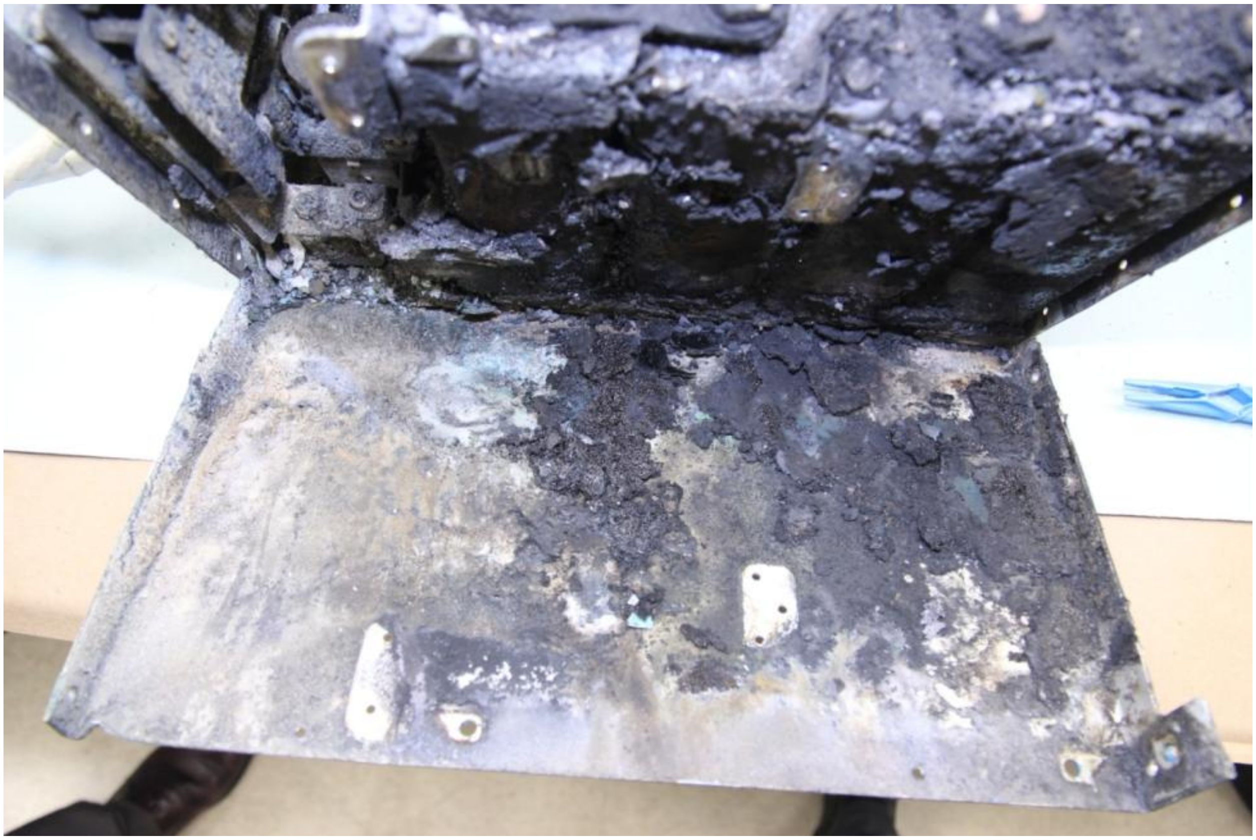

Figure 27. S4 battery box side interior.

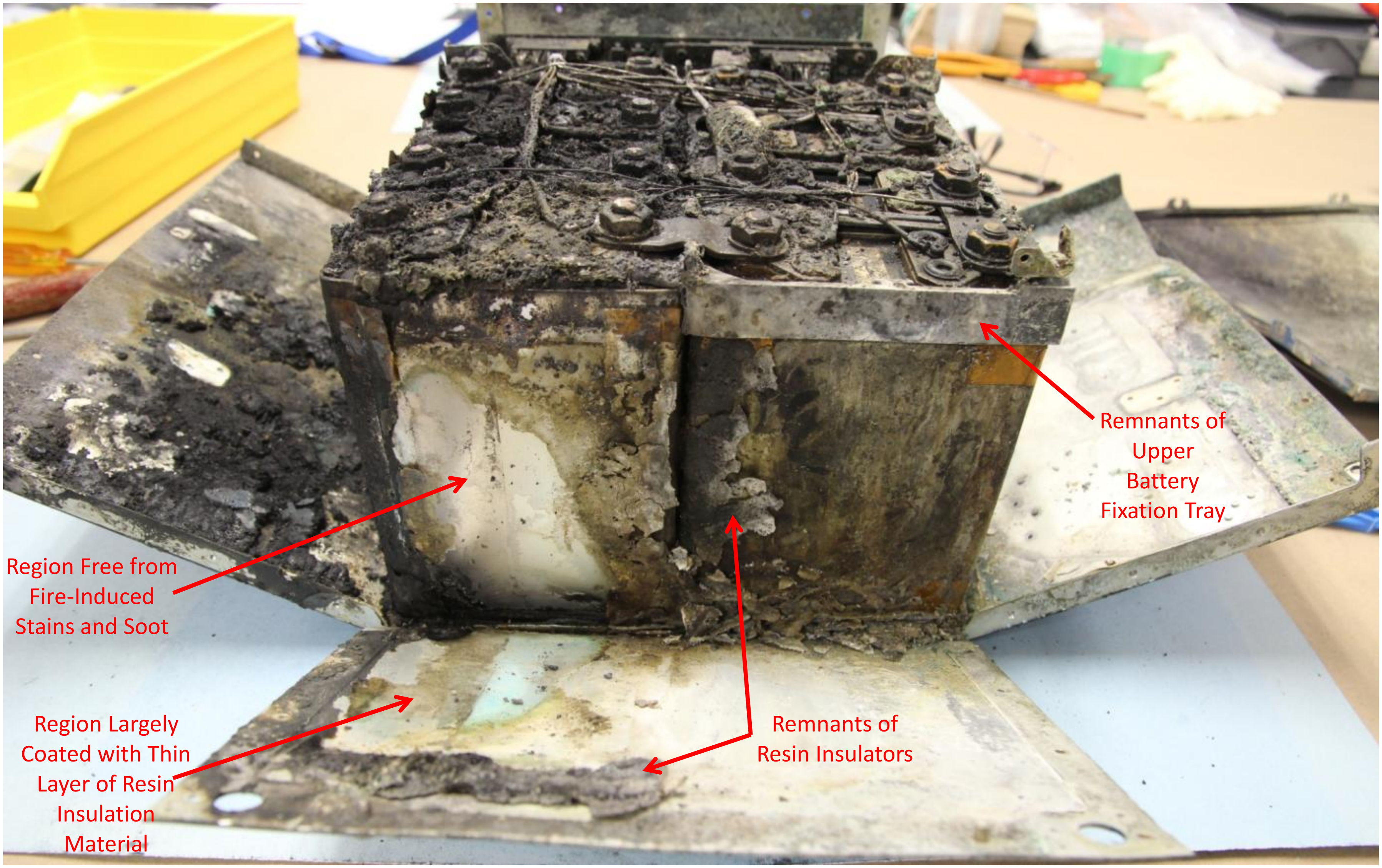

Figure 28. View of S3 with battery box panel pulled back to reveal C4 (right) and C5 (left).

Figure 29. S3 battery box side interior.

Figure 30. Top view of S4.

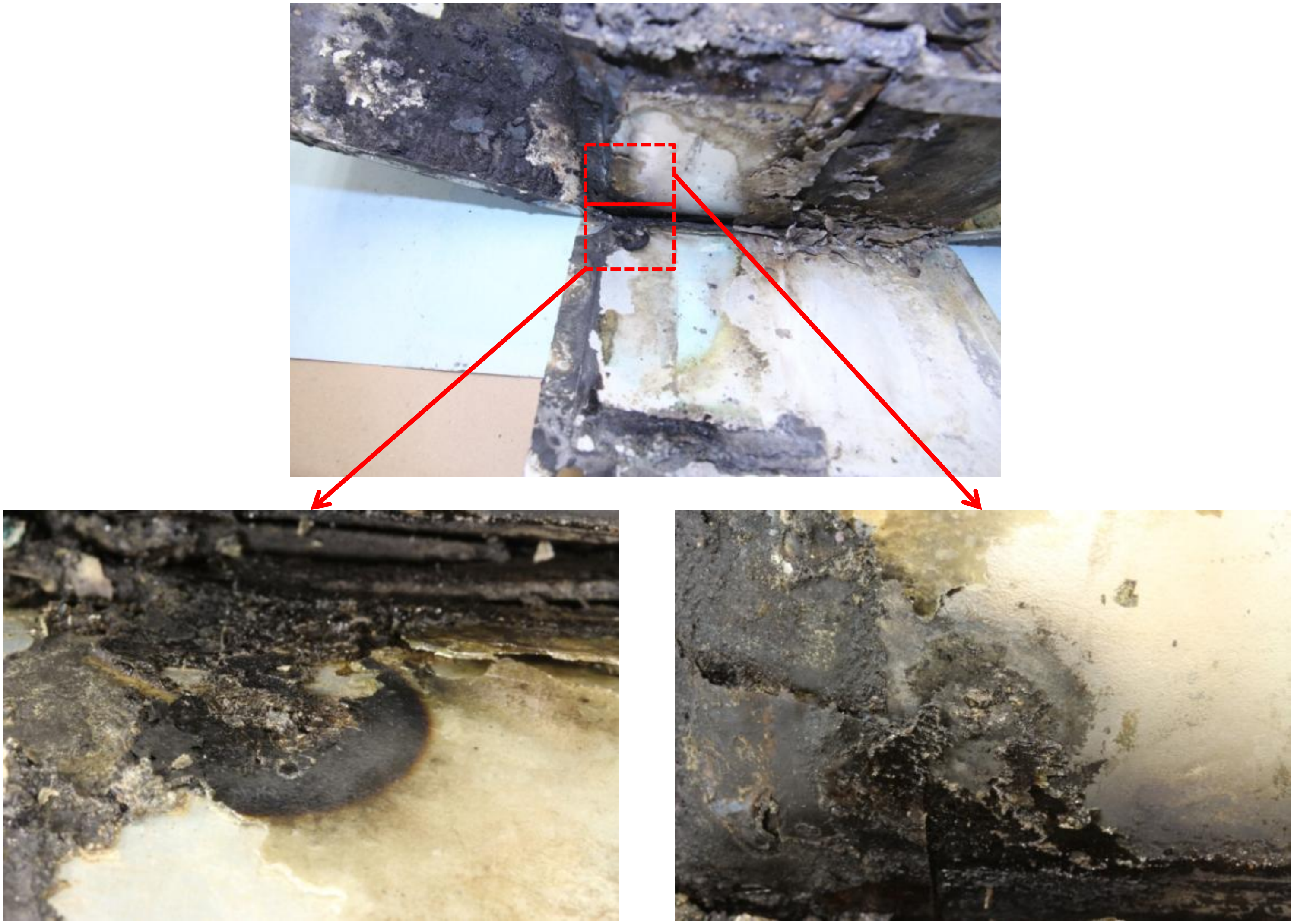

Figure 31. Closer views of a higher-temperature spot consistent with arc damage between C5 and the inside of S3 of the battery box.

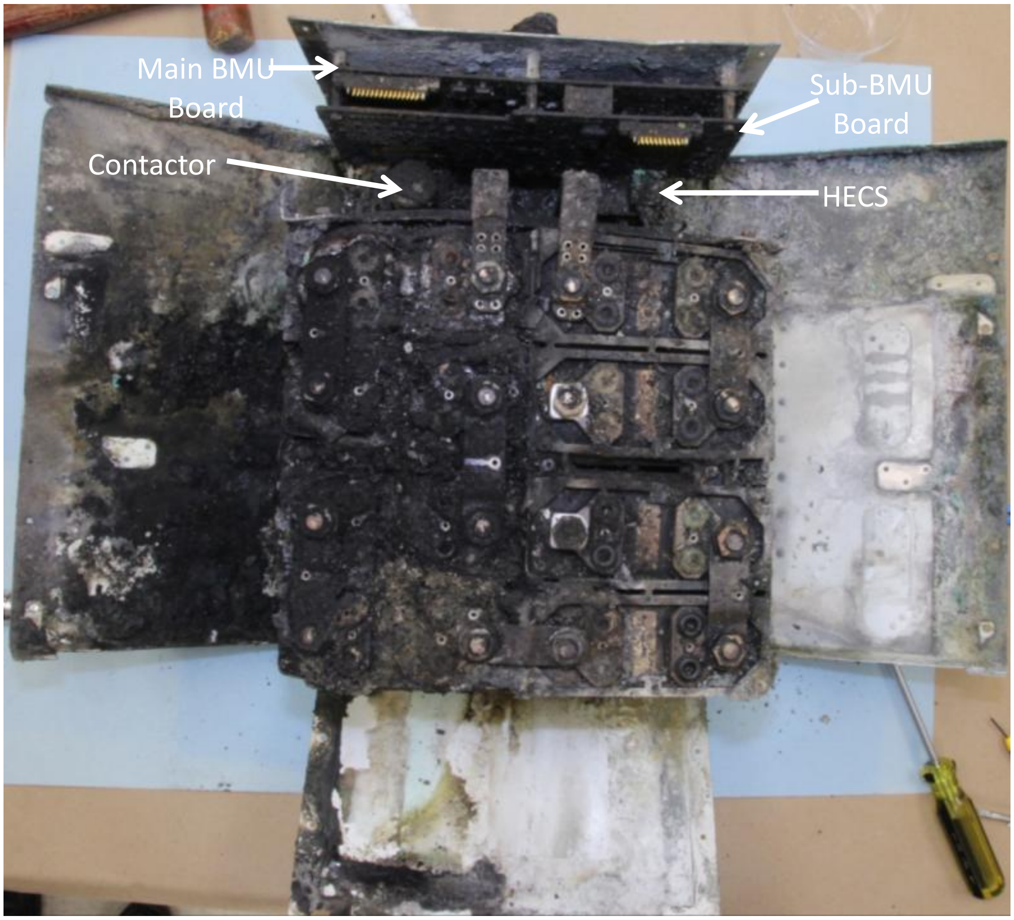

Figure 32. Top view showing the BMU, HECS, and contactor locations.

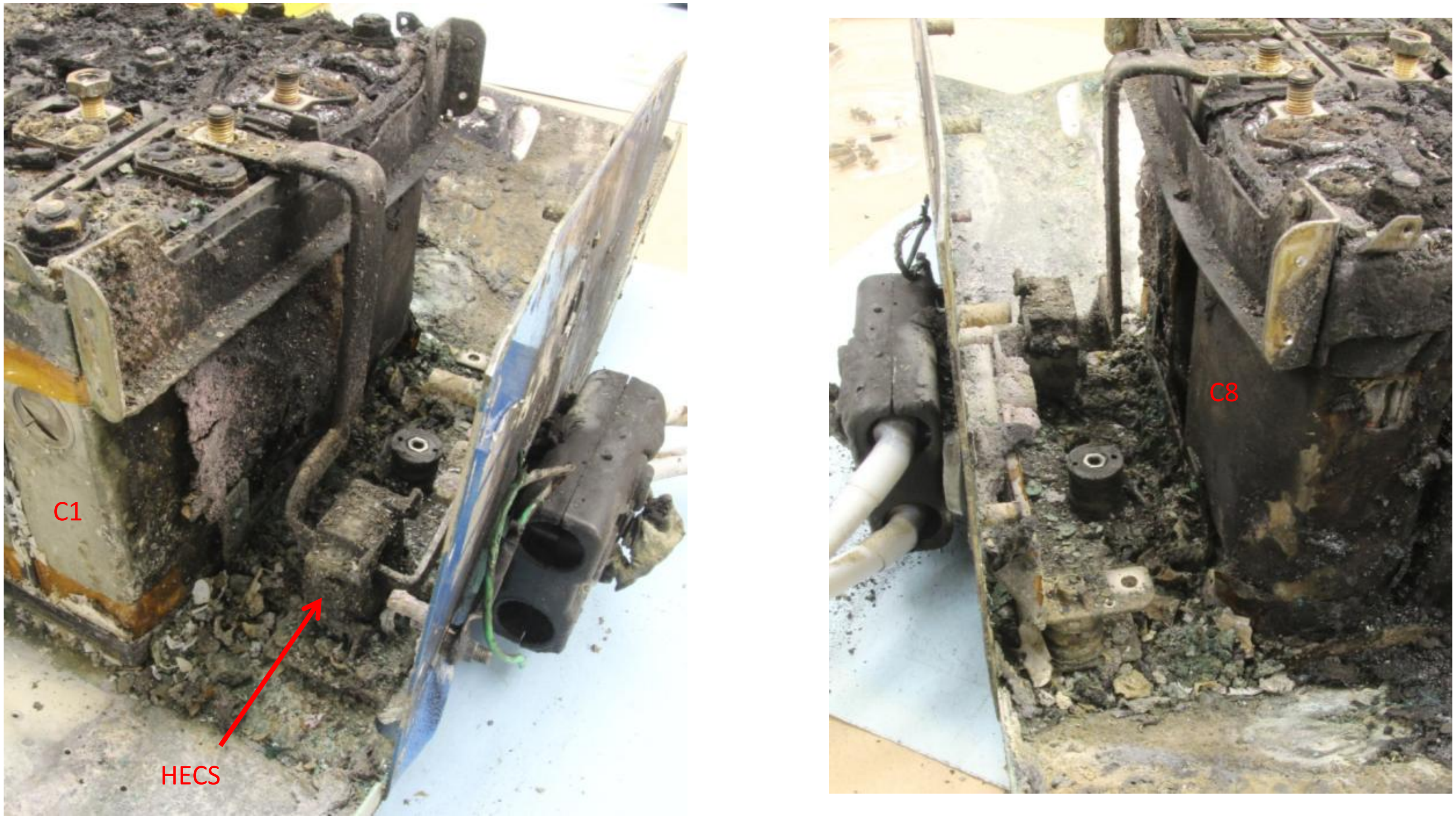

Figure 33. Photos of the BMU boards and contactor removed. The photo on the left is a view from S2. The photo on the right is a view from S4.

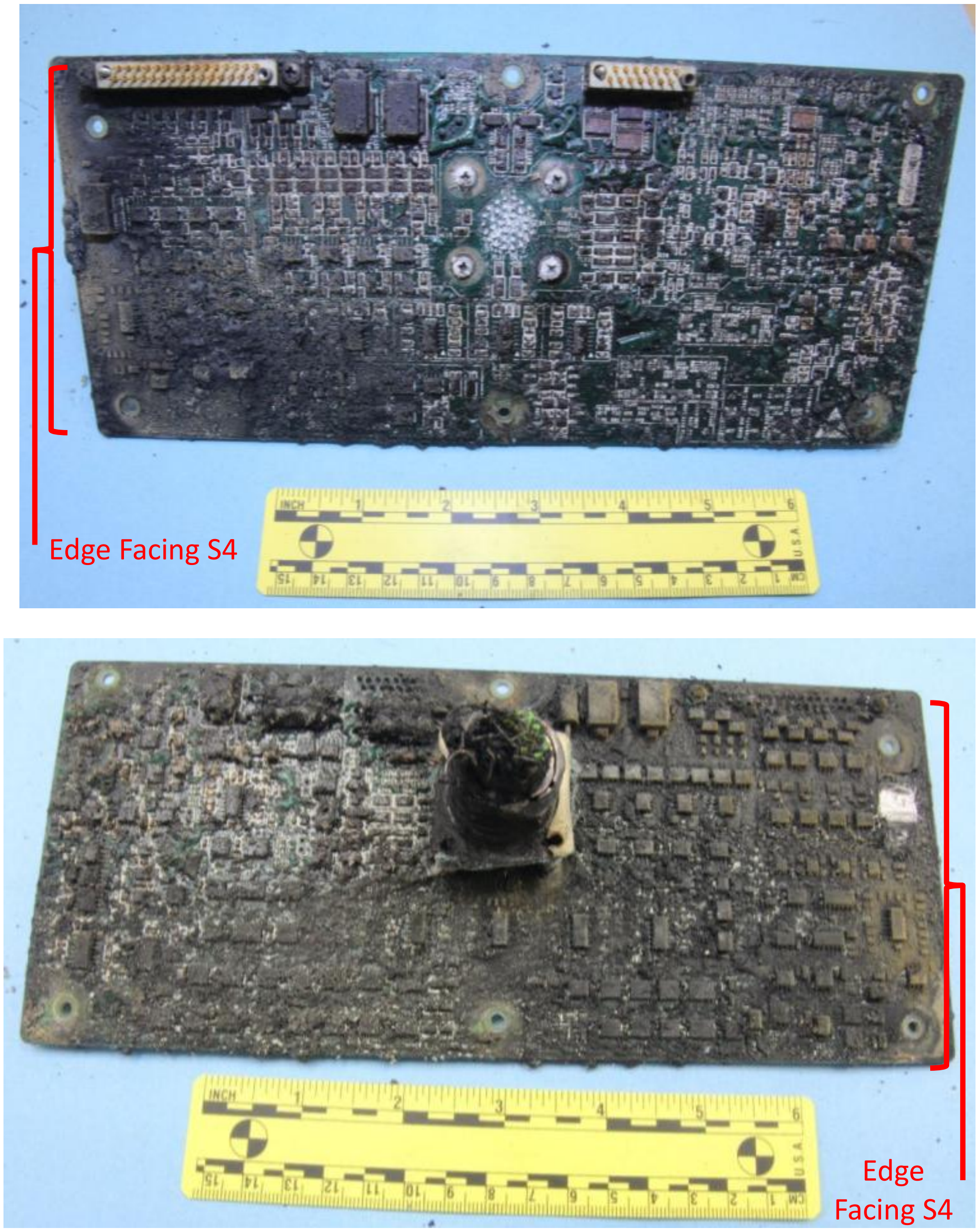

Figure 34. Main BMU board. The top photo shows the side facing the interior of the battery box. The bottom photo shows the side facing the exterior of the battery box.

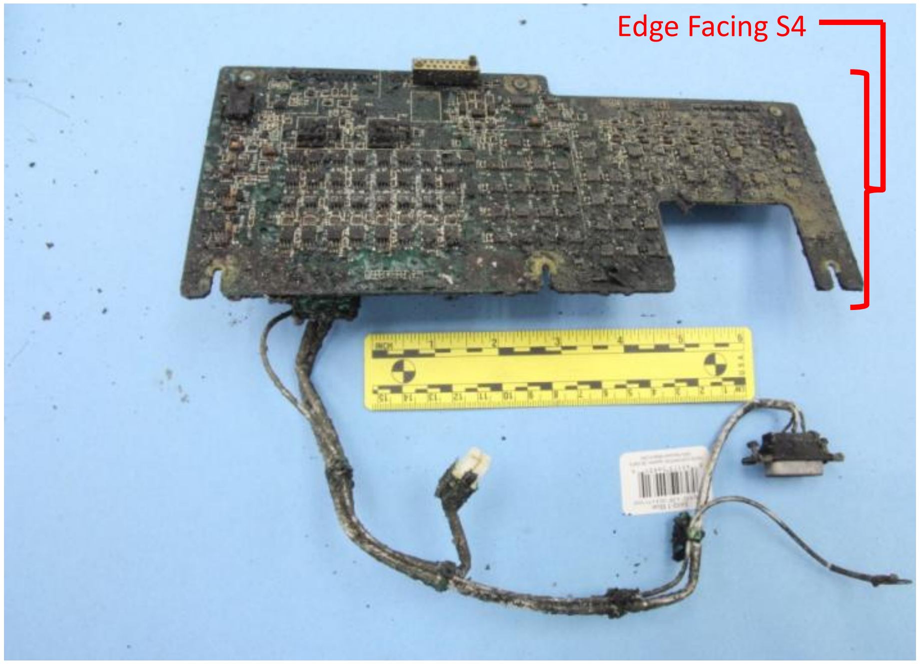

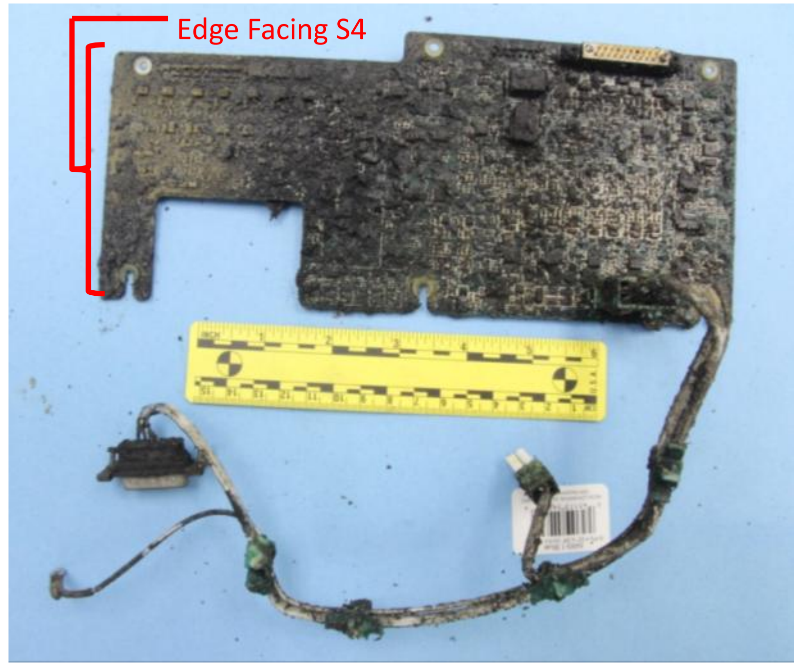

Figure 35. Sub-BMU board. The left photo shows the side facing the exterior of the battery box. The right photo shows the side facing the interior of the battery box.

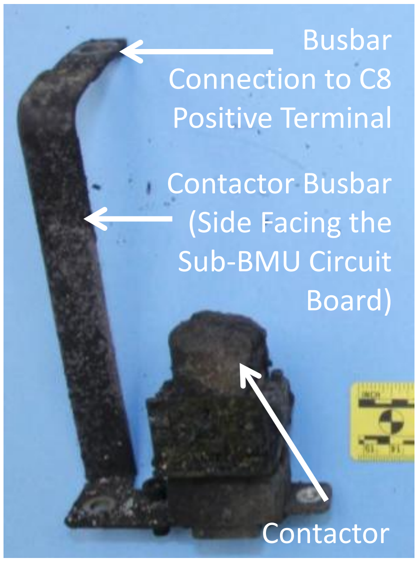

Figure 36. View of busbar from C8 positive terminal to contactor side facing sub-BMU.

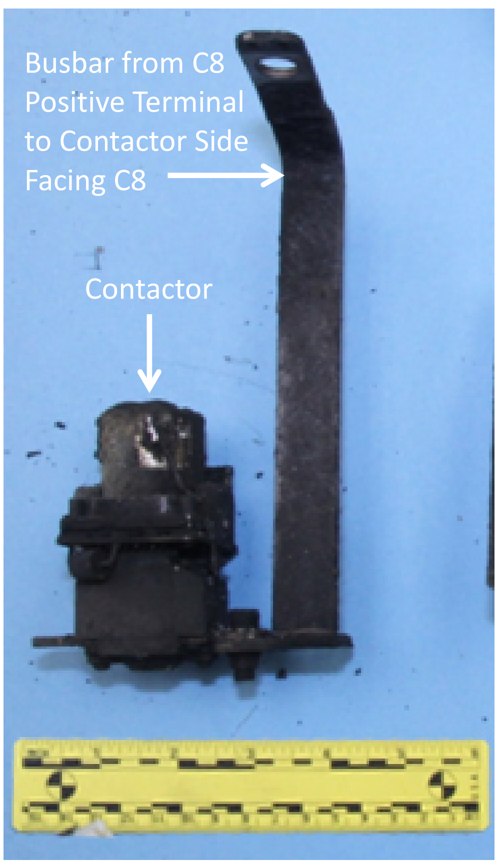

Figure 37. View of busbar from C8 positive terminal to contactor side facing C8.

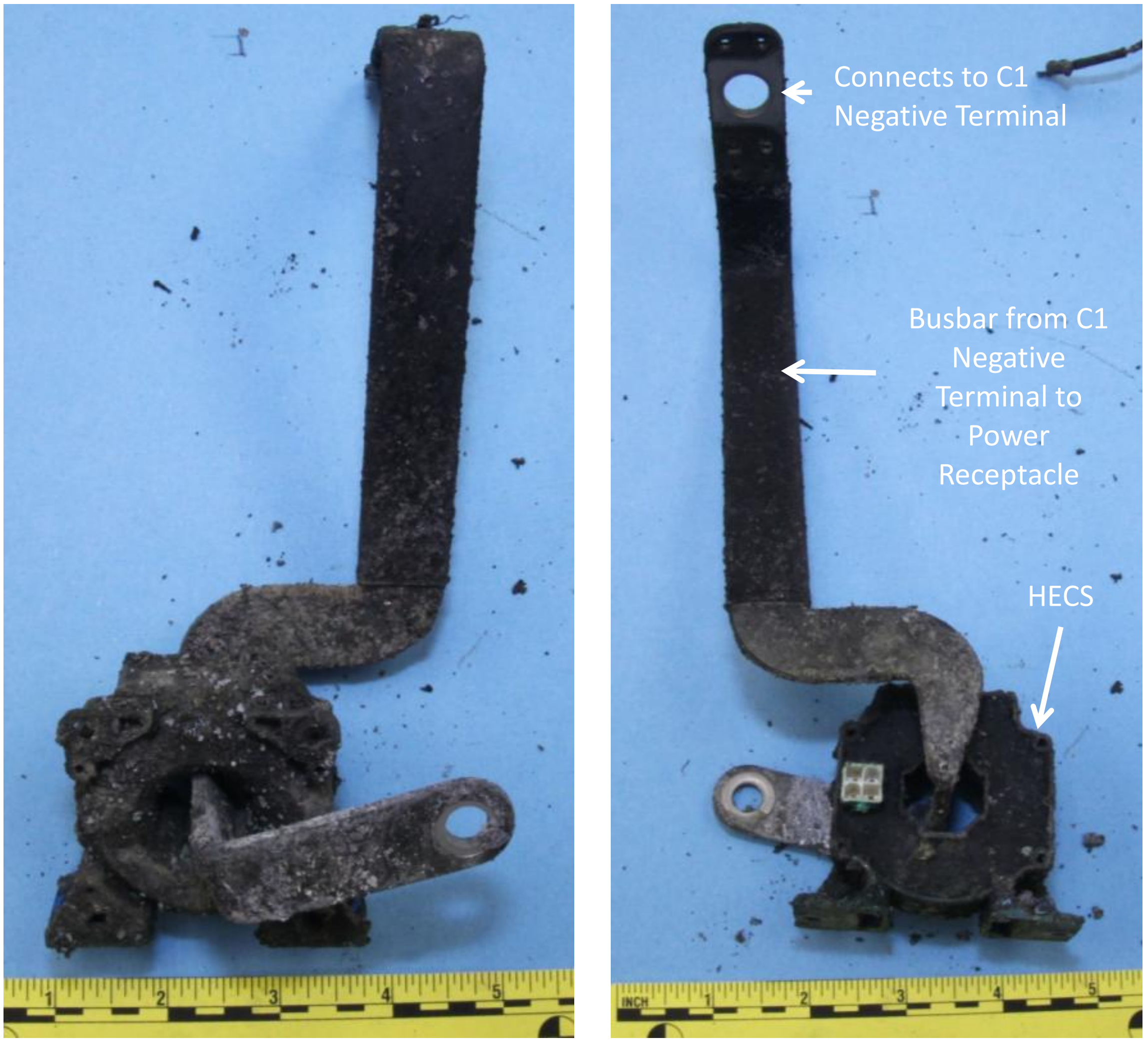

Figure 38. Busbar from C1 negative terminal to power receptacle. The photo on the left shows the side facing the sub-BMU circuit board. The photo on the right shows the side facing C1.

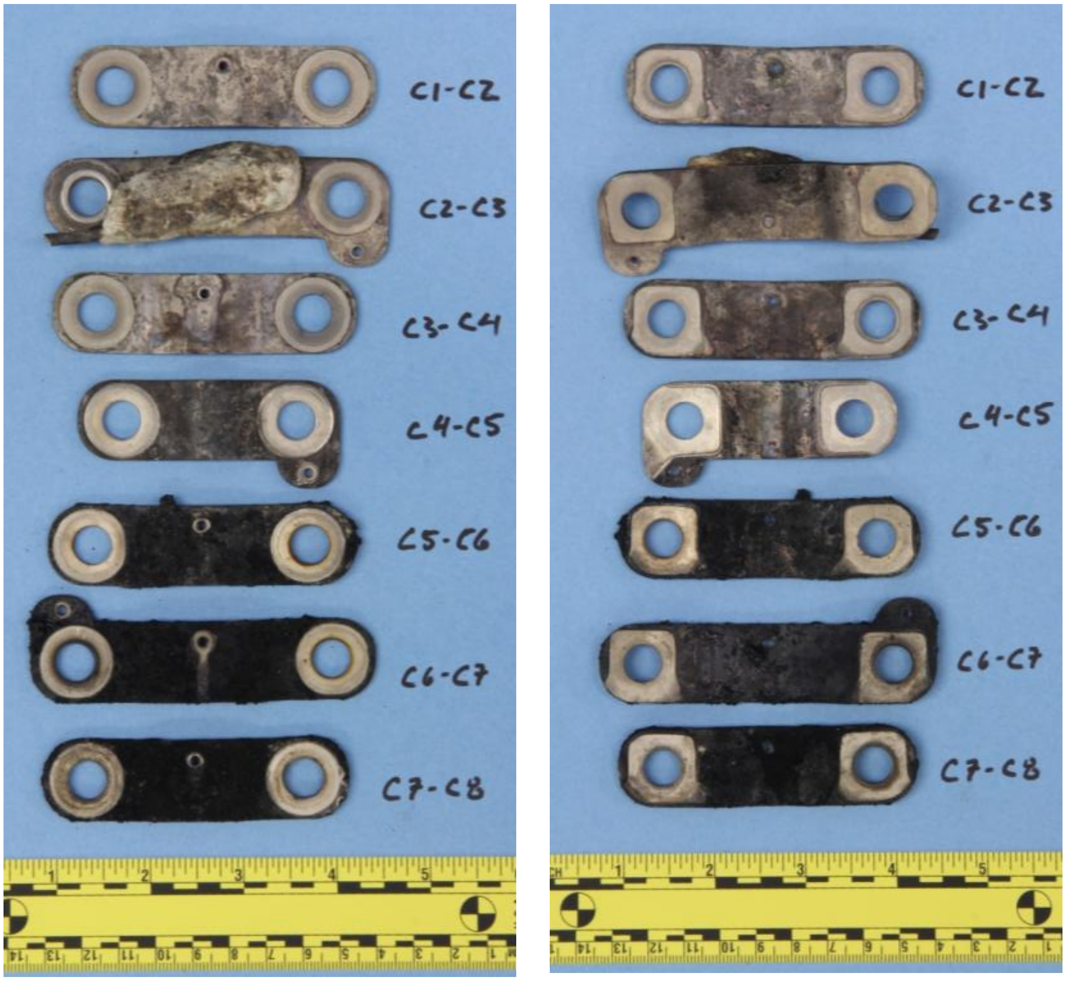

Figure 39. Views of the contact surfaces. The photo on the left shows the contact surfaces facing the washer and nut. The photo on the right shows the contact surfaces facing the battery terminal.

Figure 40. Two photos of the C1-J3 and C8-contactor busbars.

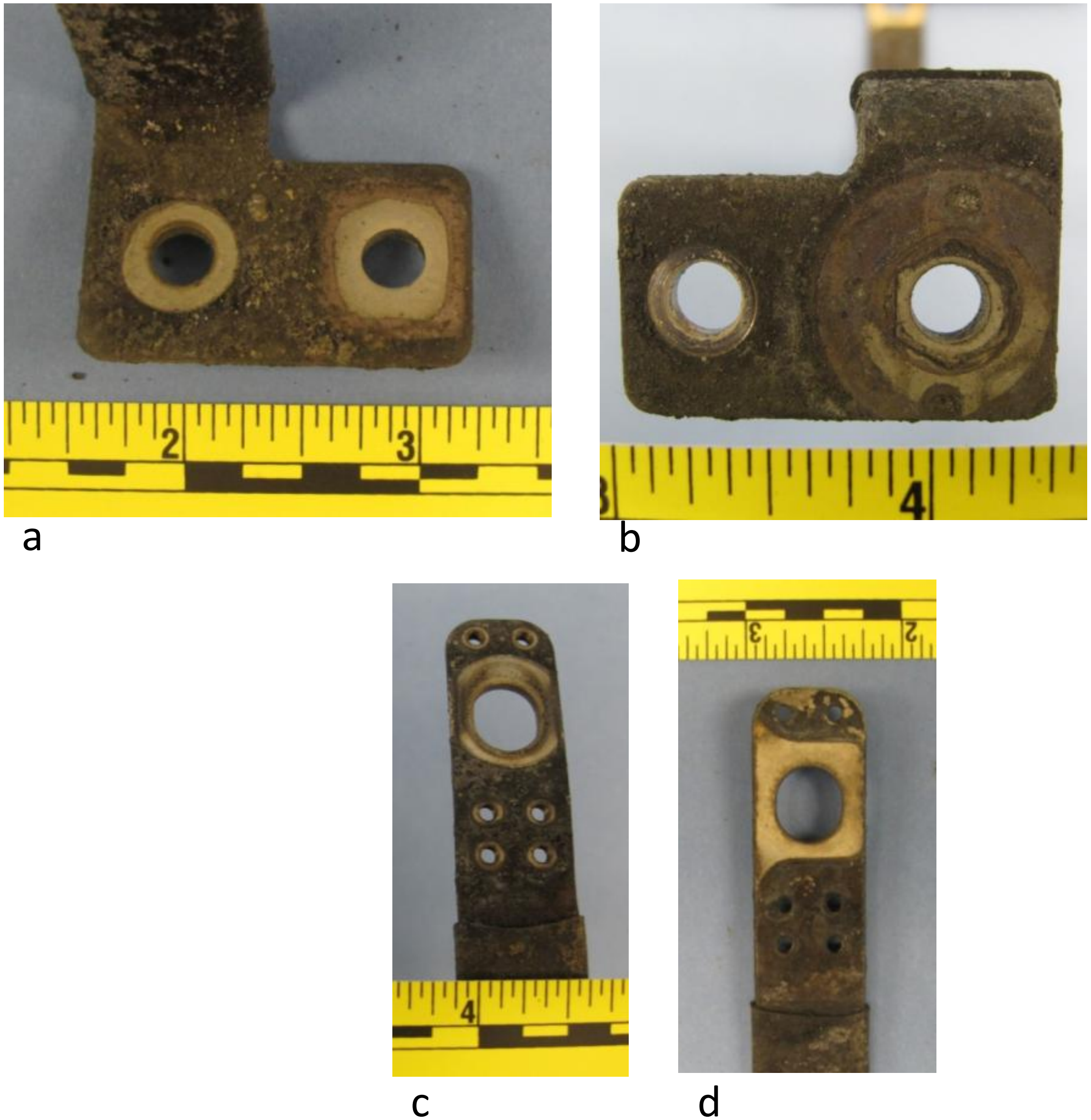

Figure 41. Connector ends of C8-contactor busbar (close-up of image shown in Figure 40).

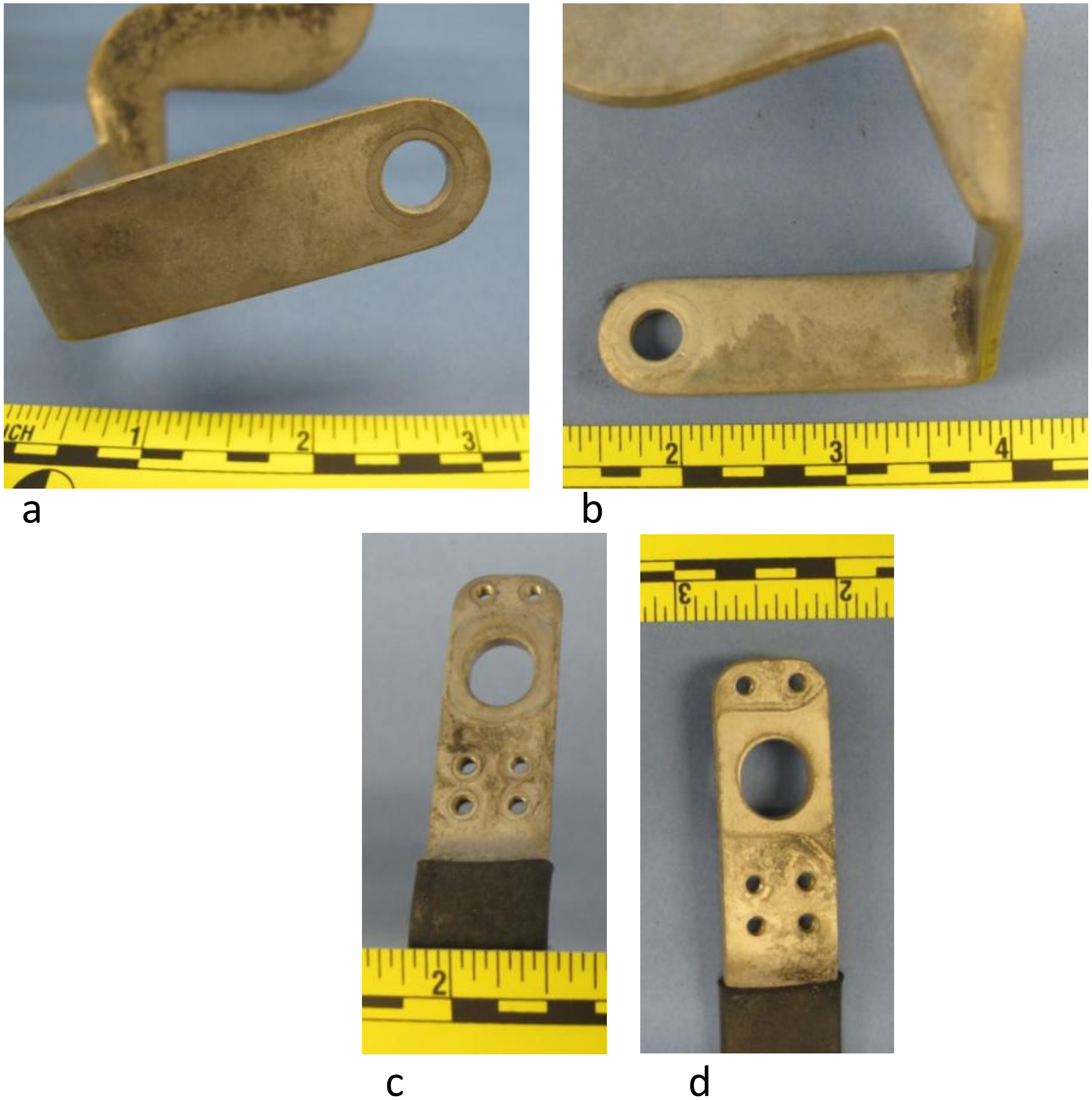

Figure 42. Four close-up views of C1-J3 busbar contact surfaces.

Figure 43. Two views of the contactor-J3 busbar.

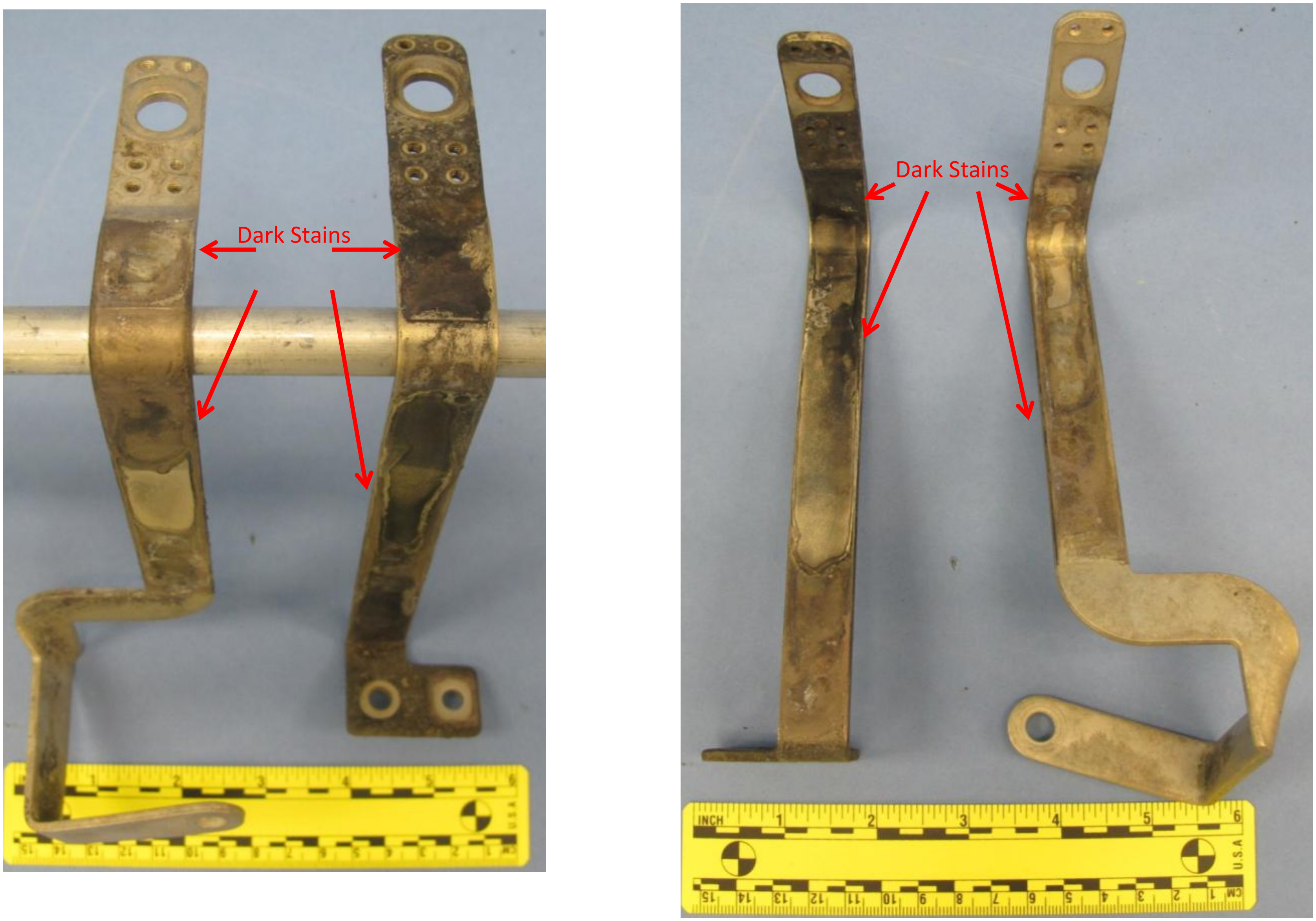

Figure 44. Two views of the C1-J3 and C8-contactor busbars.

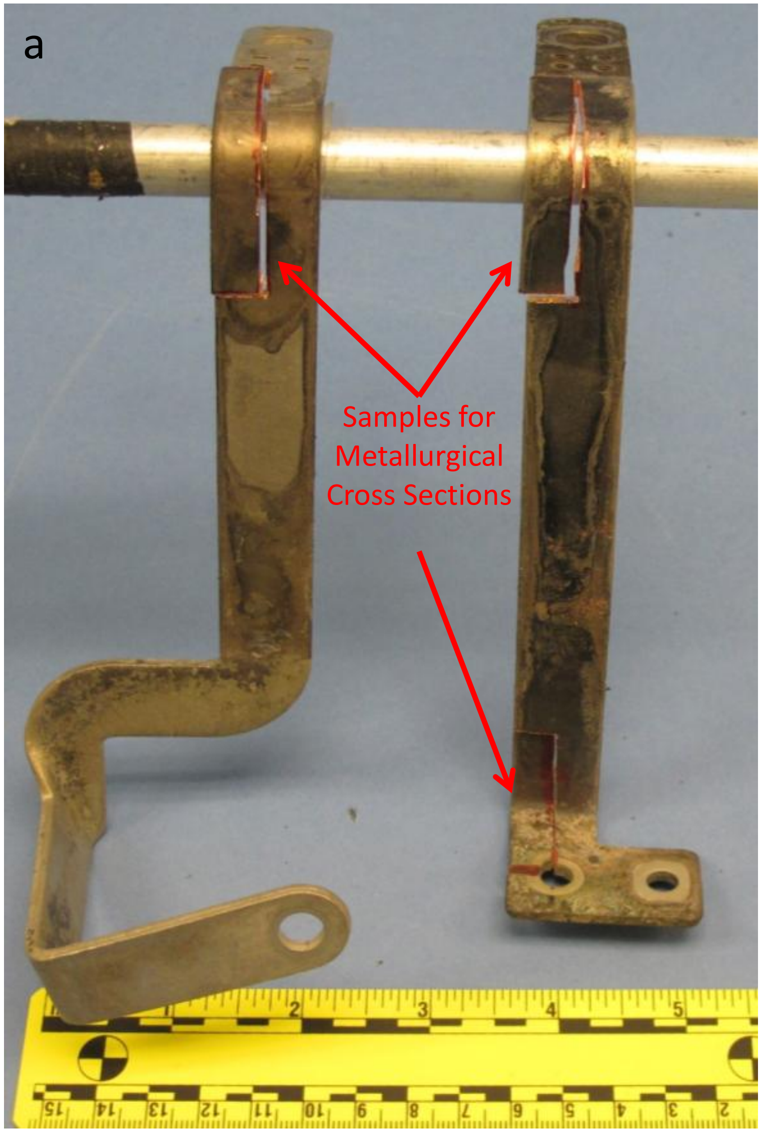

Figure 45. Sections of components from (a) C1-J3 and C8-contactor and (b) C4-C5 busbar.

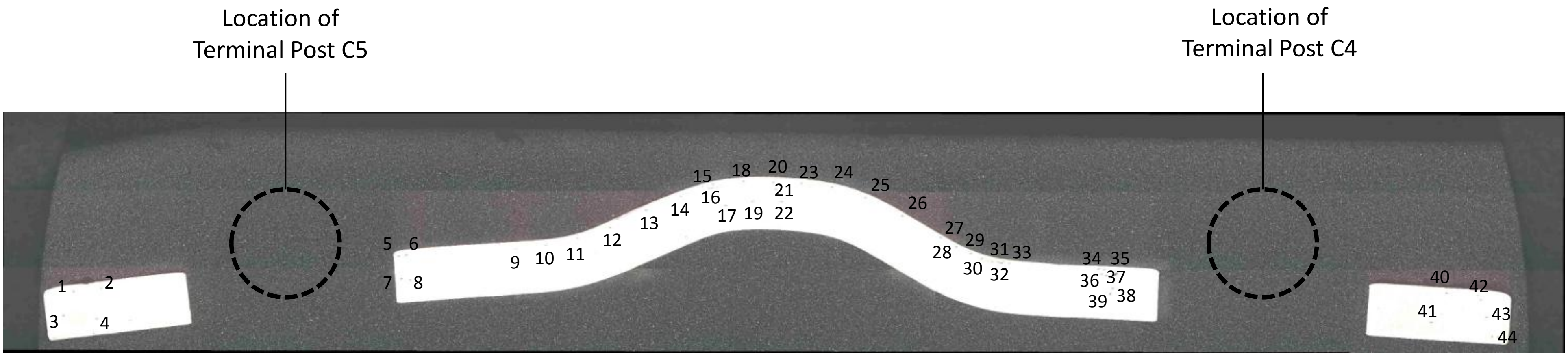

Location	Hardness (HK_{500})	Location	Hardness (HK_{500})	Location	Hardness (HK_{500})	Location	Hardness (HK_{500})
1[a]	47.4	12[a]	53.2	23[a]	51.0	34[a]	52.3
2[a]	48.3	13[a]	54.4	24[a]	53.6	35[a]	53.8
3[b]	47.3	14[a]	56.0	25[a]	54.8	36	51.5
4[b]	45.5	15[a]	62.0	26[a]	52.5	37	49.6
5[a]	48.8	16	57.4	27[a]	51.6	38[b]	44.5
6[a]	49.7	17[b]	48.2	28[b]	51.8	39[b]	46.8
7[b]	45.5	18[a]	53.0	29[a]	52.5	40[a]	50.5
8[b]	48.0	19[b]	47.1	30[b]	52.6	41[b]	47.6
9[a]	58.5	20[a]	54.8	31[a]	52.6	42[a]	60.4
10[a]	57.6	21	54.8	32[b]	52.9	43[b]	50.4
11[a]	55.0	22[b]	49.9	33[a]	56.3	44[b]	51.9

a. Indentation approximately 0.01 inch from outer surface.
b. Indentation approximately along centerline.

Figure 46. Microhardness indentation locations of C4-C5 busbar.

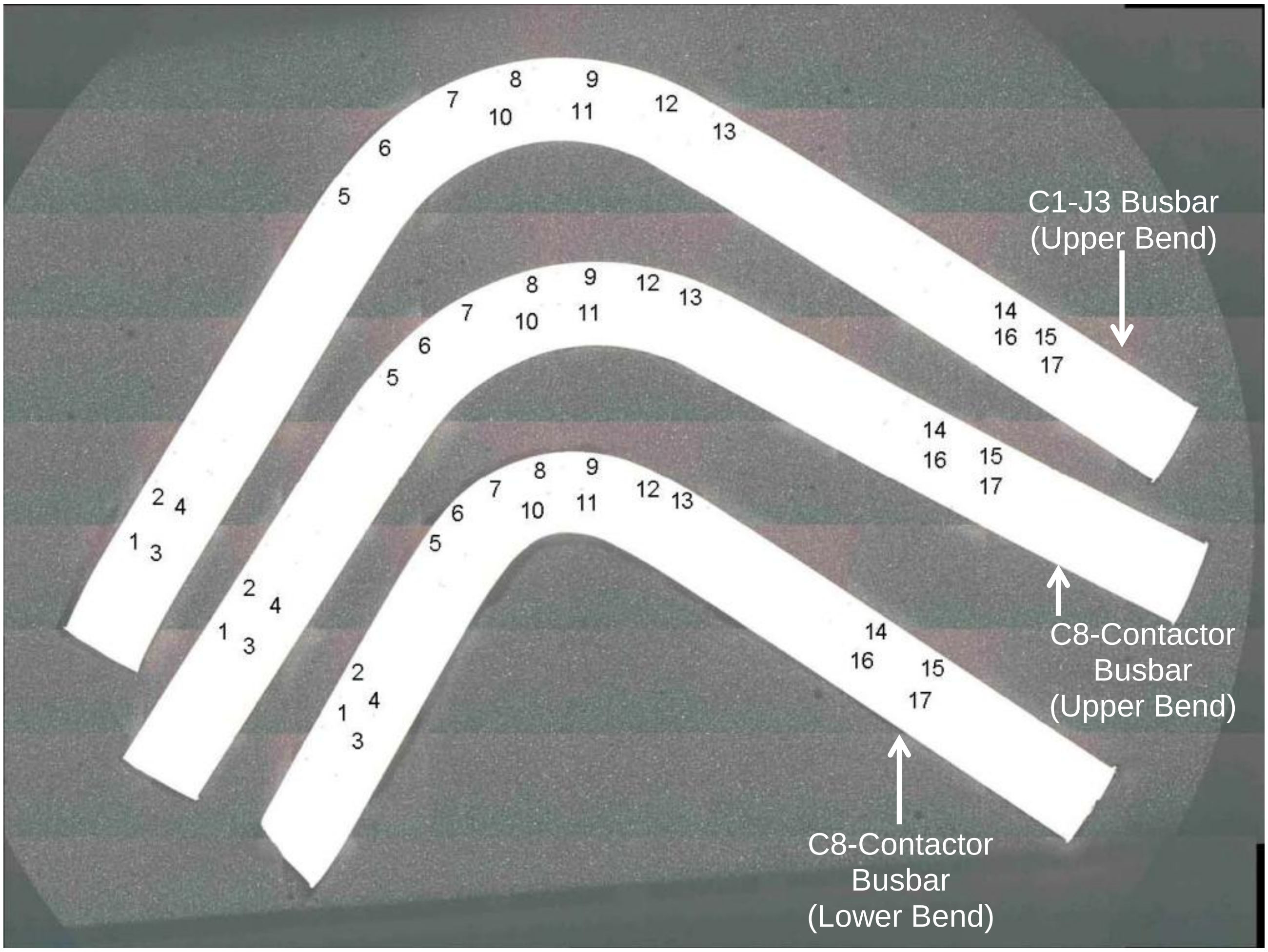

	Hardness (HK_{500})		
Location	C1-J3 Busbar (Upper Bend)	C8-Contactor Busbar (Upper Bend)	C8-Contactor Busbar (Lower Bend)
1[a]	53.6	57.4	53.9
2[a]	54.6	58.8	55.0
3[b]	52.2	56.0	54.8
4[b]	52.8	55.2	54.2
5[a]	54.6	53.2	59.8
6[a]	53.8	56.4	60.3
7[a]	52.0	53.2	59.8
8[a]	51.0	55.8	56.5
9[a]	53.0	59.2	57.7
10[b]	54.4	58.5	53.0
11[b]	57.2	54.7	53.5
12[a]	56.4	54.4	58.1
13[a]	53.6	56.6	57.6
14[a]	55.4	56.6	56.4
15[a]	53.7	55.9	56.2
16[b]	54.8	56.8	56.6
17[b]	54.8	55.5	56.1

a. Indentation approximately 0.01 inch from outer surface.
b. Indentation approximately along centerline.

Figure 47. Microhardness indentation locations of the C1 J3 and C8 contactor busbars.

Figure 48. S3 of the exterior of the battery box. The highlighted area shows the small protrusion on the lower left side. This area is magnified in Figure 49.

Figure 49. The protrusion from the exterior of S3 of the battery box, as received.

Figure 50. Close-up view of the protrusion on the battery box exterior, as received (~200X).

Figure 51. Close-up view of the protrusion on the battery box interior, as received (~200X).

Figure 52. The protrusion on the exterior of the battery box, after cleaning (~50X).

Figure 53. The protrusion on the exterior of the battery box, after cleaning (~200X). The largest holes (arrows) are labeled and exhibit a light-blue color from the backing paper used during photographing.

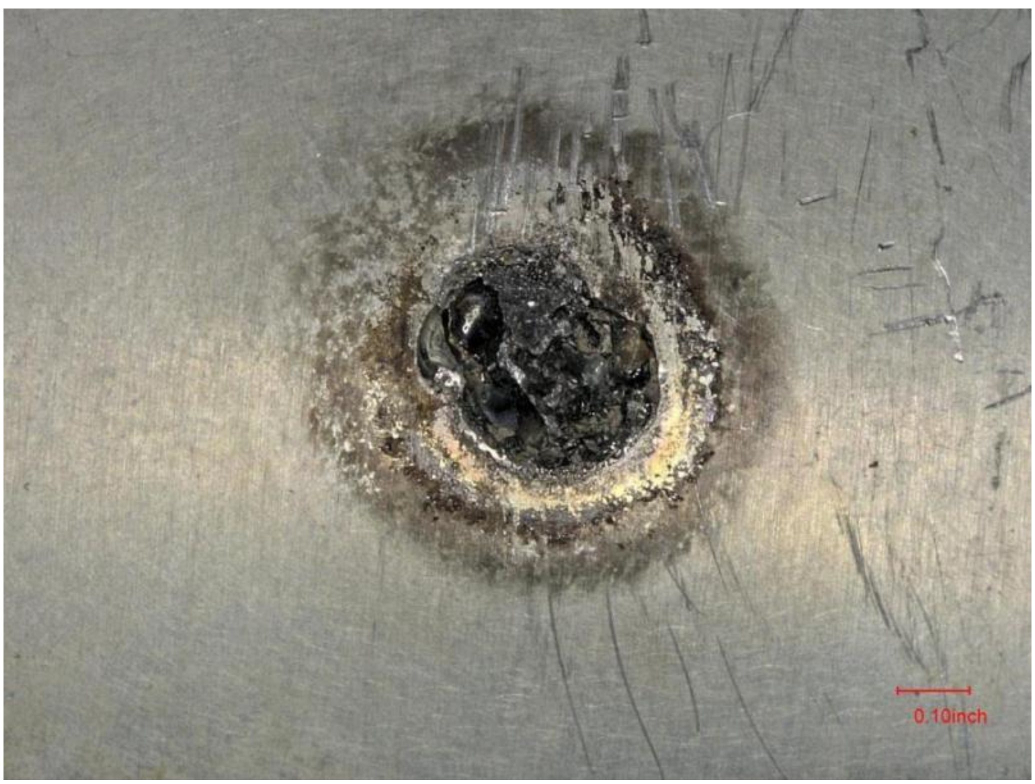

Figure 54. The protrusion on the interior of the battery box, after cleaning (~200X).

Figure 55. The protrusion on the interior of the battery box, after cleaning (~200X). The largest holes (arrows) are labeled and exhibit a light-blue color from the backing paper used during photographing.

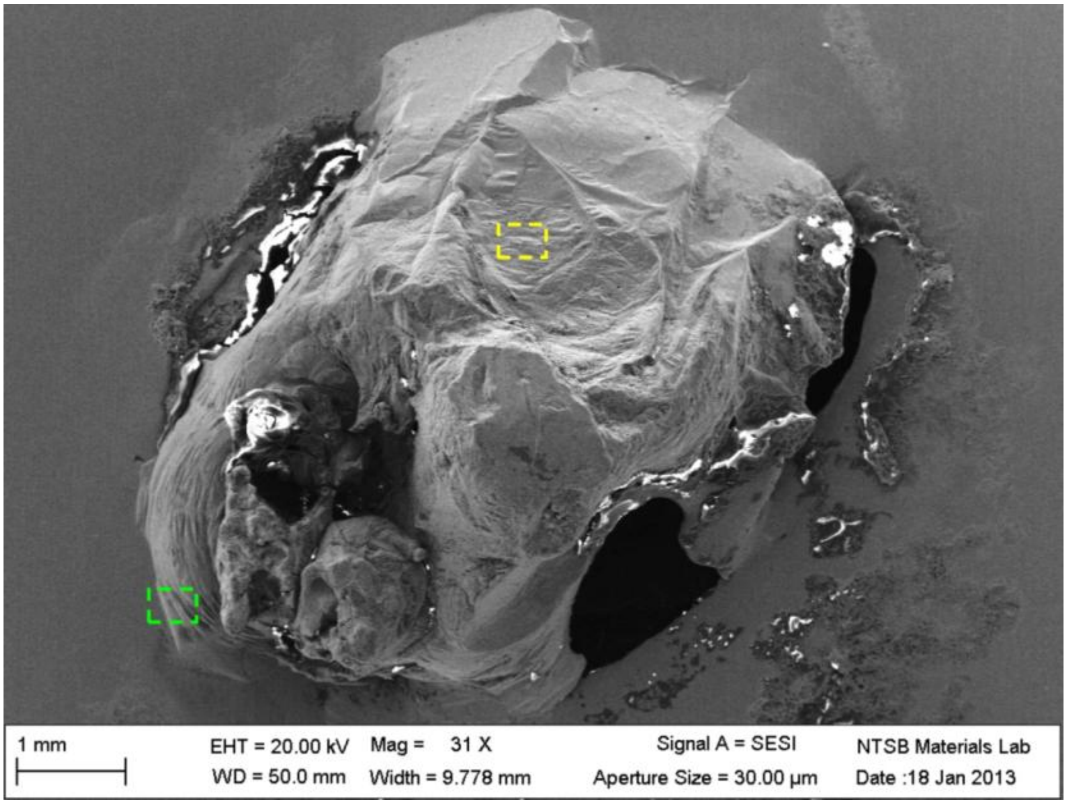

Figure 56. SEM micrograph of the protrusion from the exterior. The yellow boxed area is highlighted in Figure 57, and the green boxed area is highlighted in Figure 58.

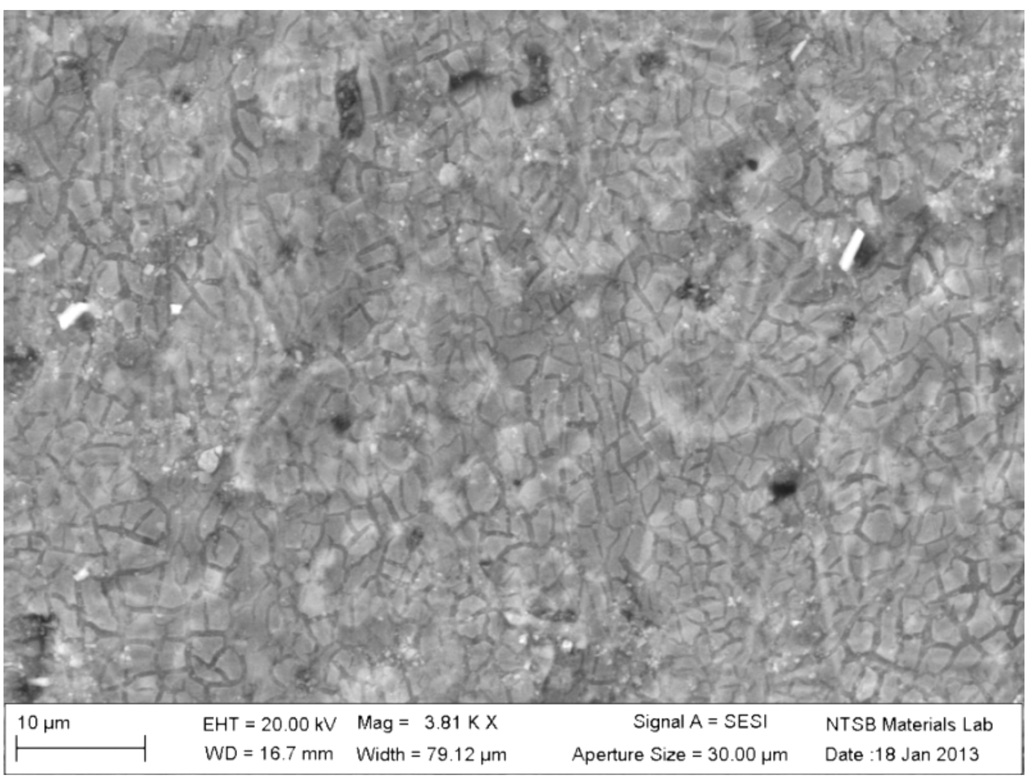

Figure 57. SEM micrograph of the boxed area in Figure 56. The pattern is consistent with a fractured surface aluminum oxide layer that forms on aluminum alloys as it solidifies and cools.

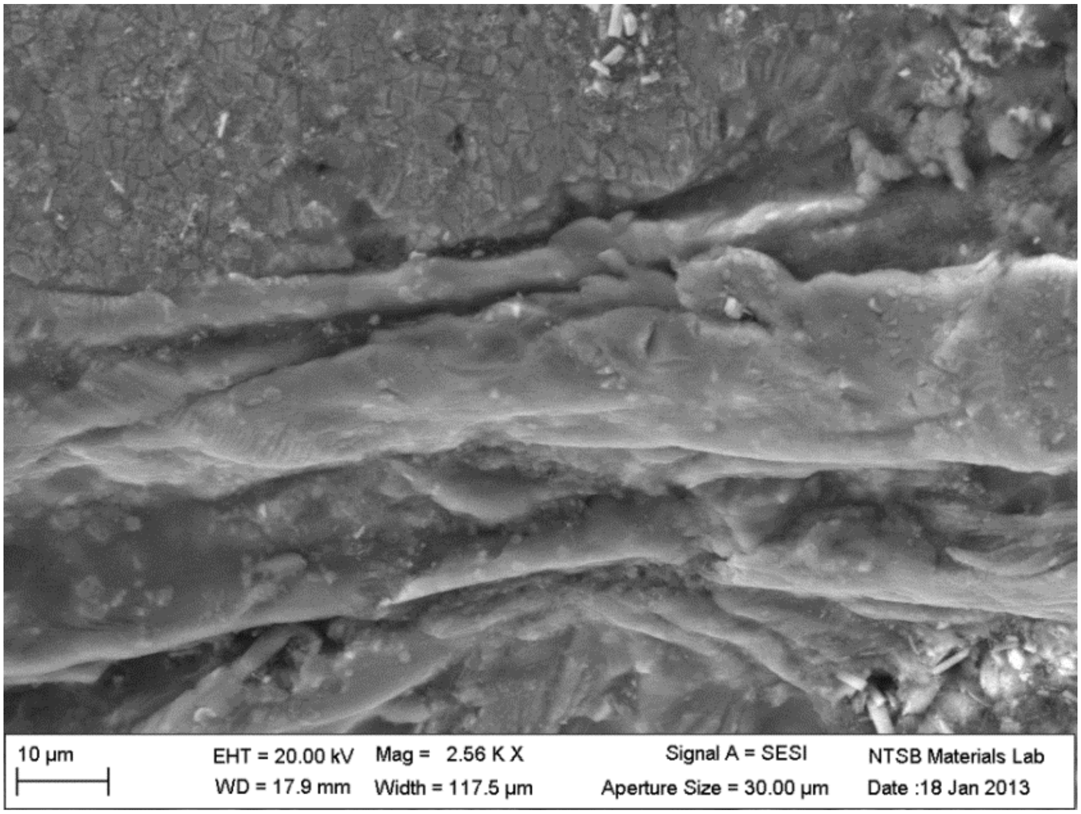

Figure 58. SEM micrograph of the boxed area in Figure 56. The reticulated morphology of the base of the protrusion is typical of contracting experienced by metals during solidification.

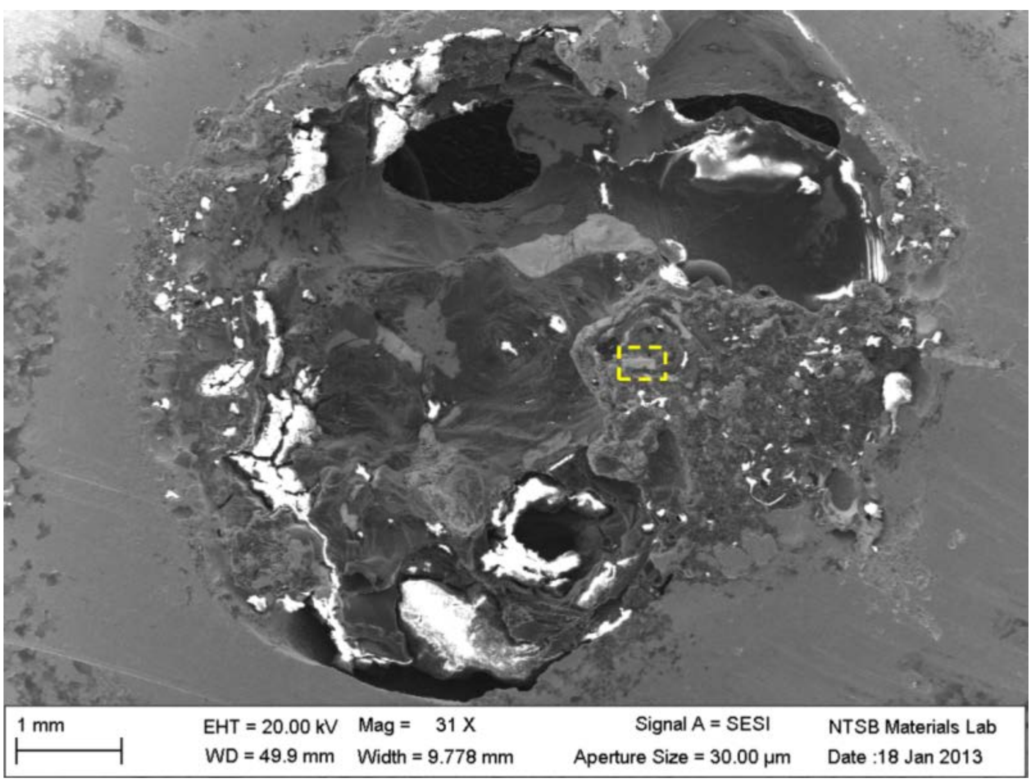

Figure 59. SEM micrograph of the protrusion from the interior. The boxed area is highlighted in Figure 60.

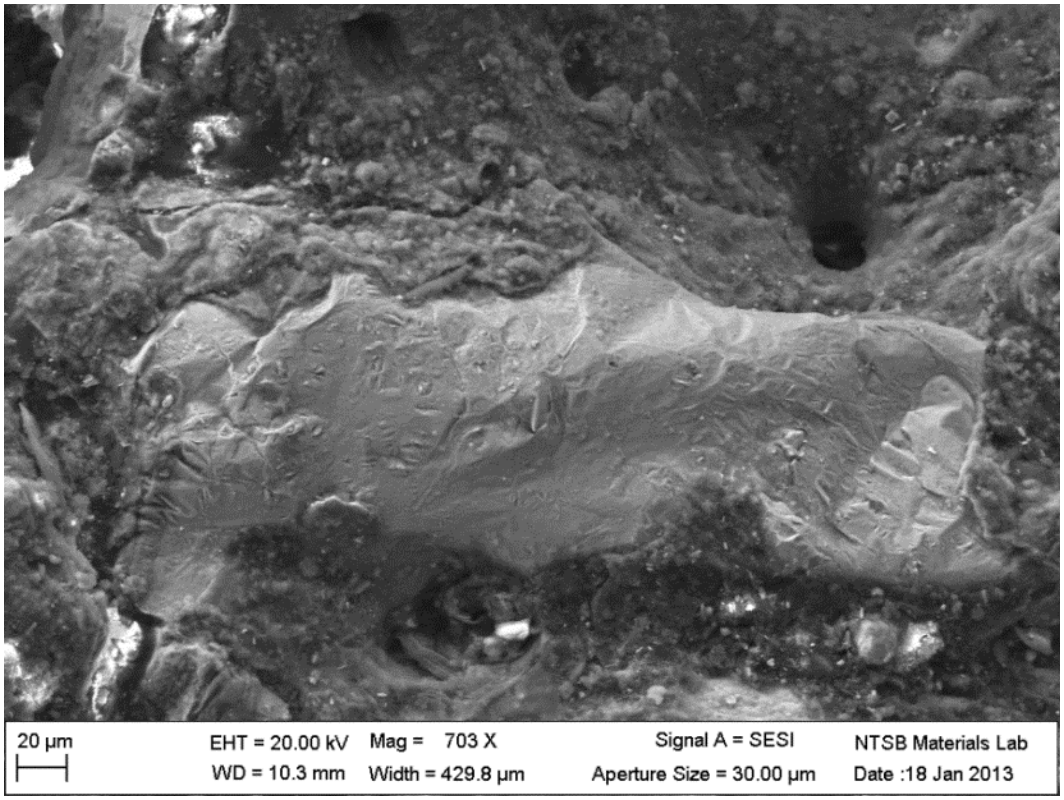

Figure 60. SEM micrograph of an embedded iron-based compound, showing reticulation consistent with solidification.

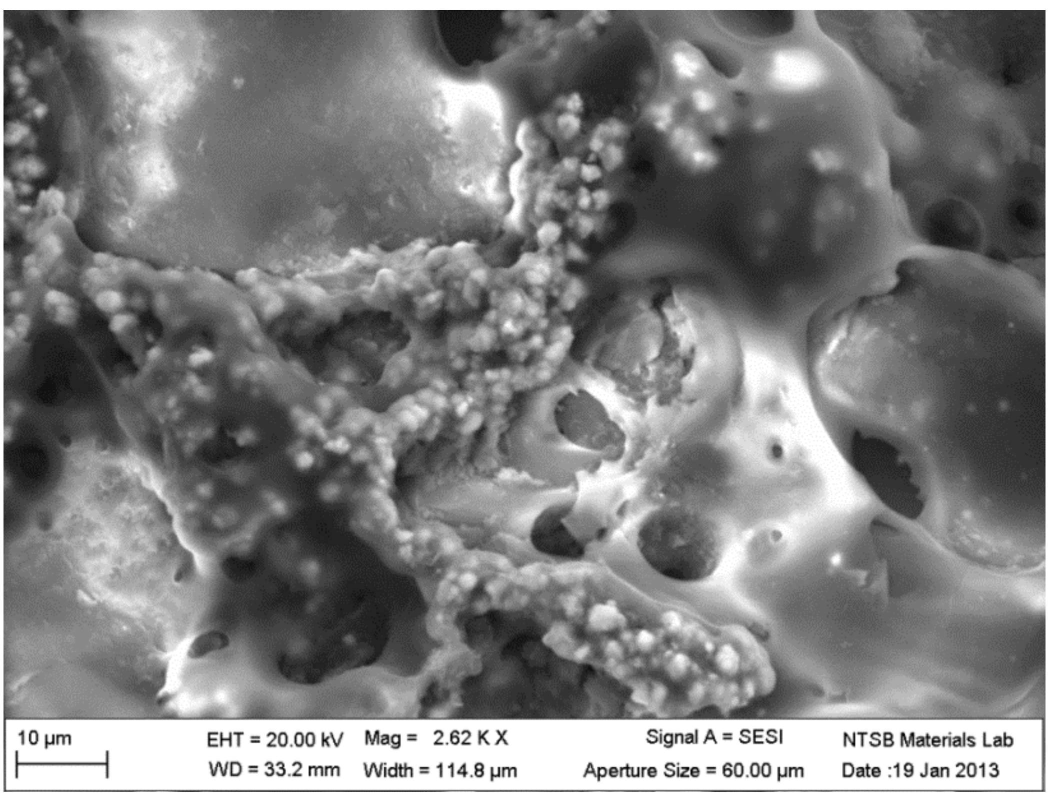

Figure 61. SEM micrograph of cobalt-based oxide particles embedded in carbon-rich decomposition products near the defect.

Figure 62. The cell case of C5, facing the interior of S3 of the battery box. Four areas were found that exhibited heavy decomposition deposits about a round hole—these areas are labeled 1 through 4 (circles).

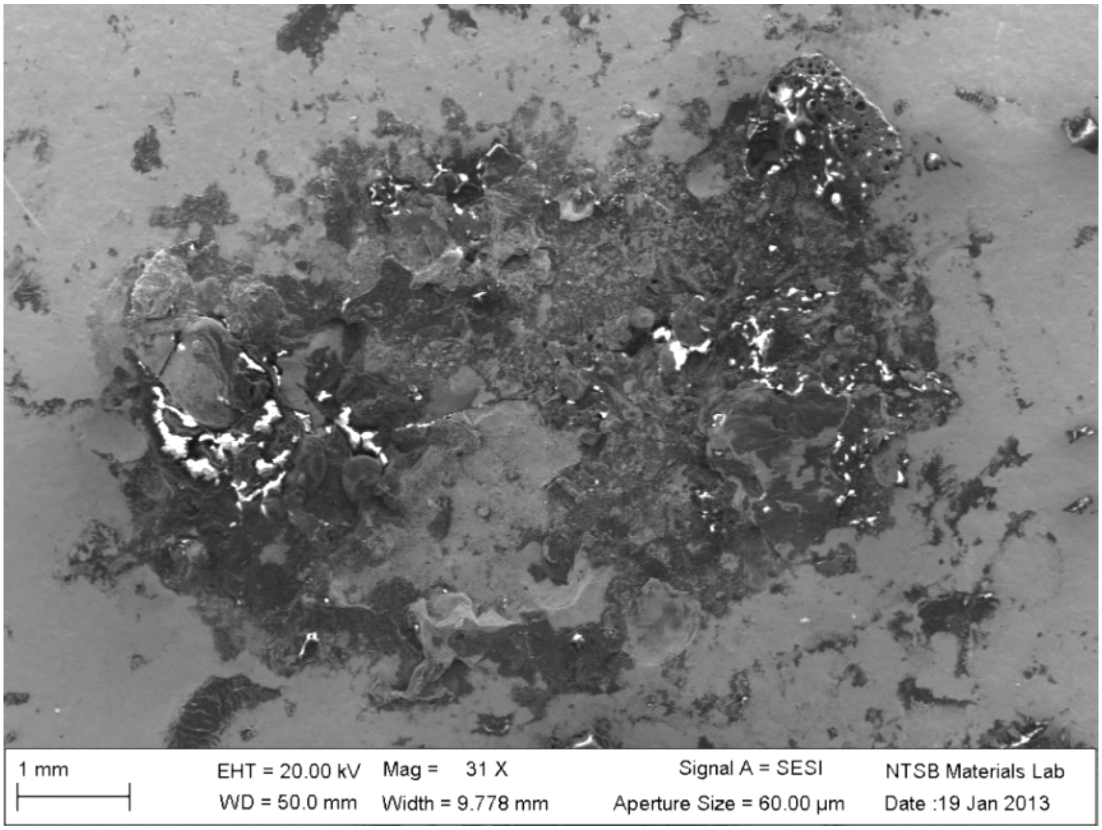

Figure 63. SEM micrograph of the hole 1 on the C5 cell case, from the exterior.

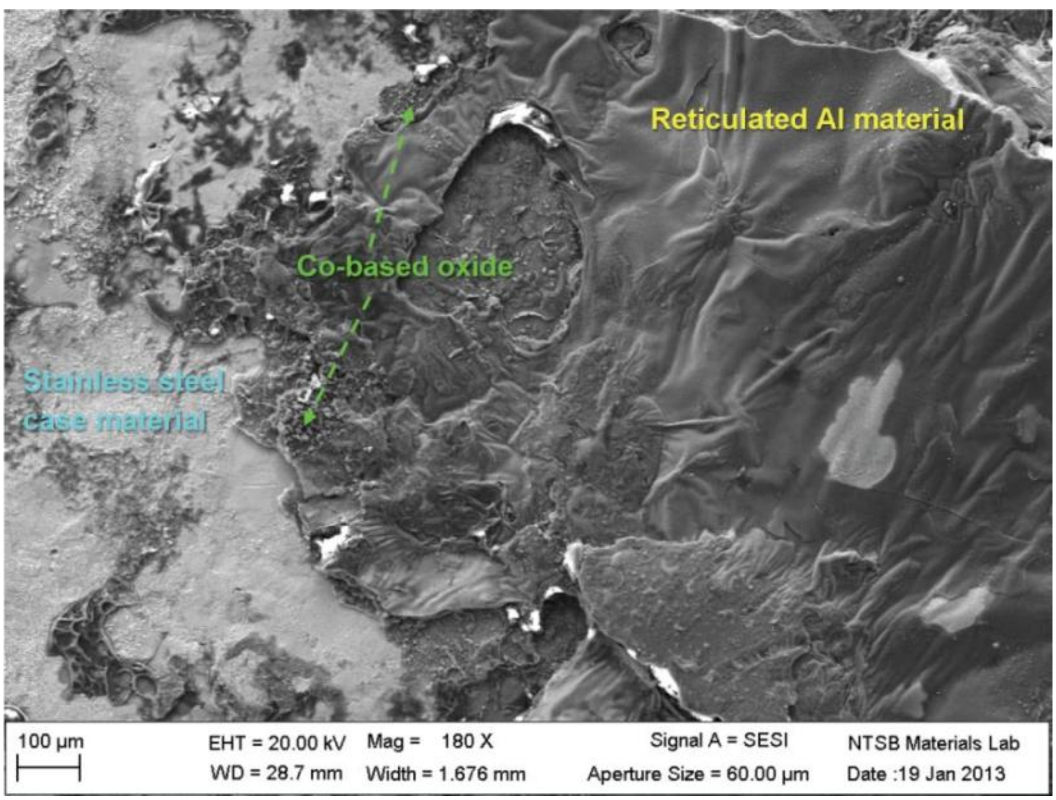

Figure 64. SEM micrograph of reticulated aluminum (dark) on the stainless steel case material (light) from the exterior of hole 1.

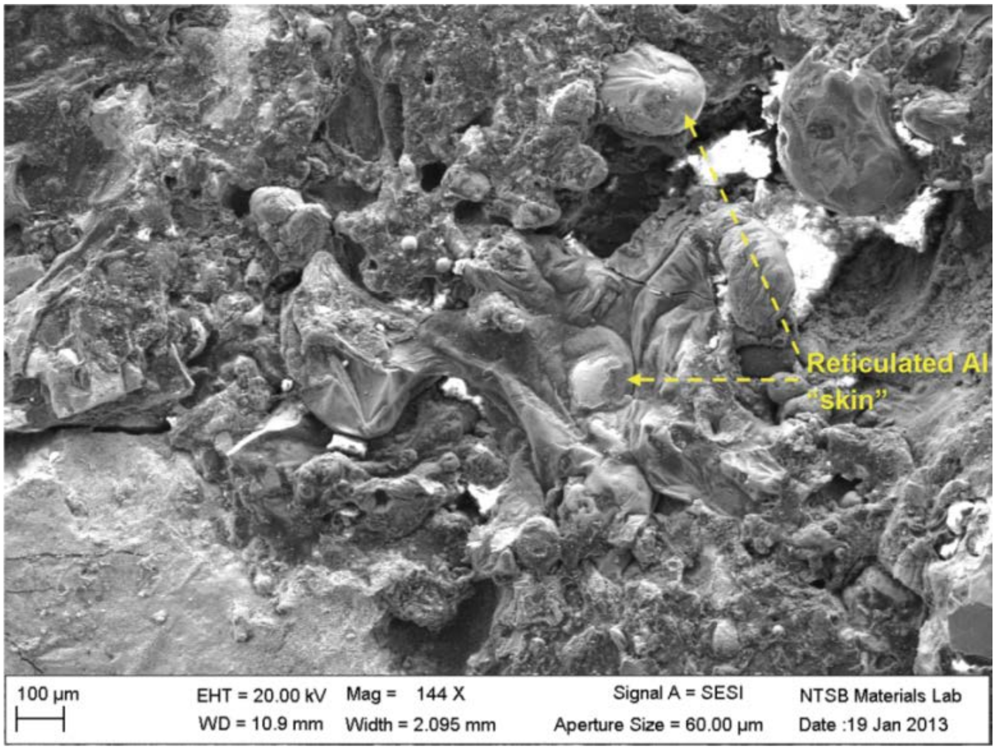

Figure 65. SEM micrograph of hole 1 from the exterior of the C5 cell case. This region exhibited rounded protrusions consistent with resolidified steel encompassed by an external layer of aluminum alloy.

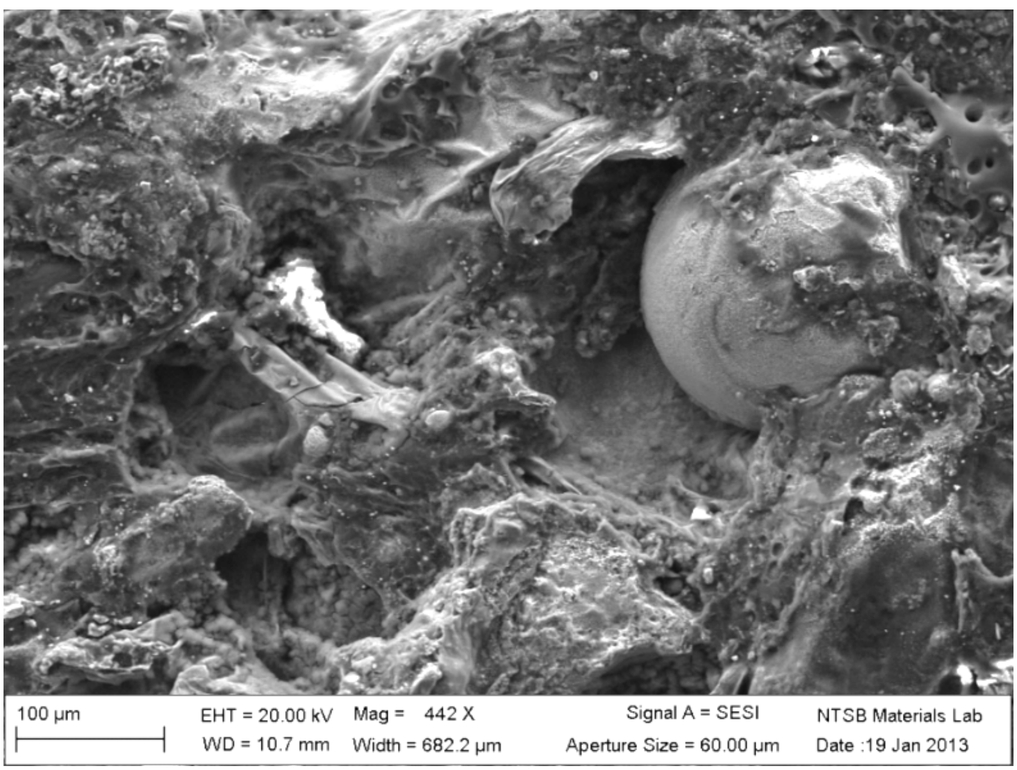

Figure 66. SEM micrograph of steel sphere embedded in combustion products in the interior of hole 1 on the C5 cell case.

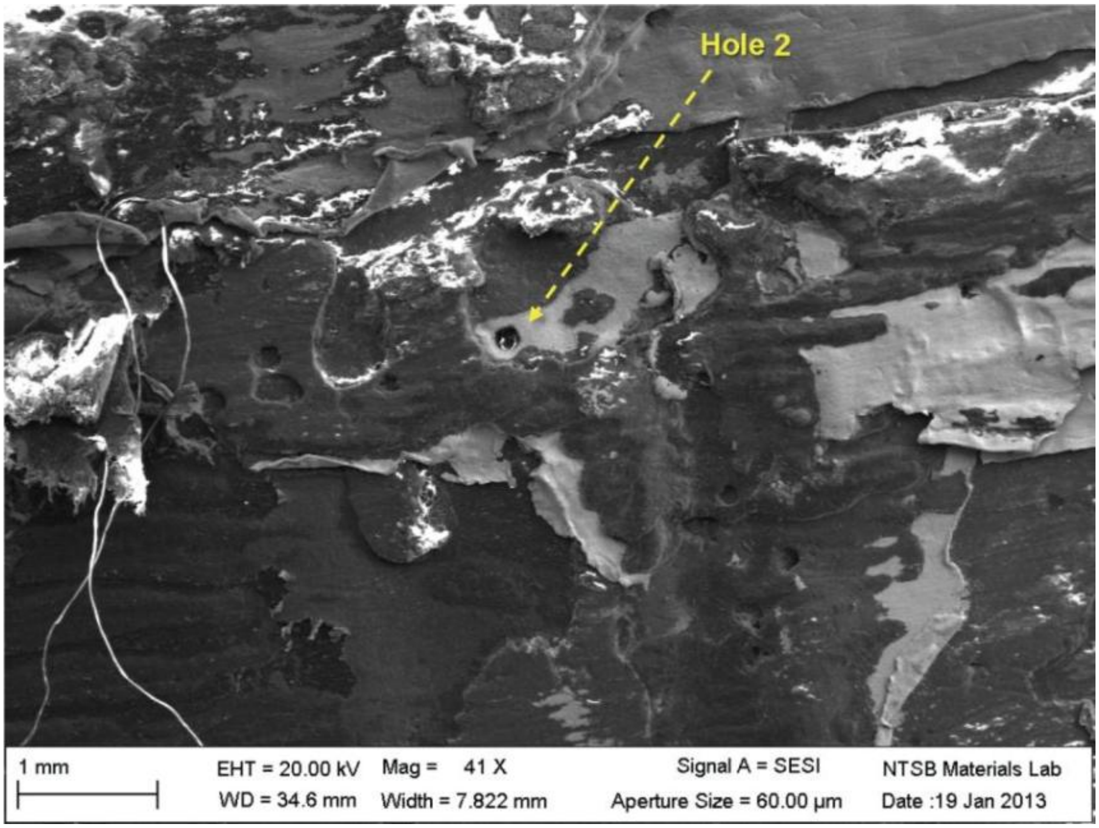

Figure 67. SEM micrograph of hole 2, from the interior of the C5 cell case.

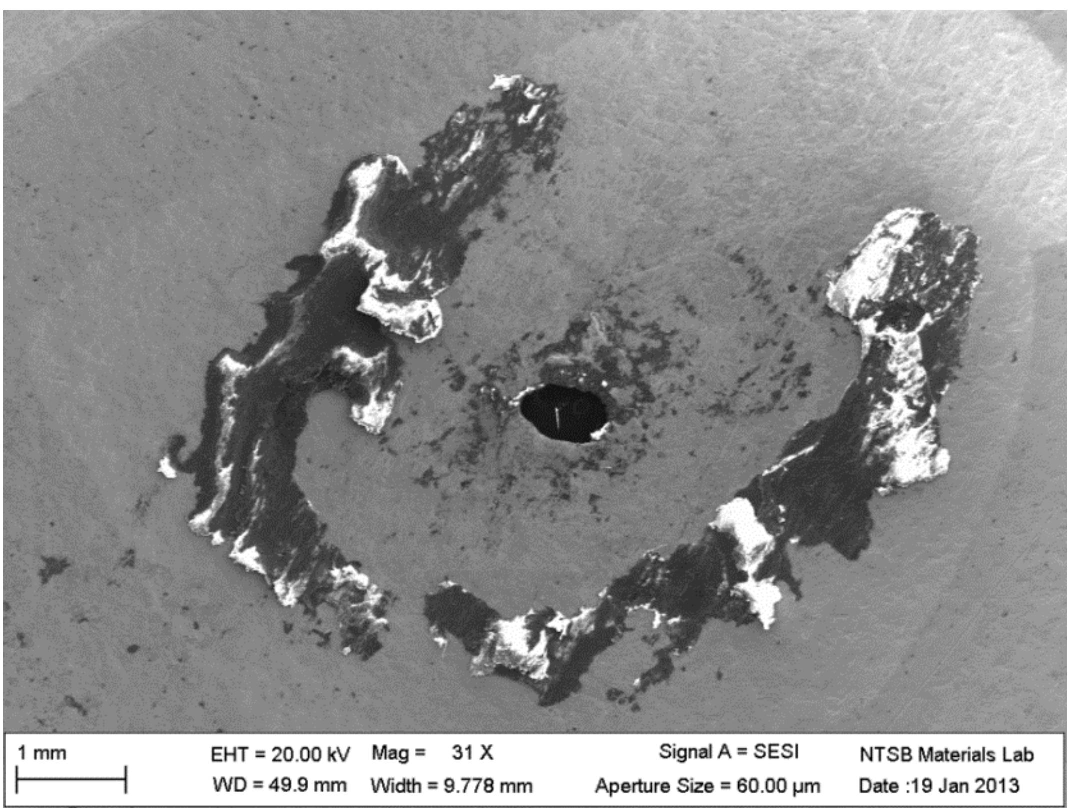

Figure 68. SEM micrograph of hole 3, from the interior of the C5 cell case.

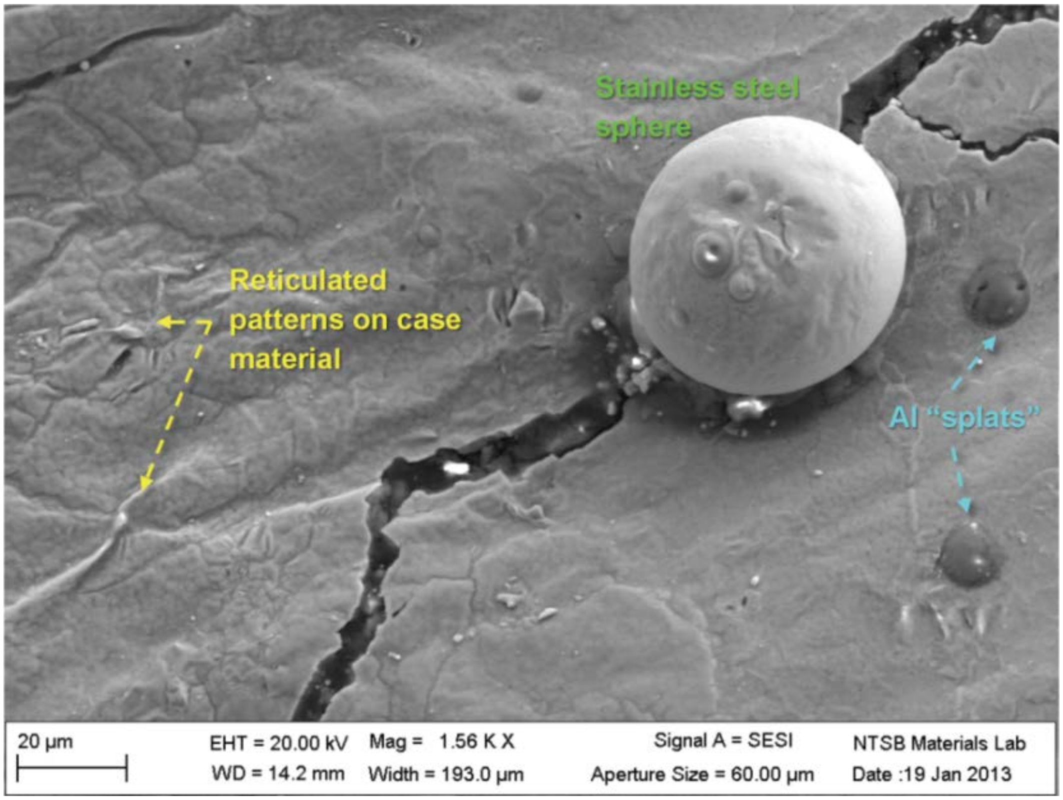

Figure 69. SEM micrograph of a spherical particle of stainless steel found near the exterior side of hole 3.

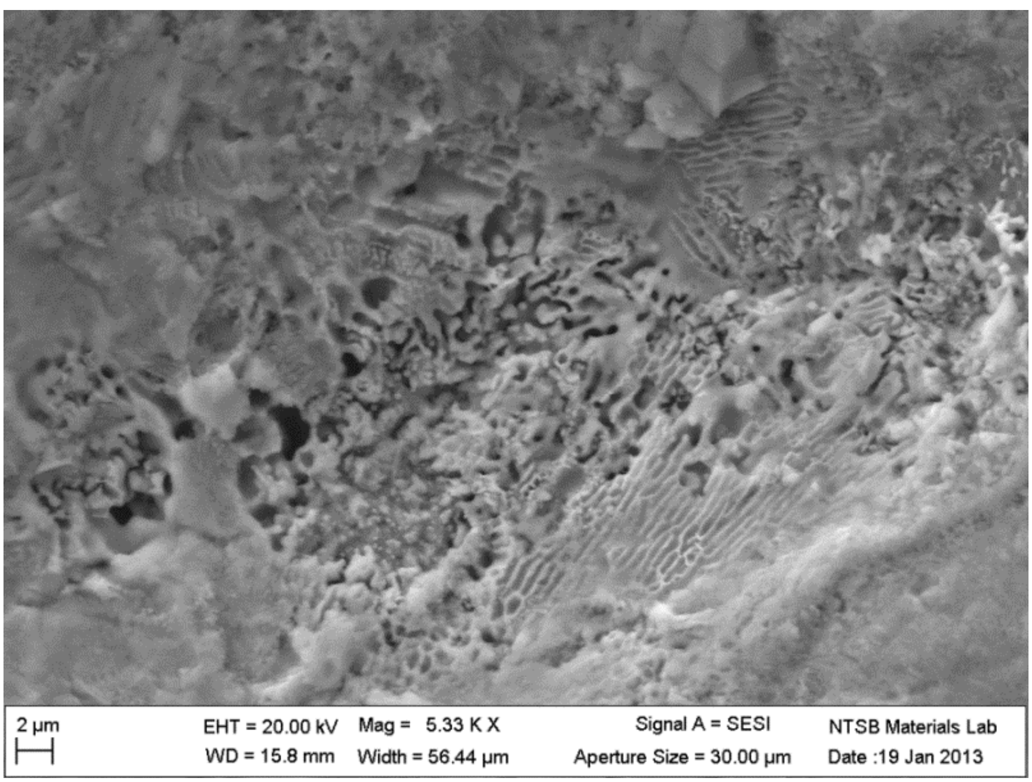

Figure 70. SEM micrograph of lamellar structure consistent with incipient melting near the exterior of hole 4.

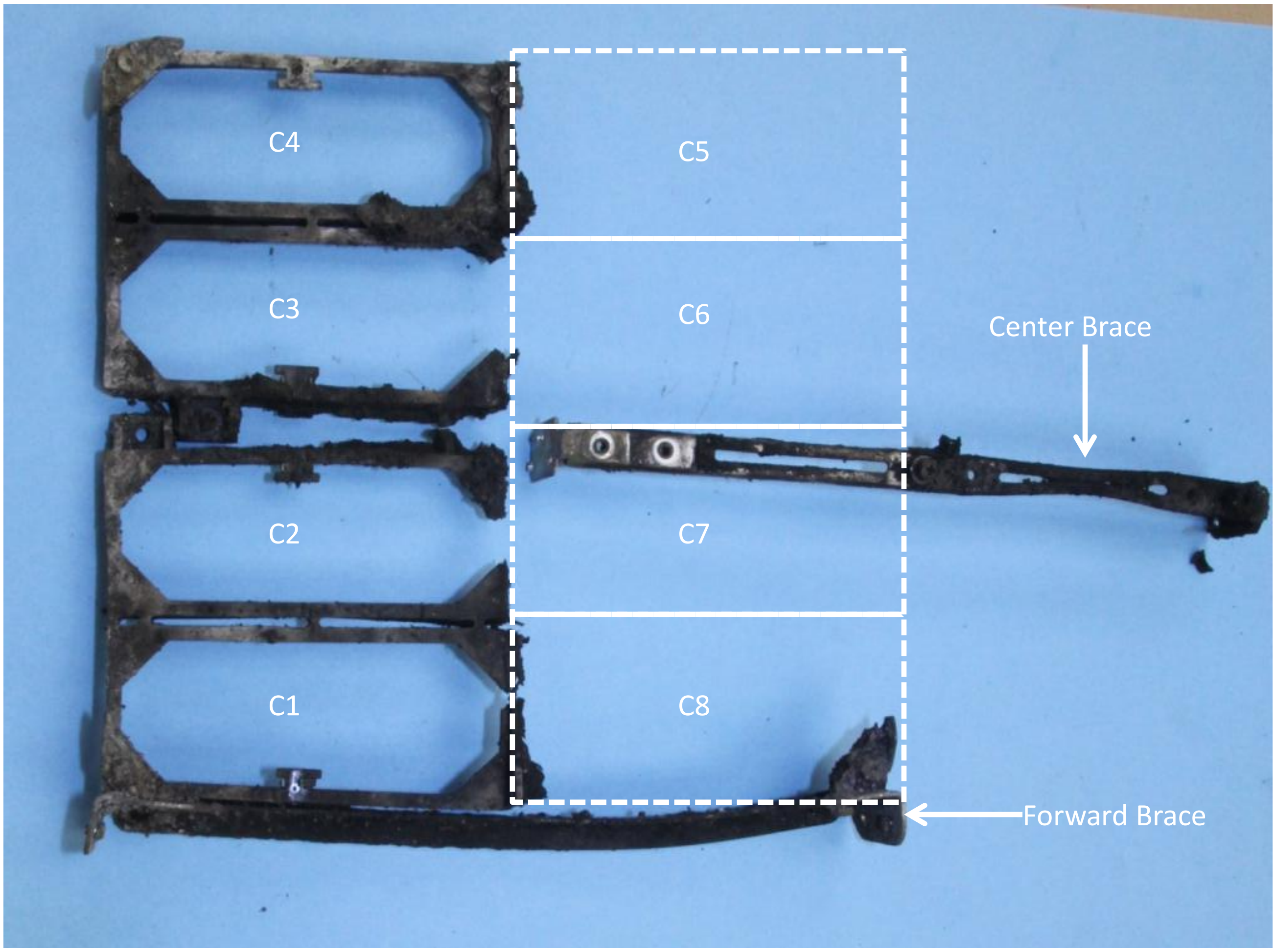

Figure 71. Upper fixation tray and center and forward braces, as removed.

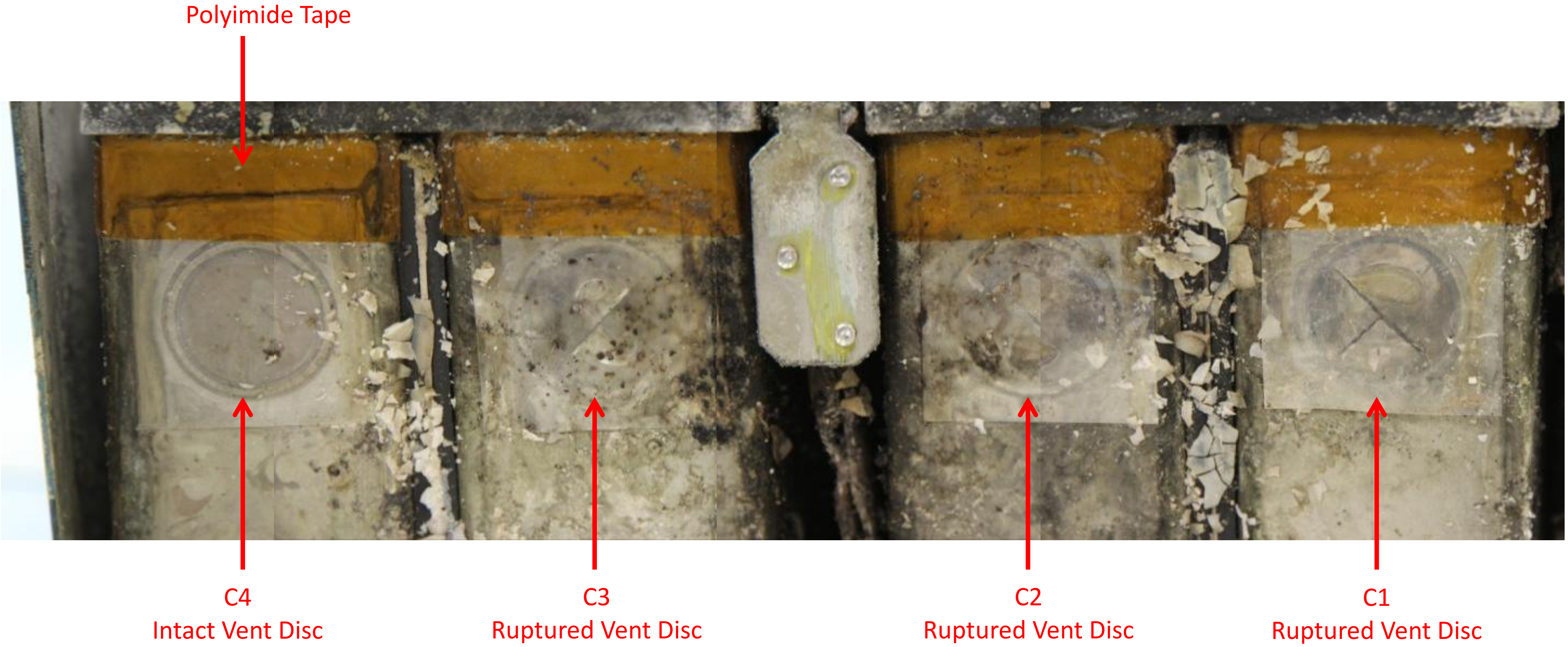

Figure 72. Composite image showing a closer view of the vent discs on C1 through C4.

Figure 73. C1 removed (viewed from S2).

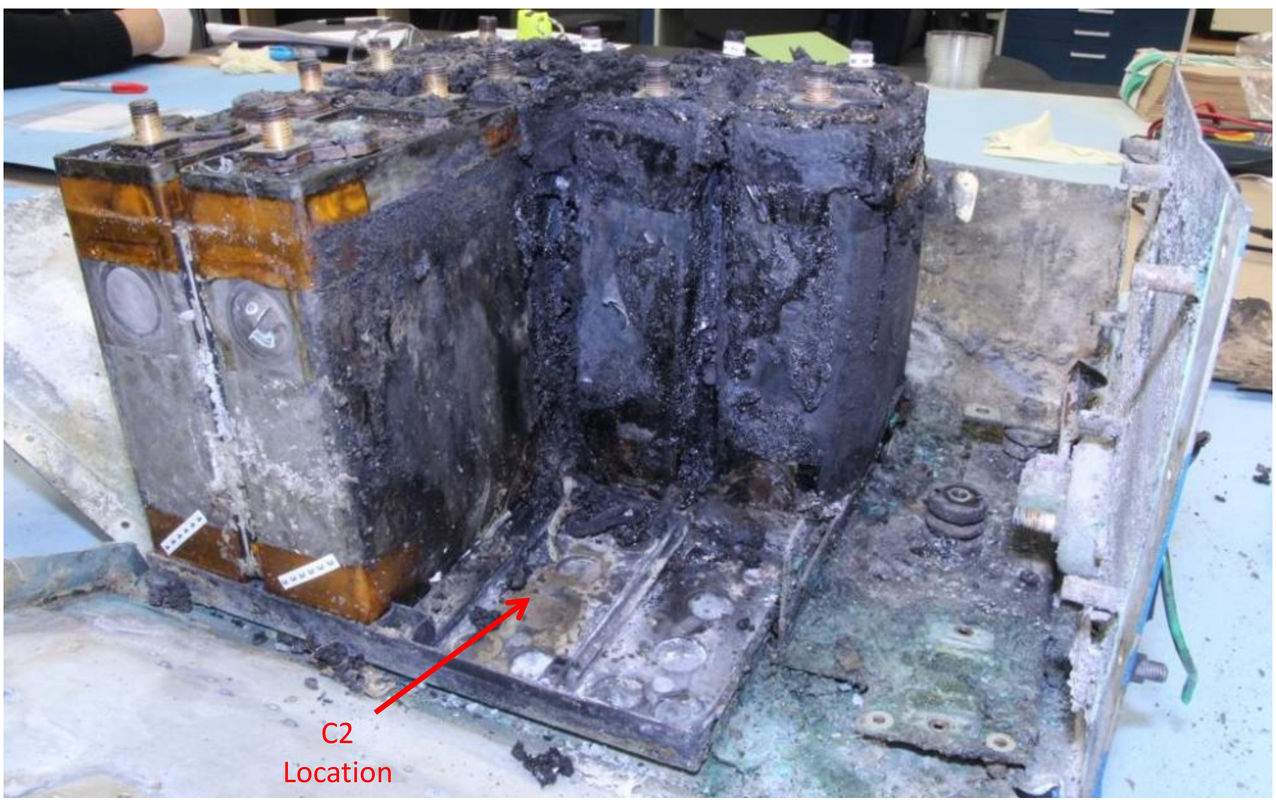

Figure 74. C2 removed (viewed from S2).

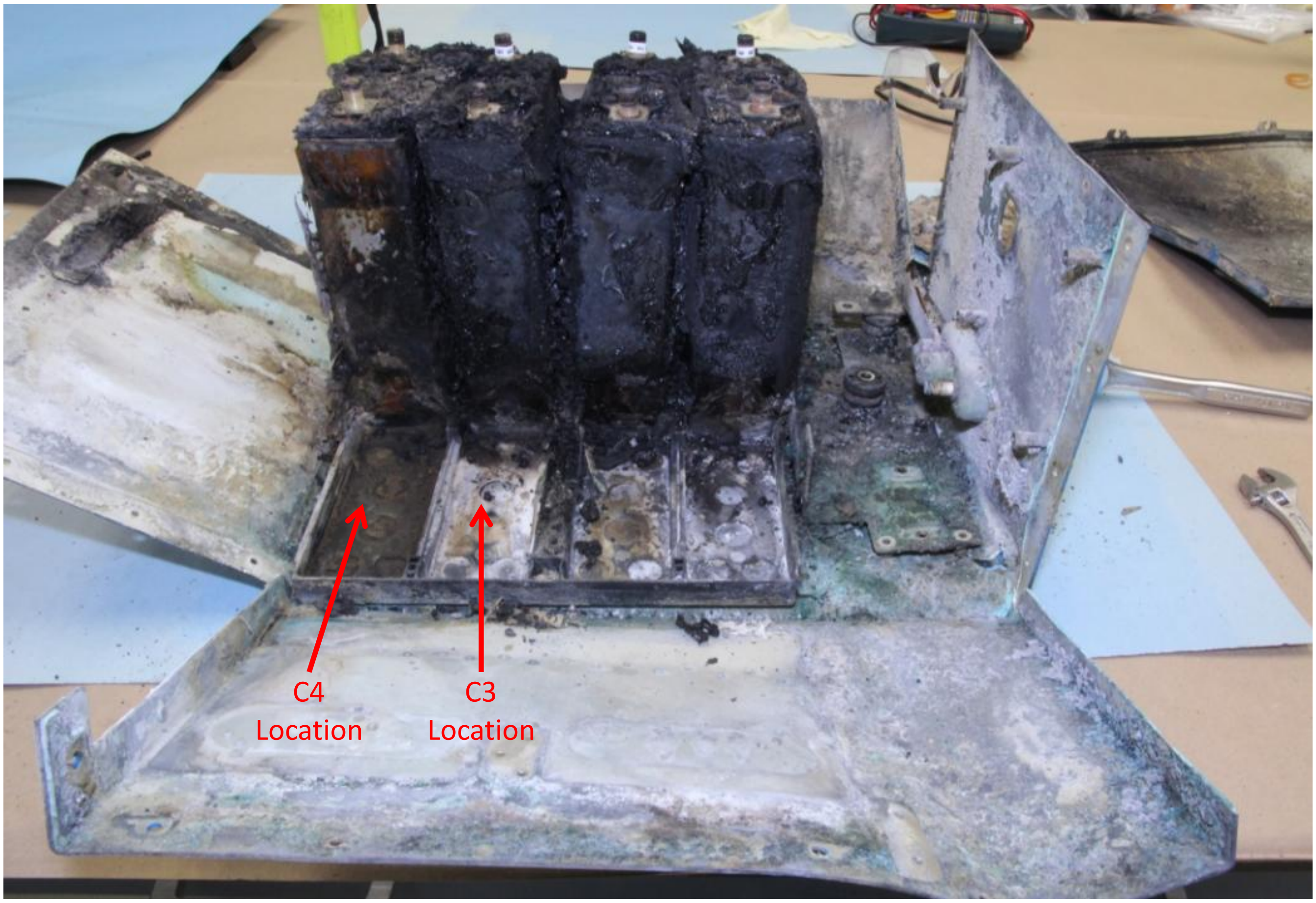

Figure 75. C1 through C4 removed (viewed from S2).

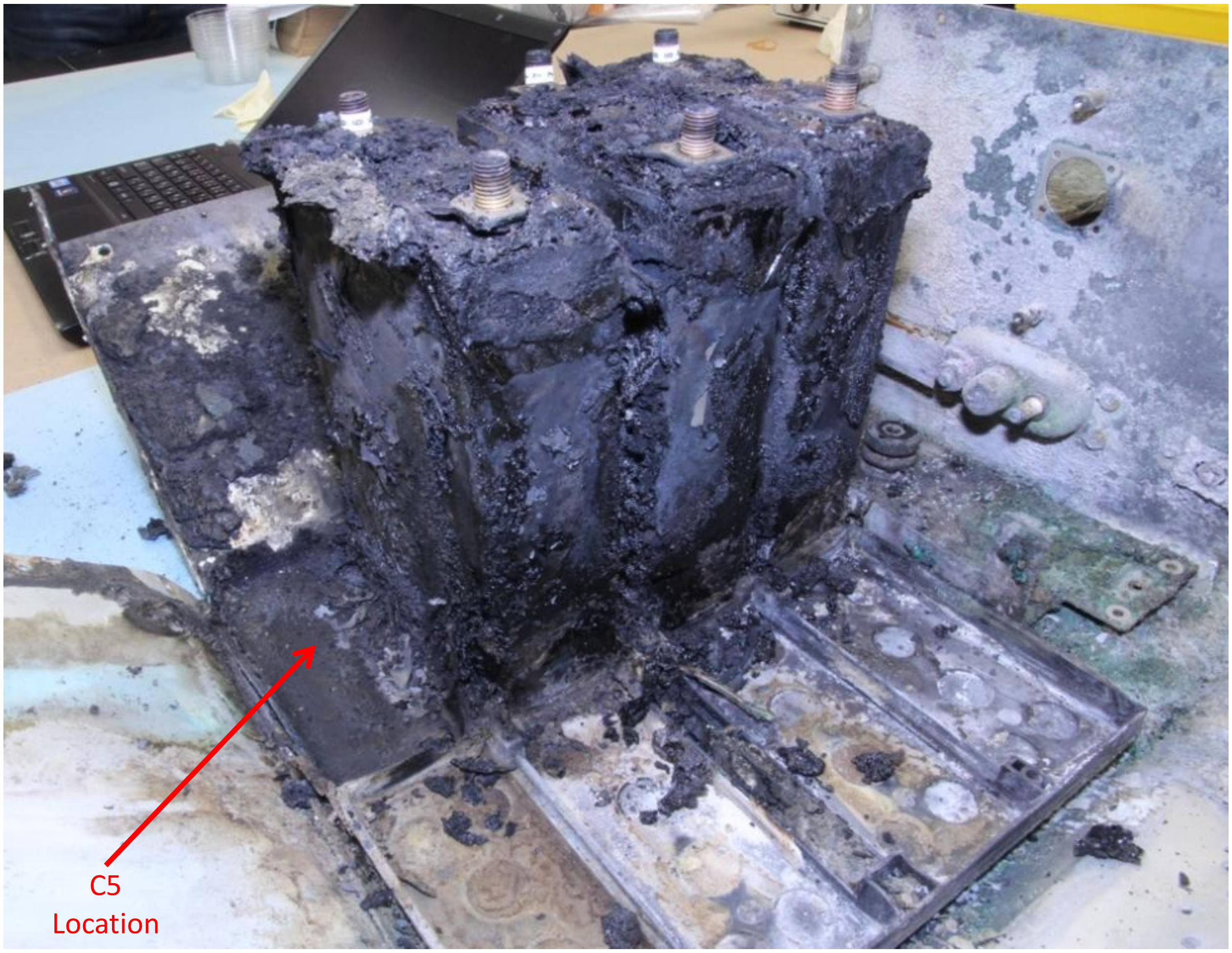

Figure 76. C1 through C5 removed (viewed from S2).

Figure 77. C6 through C8 and the lower fixation tray.

Figure 78. Battery box with all cells removed (viewed from the top of the battery box).

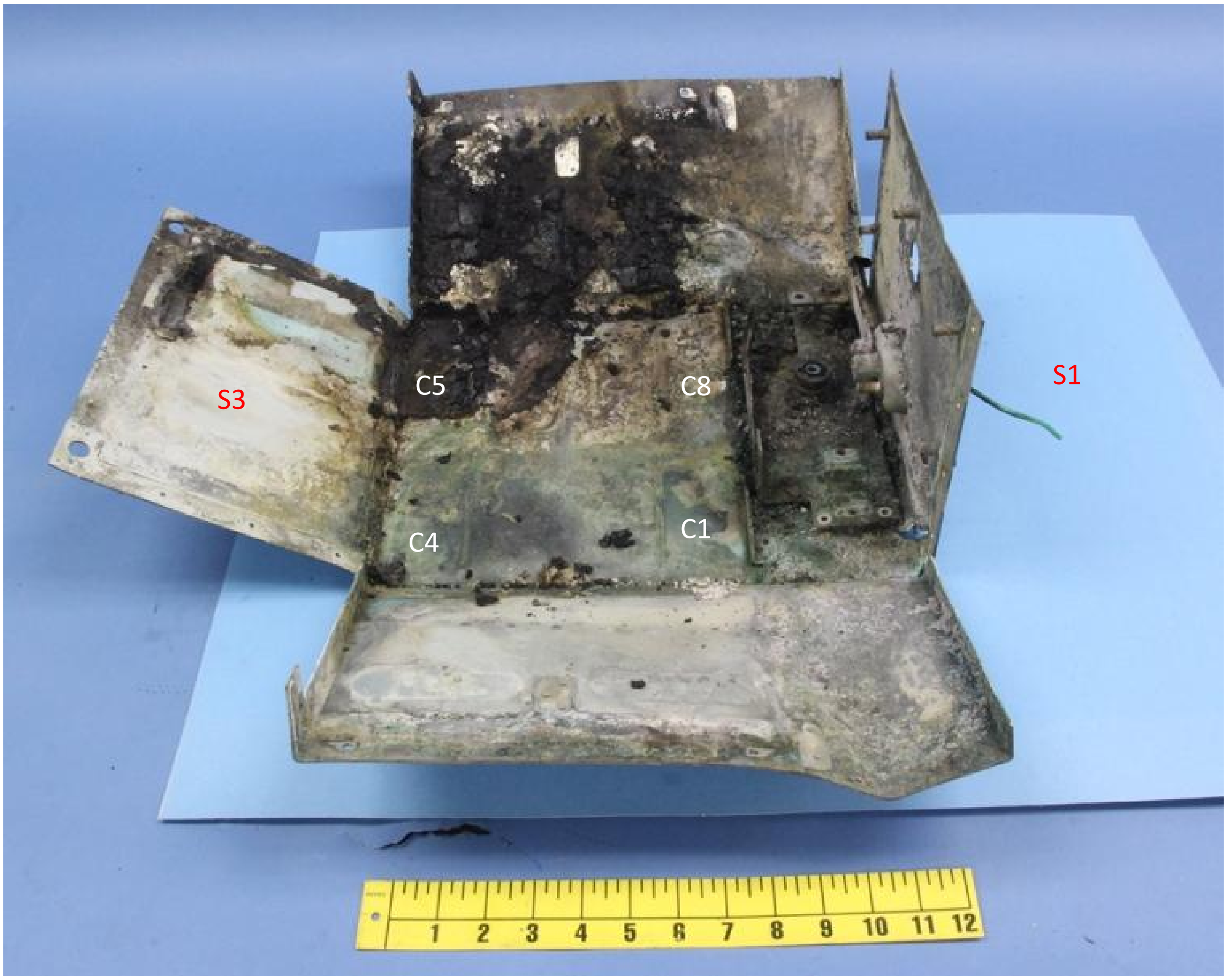

Figure 79. Battery box with all cells removed (viewed from S2).

Figure 80. Battery box with all cells removed (another view from the top of the battery box).

Figure 81. Upper fixation trays (top down view) of the JAL exemplar, main battery.

Cell 1

Cell 8

Figure 82. Lower fixation tray of the JAL exemplar, main battery.

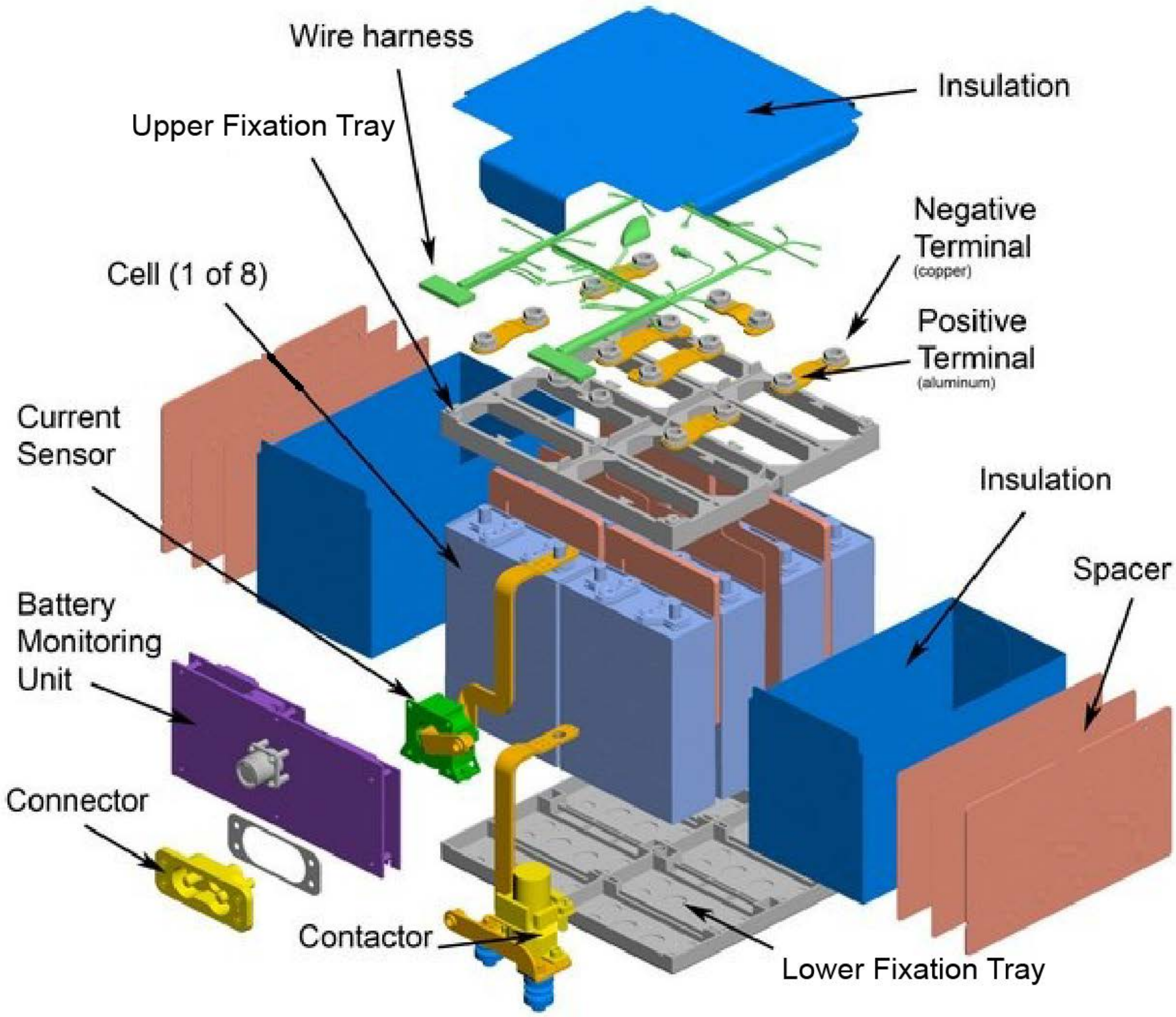

Figure 83. BPA-TP sheath surrounding the physical grouping of four cells of the JAL exemplar, main battery.

Figure 84. S2 folded down.

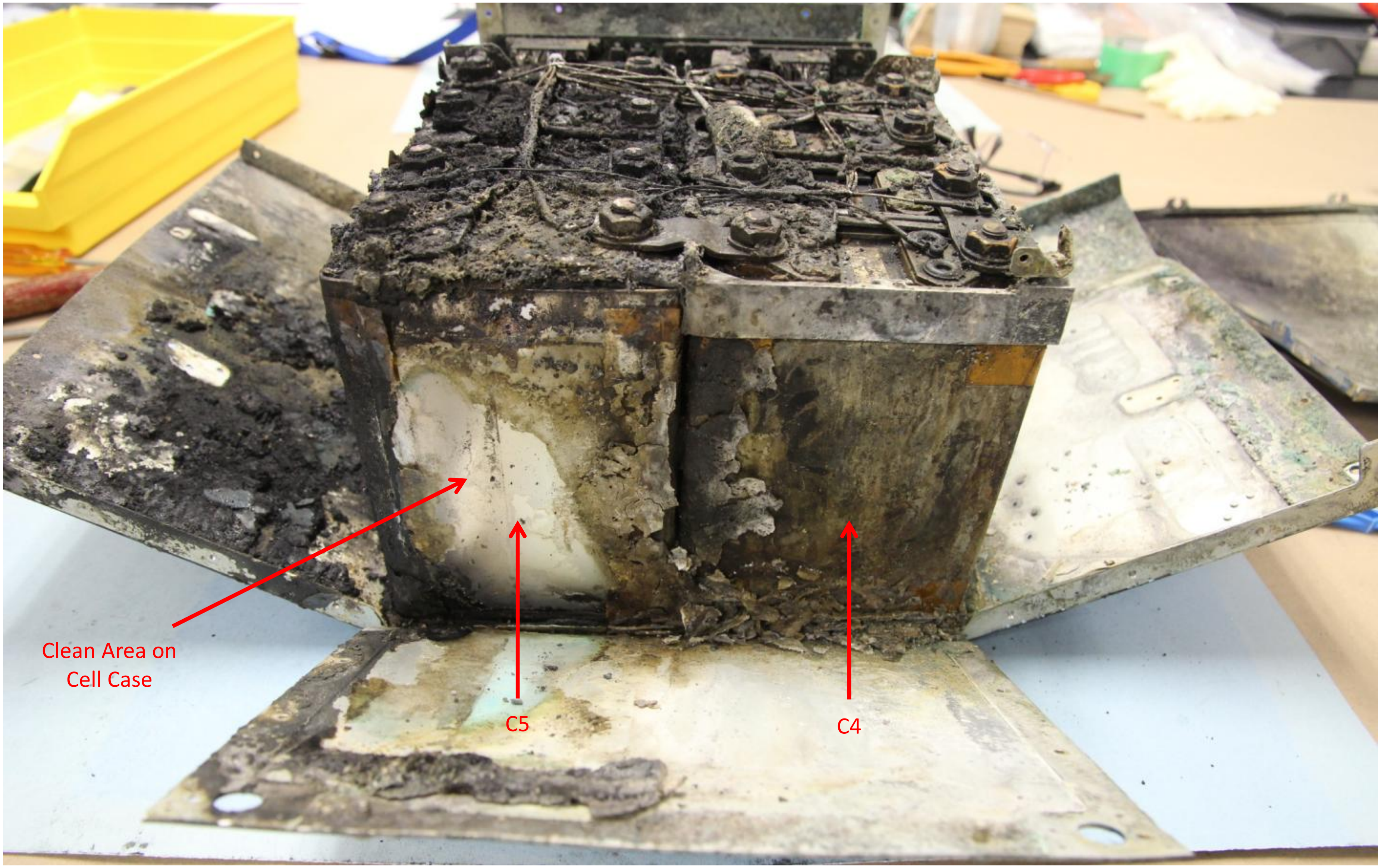

Figure 85. S3 folded down.

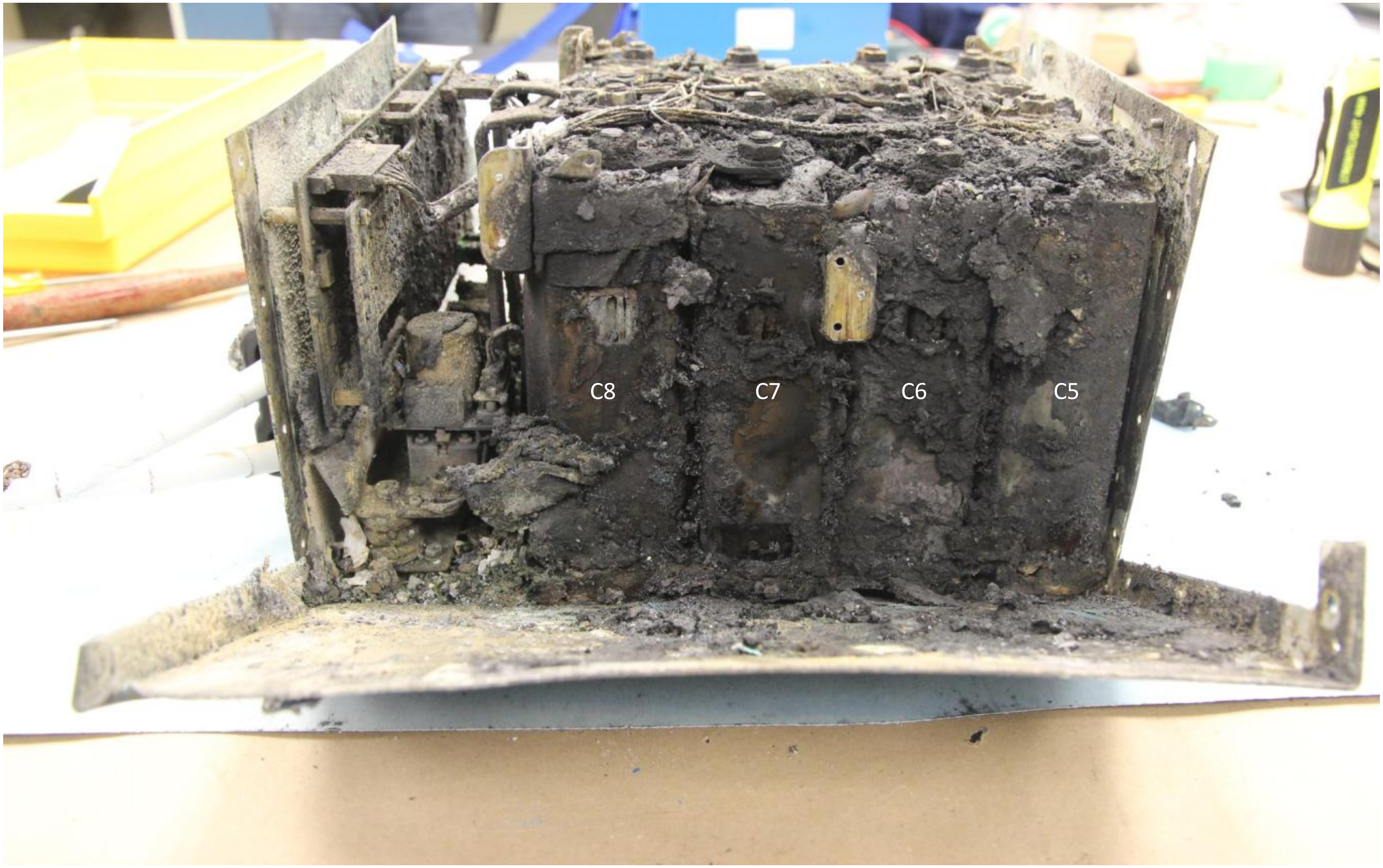

Figure 86. S4 folded down.

Figure 87. Battery box with C2 removed (viewed from S2).

Figure 88. Battery box with C1 through C4 removed (viewed from S2).

Figure 89. Bottom view of lower fixation tray, which is made of thermoplastic polyester.

Figure 90. Top view of lower fixation tray.

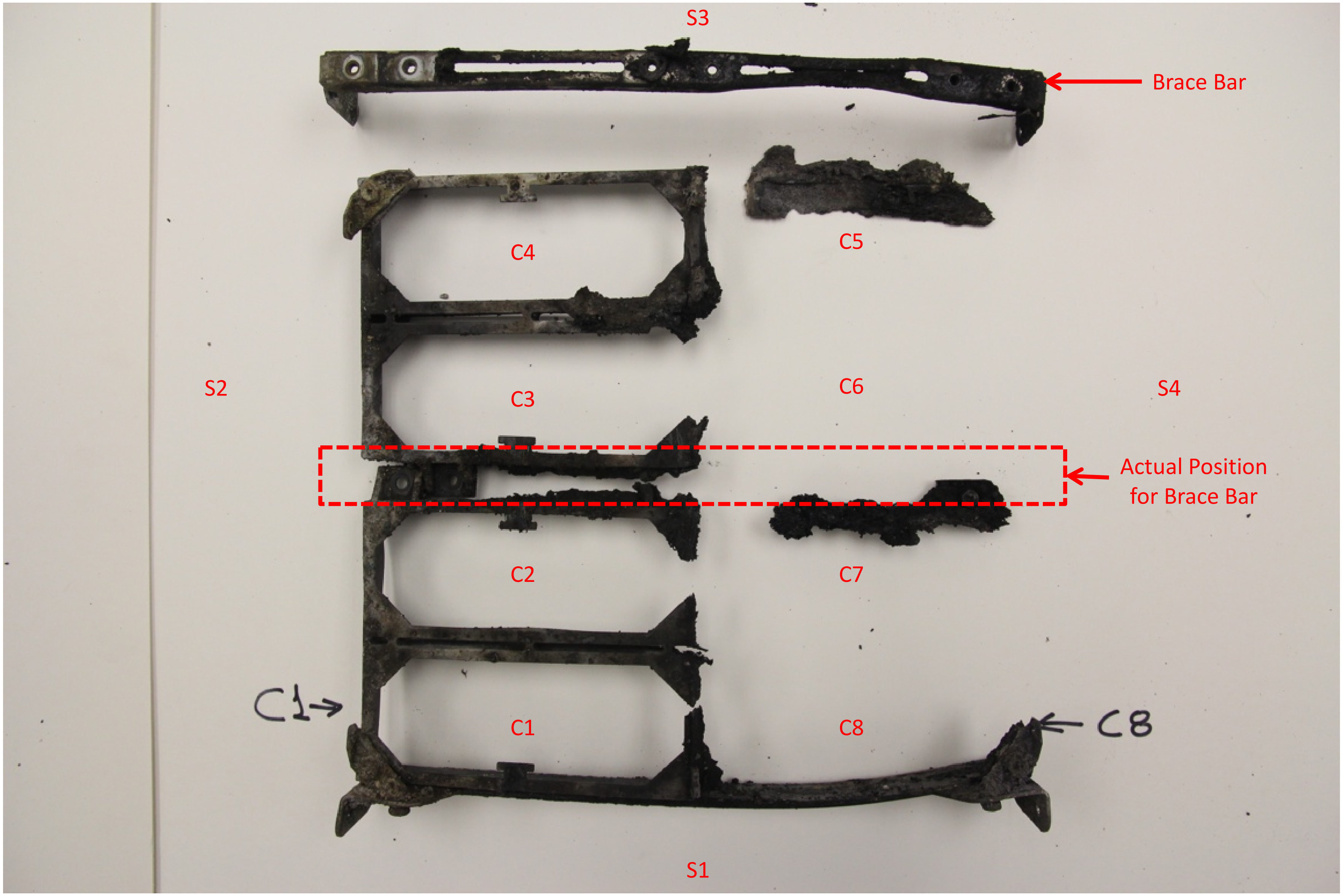

Figure 91. Upper fixation tray and brace bar.

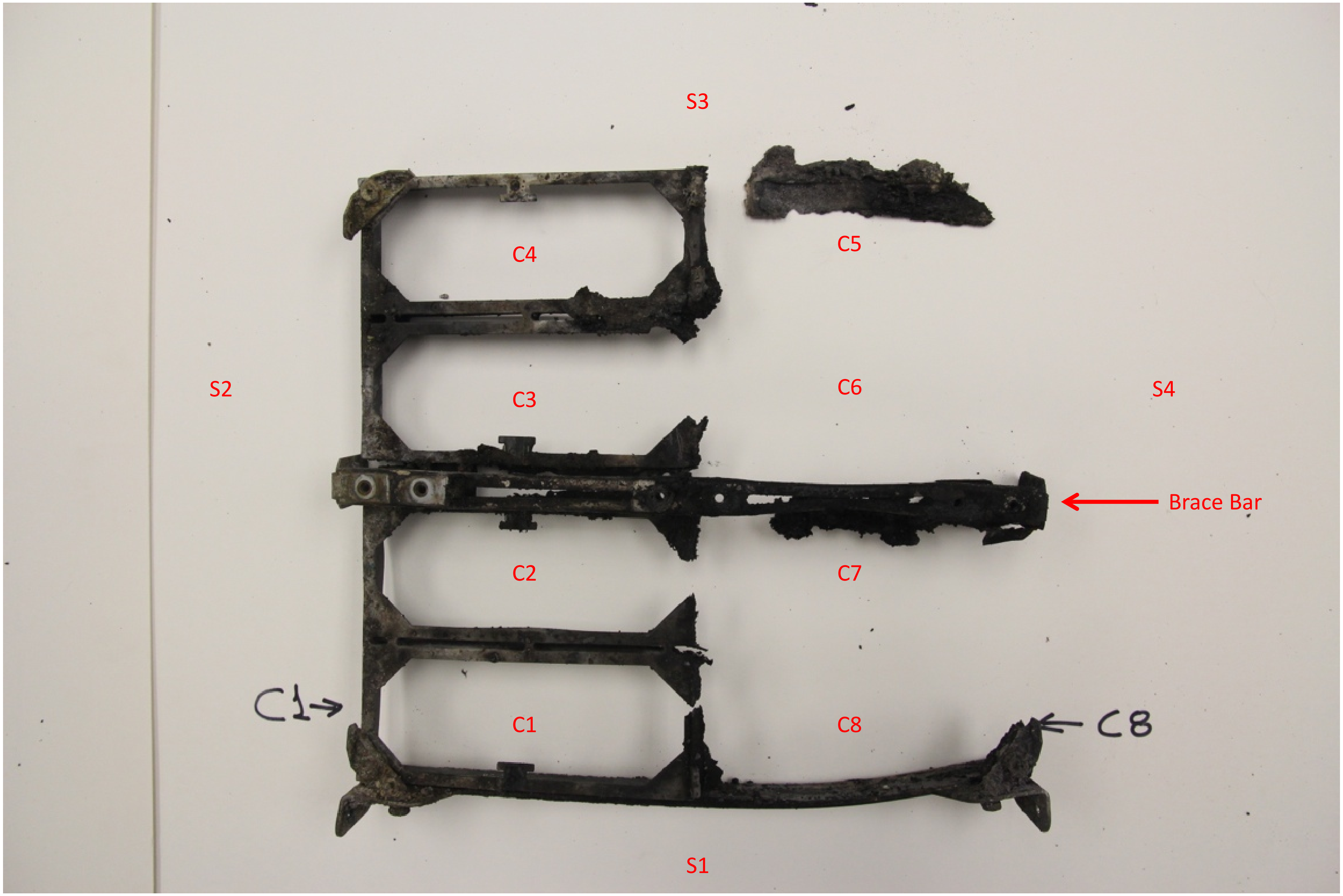

Figure 92. Top fixation tray with brace bar in position.

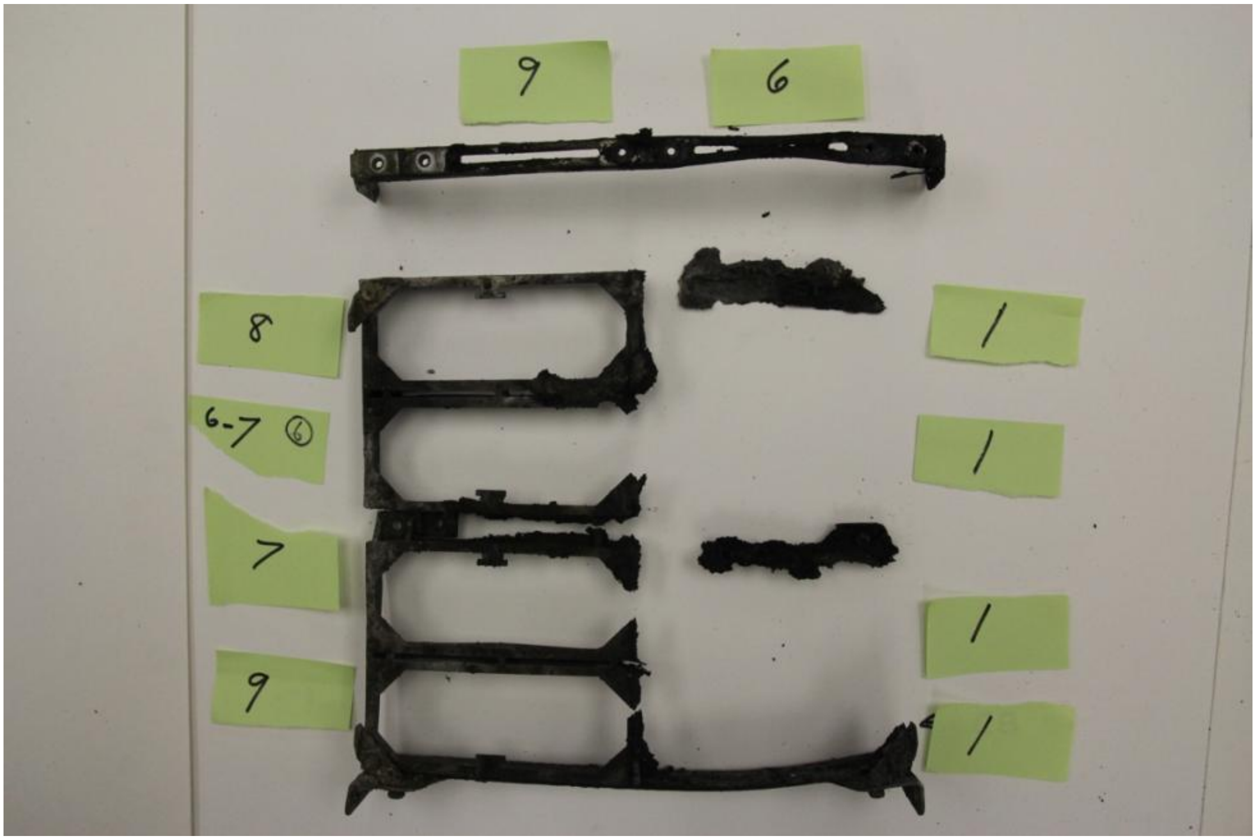

Figure 93. Upper fixation tray and brace bar damage assessment (10 = least damaged, 1 = most damaged).

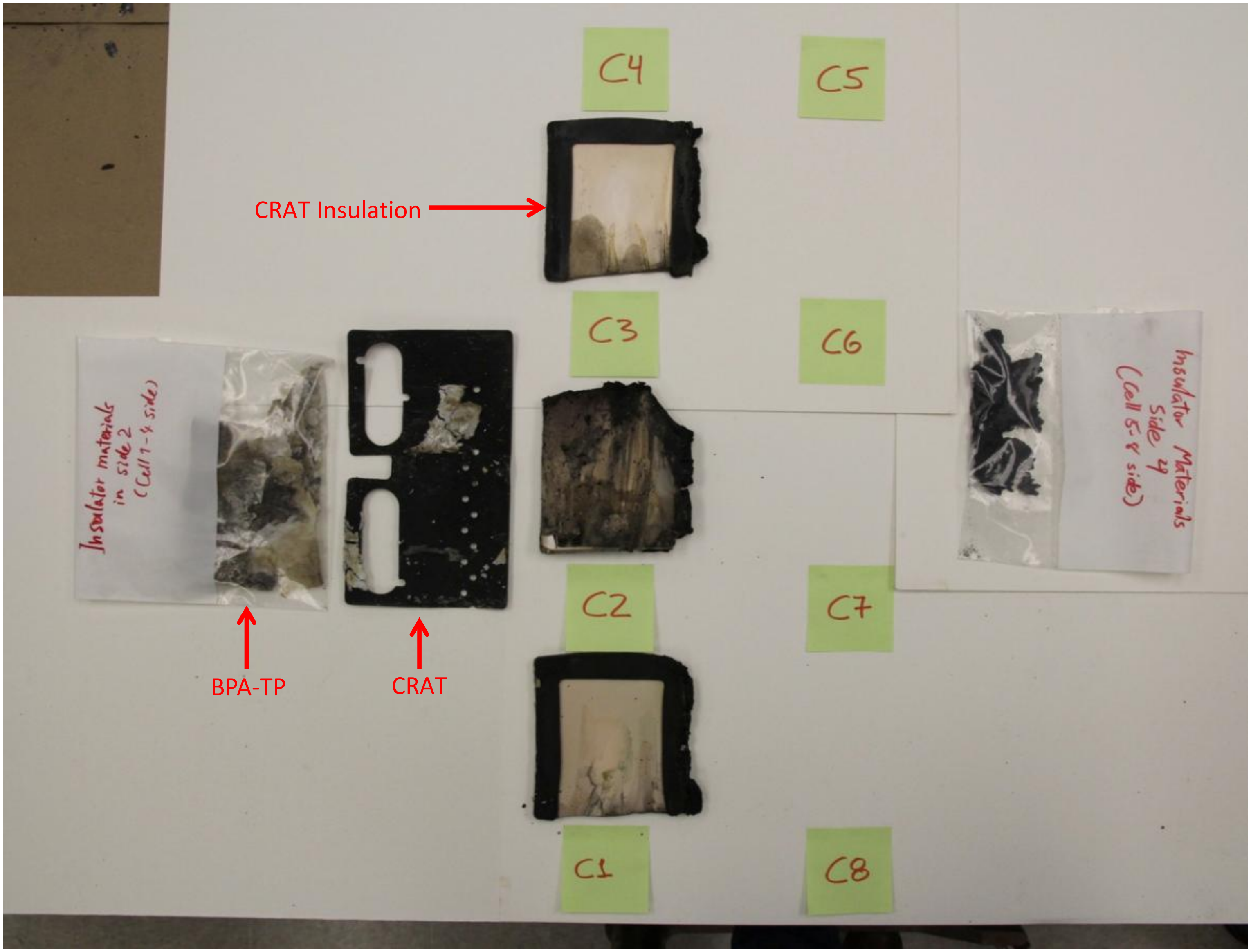

Figure 94. Insulation recovered from the battery box.

Figure 95. Battery box with C1 removed (viewed from S2).

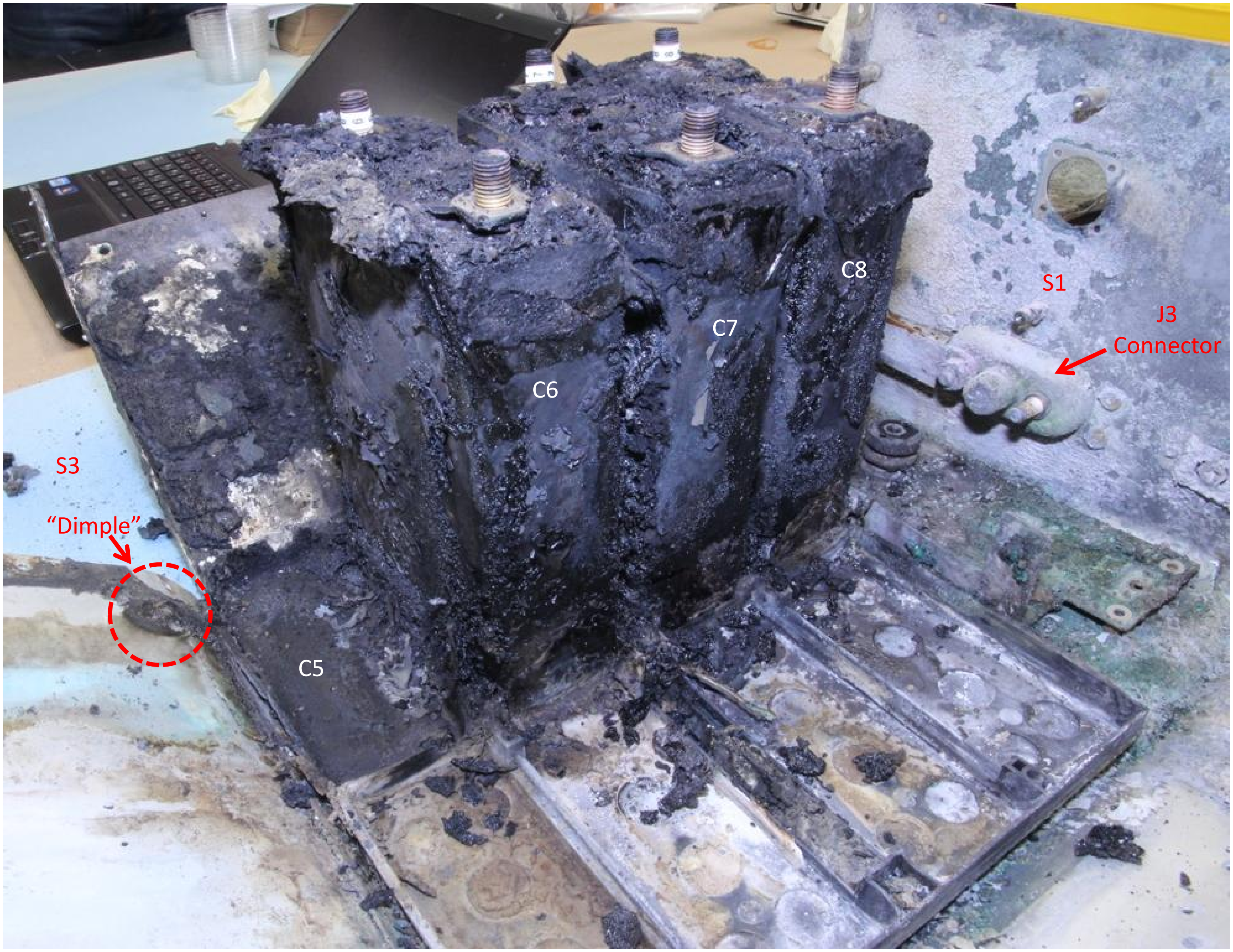

Figure 96. Battery box with C1 through C5 removed (viewed from S2).

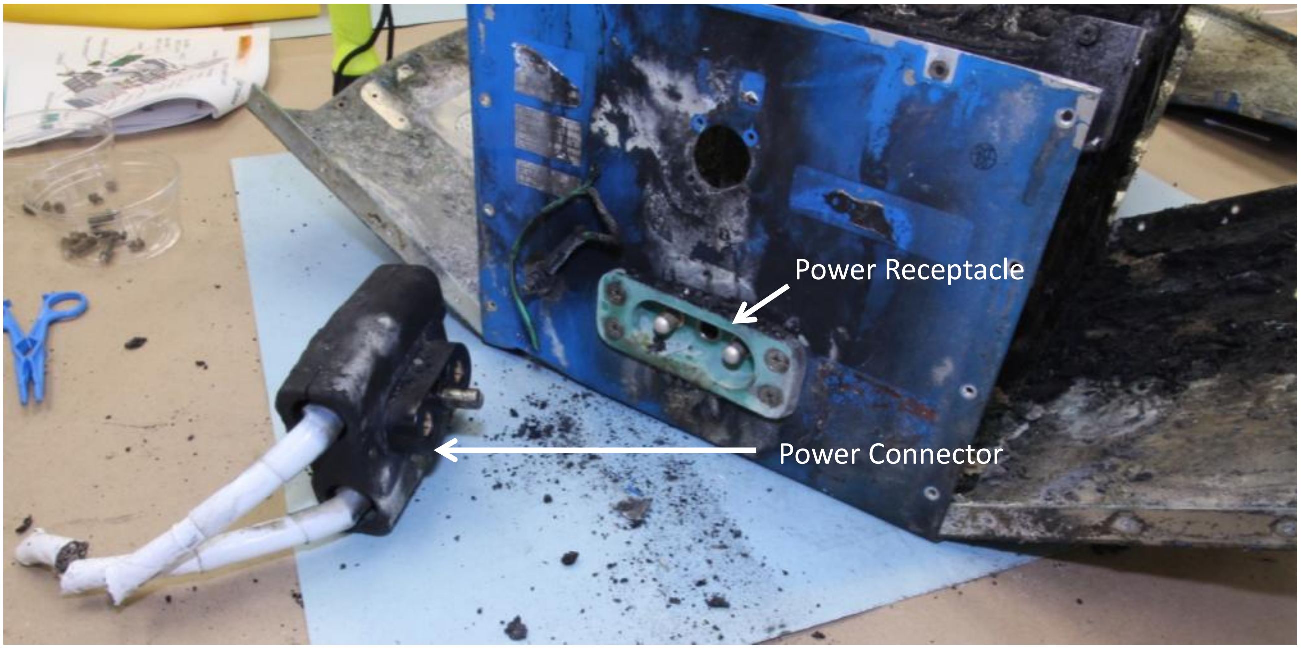

Figure 97. View of the J3 power connector and power receptacle.

Figure 98. Close-up view of the J3 power receptacle showing thermally-deformed material.

Figure 99. Close-up view of both the J3 power connector and the power receptacle.

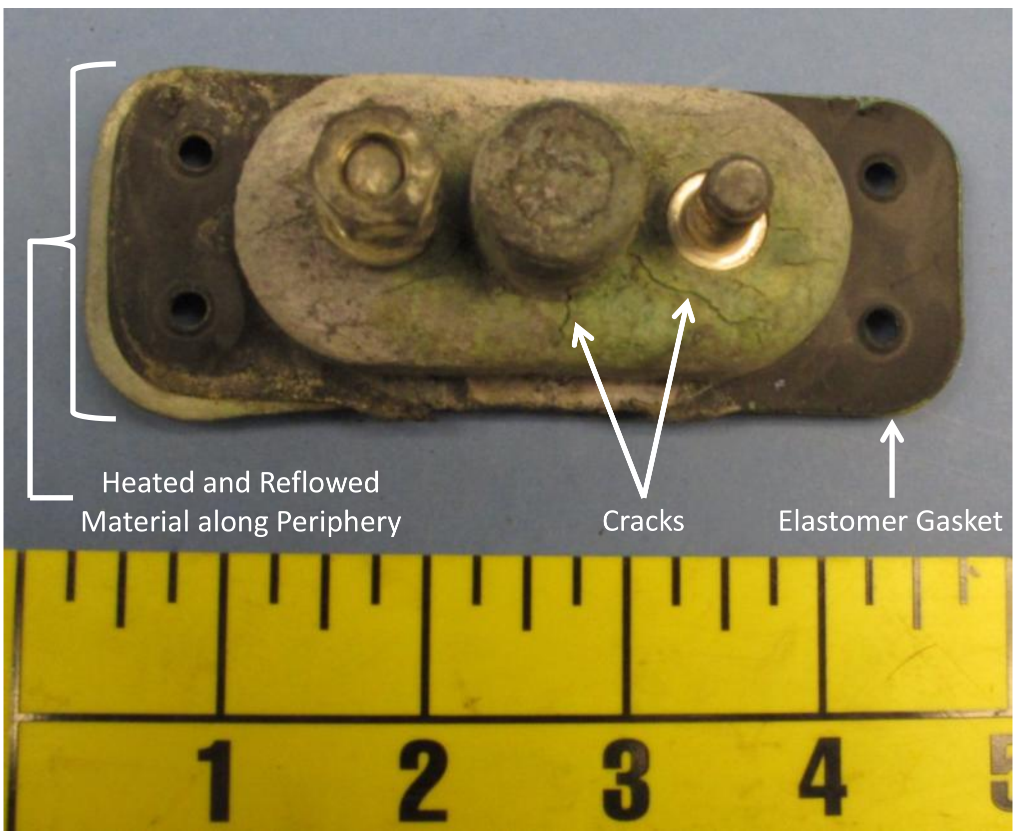

Figure 100. Close-up view of the J3 power receptacle showing heated and reflowed material.

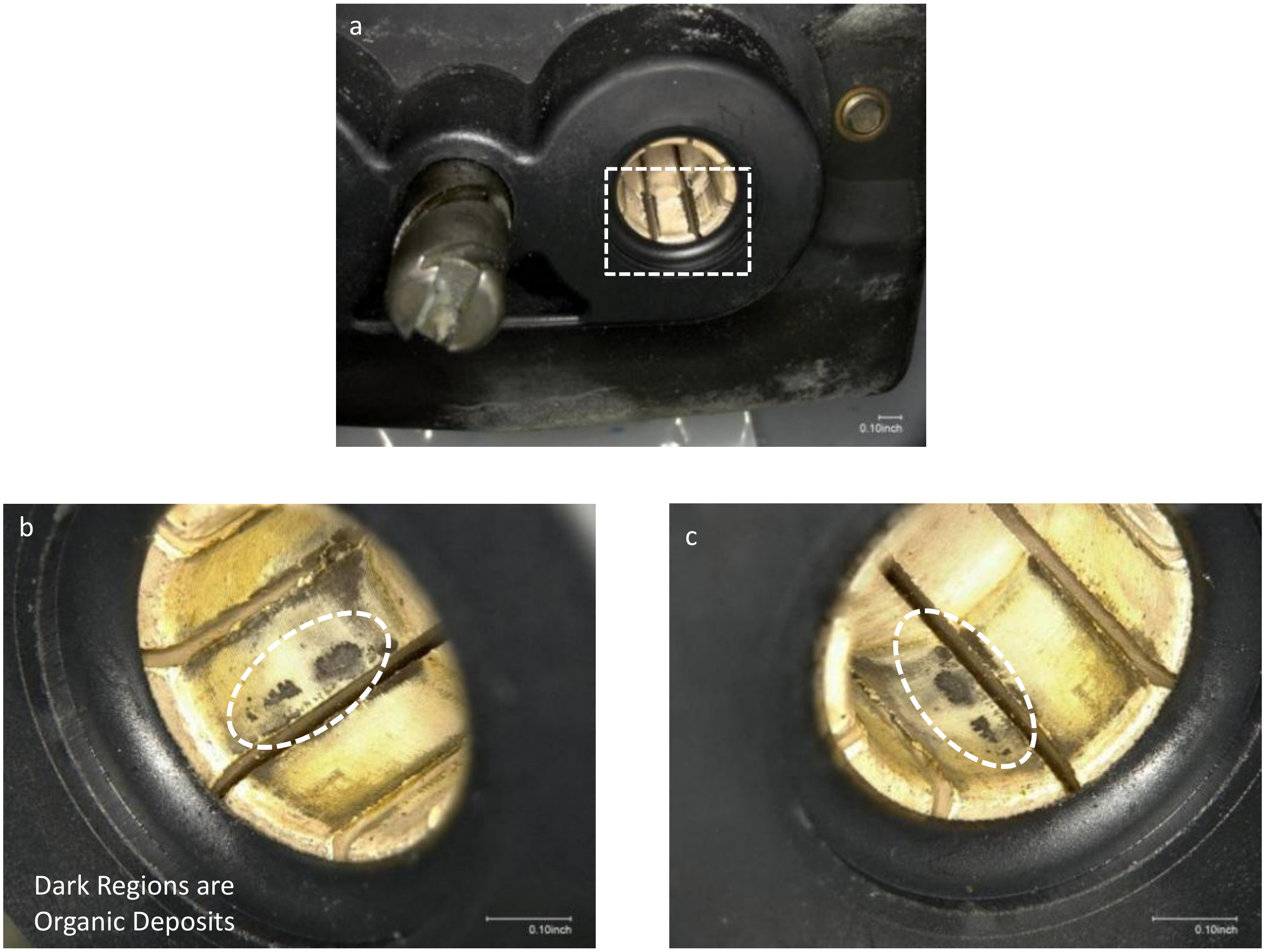

Figure 101. Close-up views of the J3 power connector showing organic deposits.

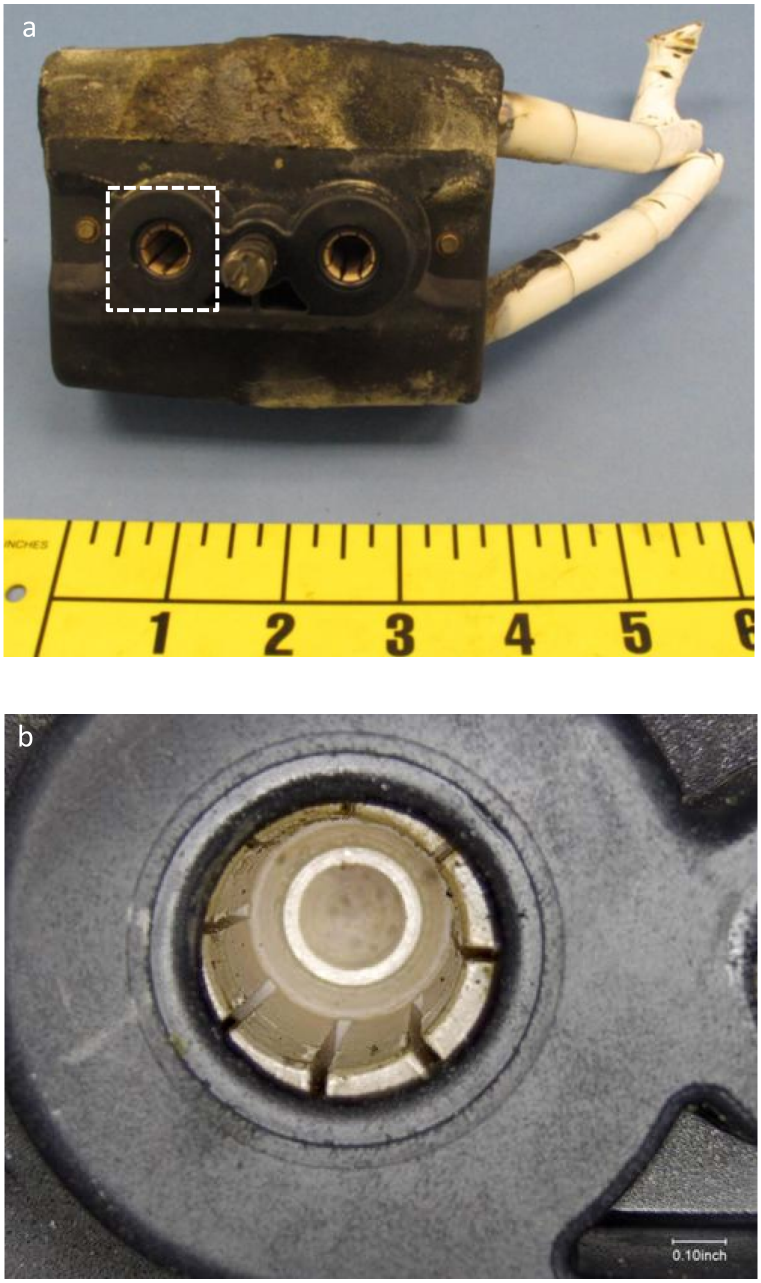

Figure 102. Close-up views of the power connector.

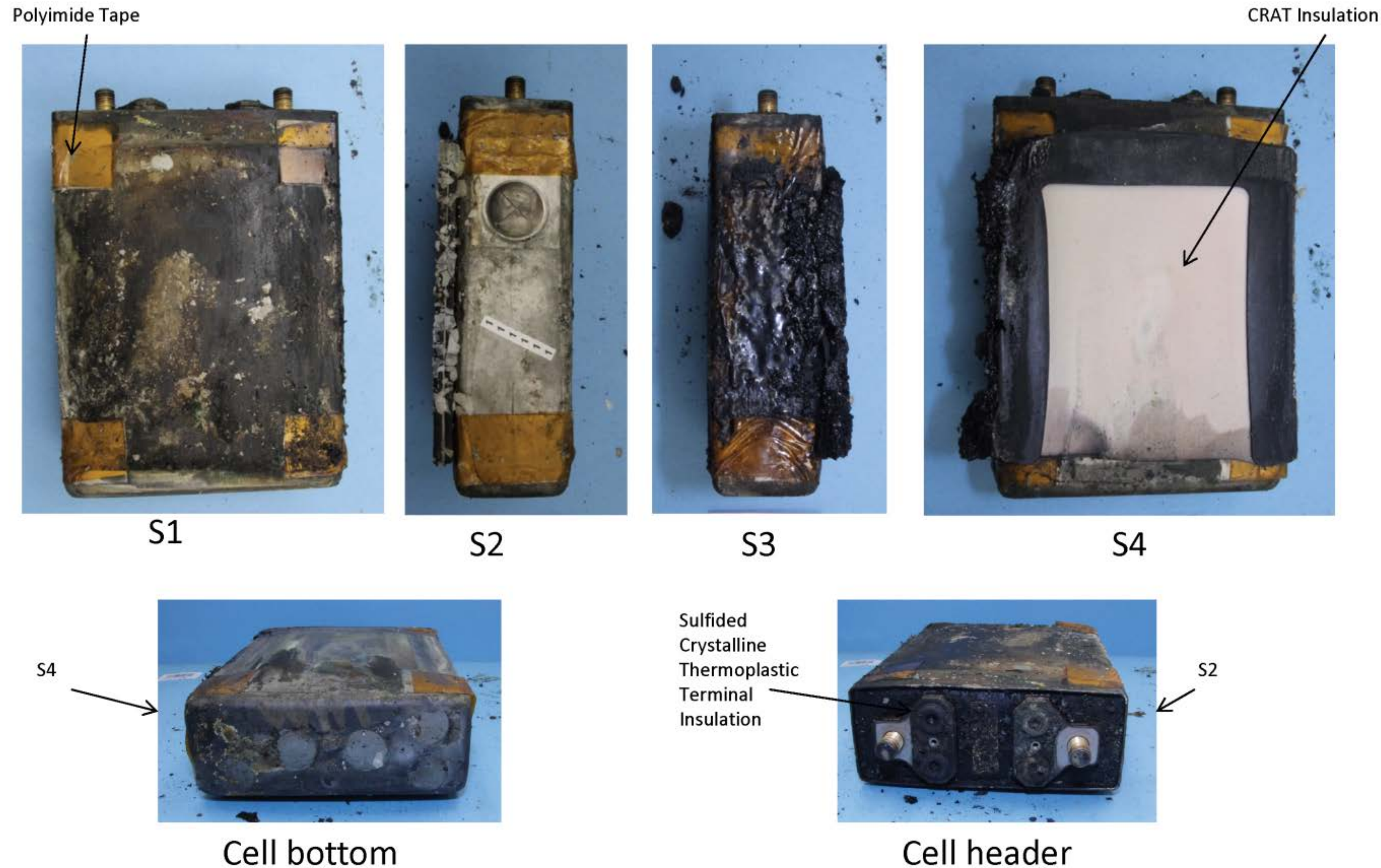

Figure 103. C1 (as removed).

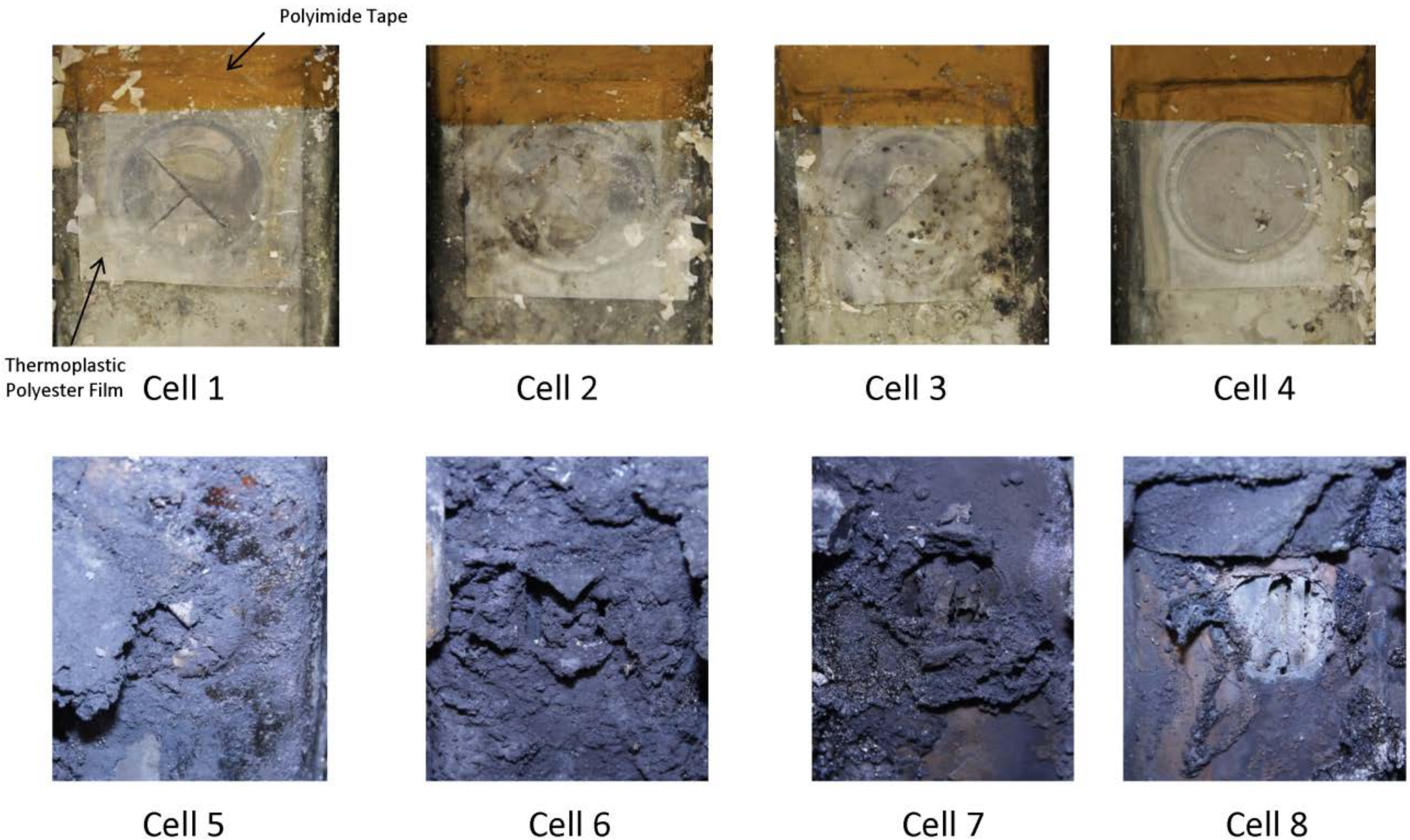

Figure 104. Close-up views of the vent disc for C1 through C8.

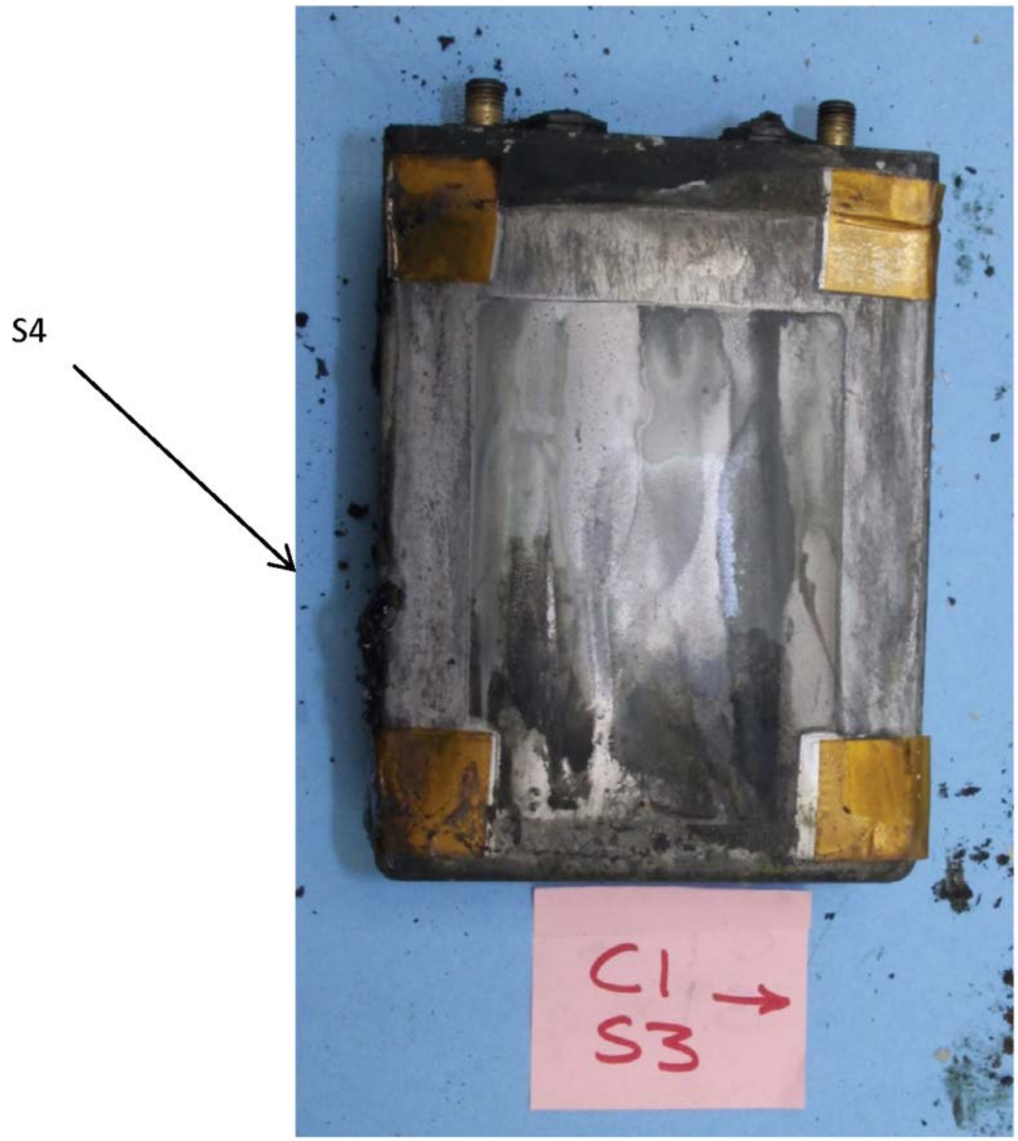

Figure 105. C1 (side S3 with insulation removed).

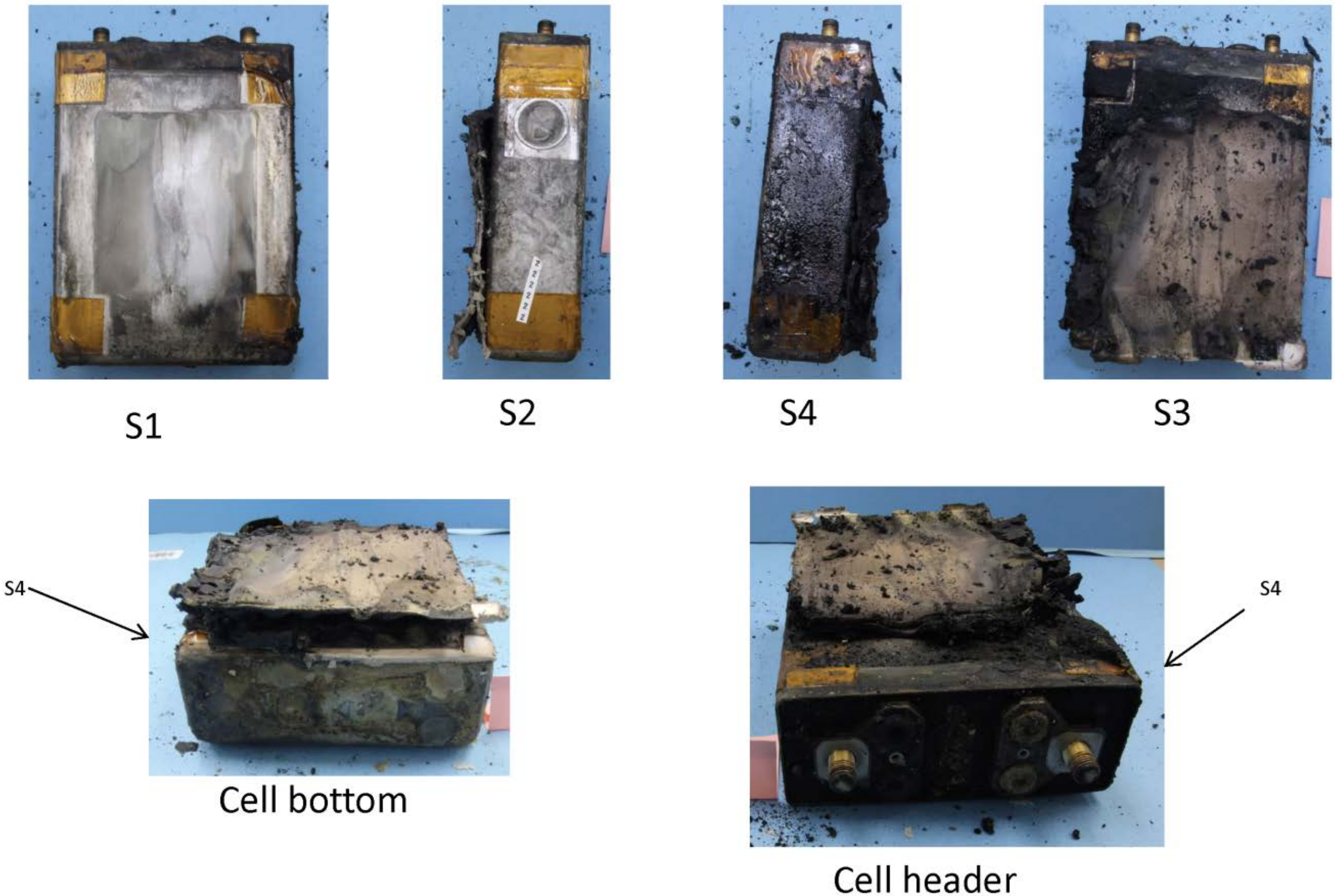

Figure 106. C2 (as removed).

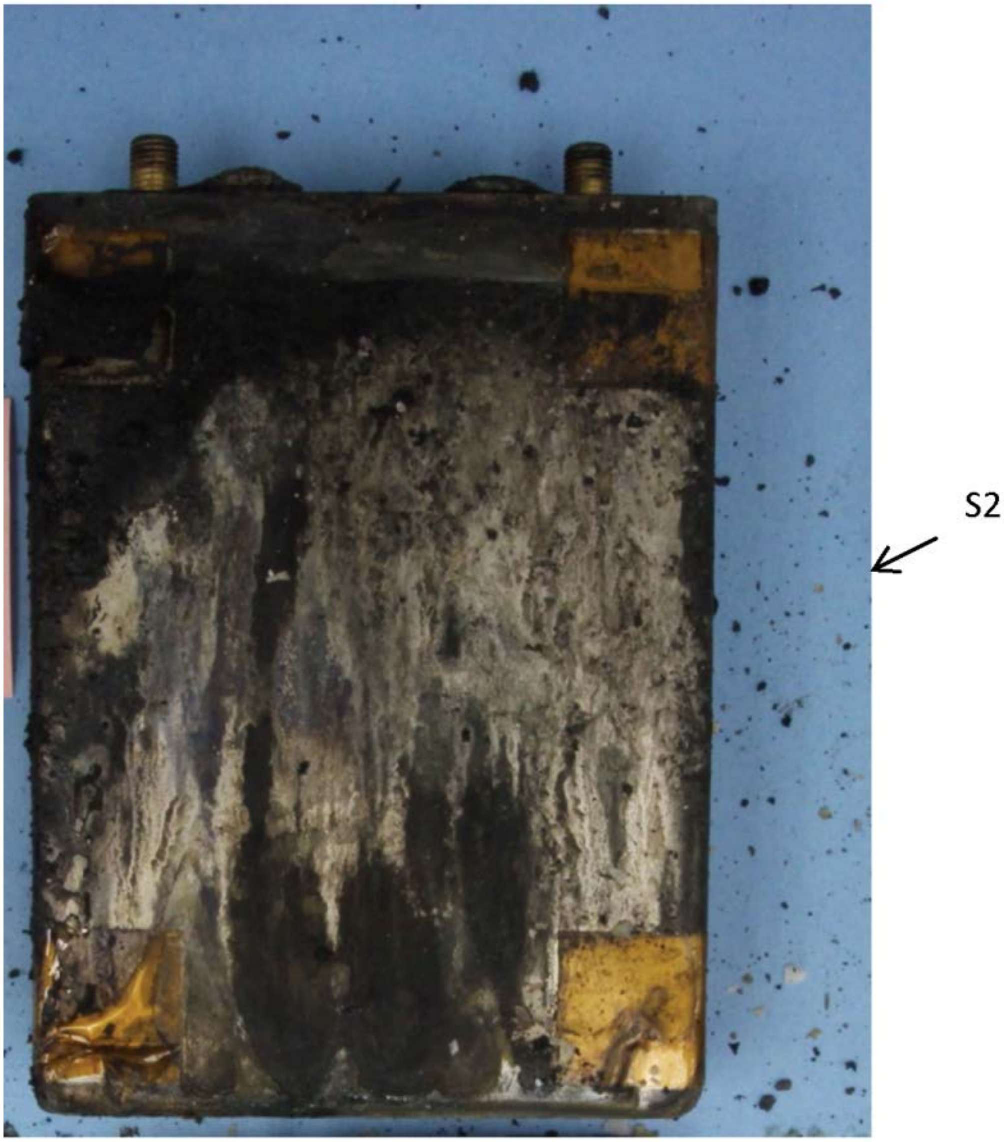

Figure 107. C2 (side S3 with insulation removed).

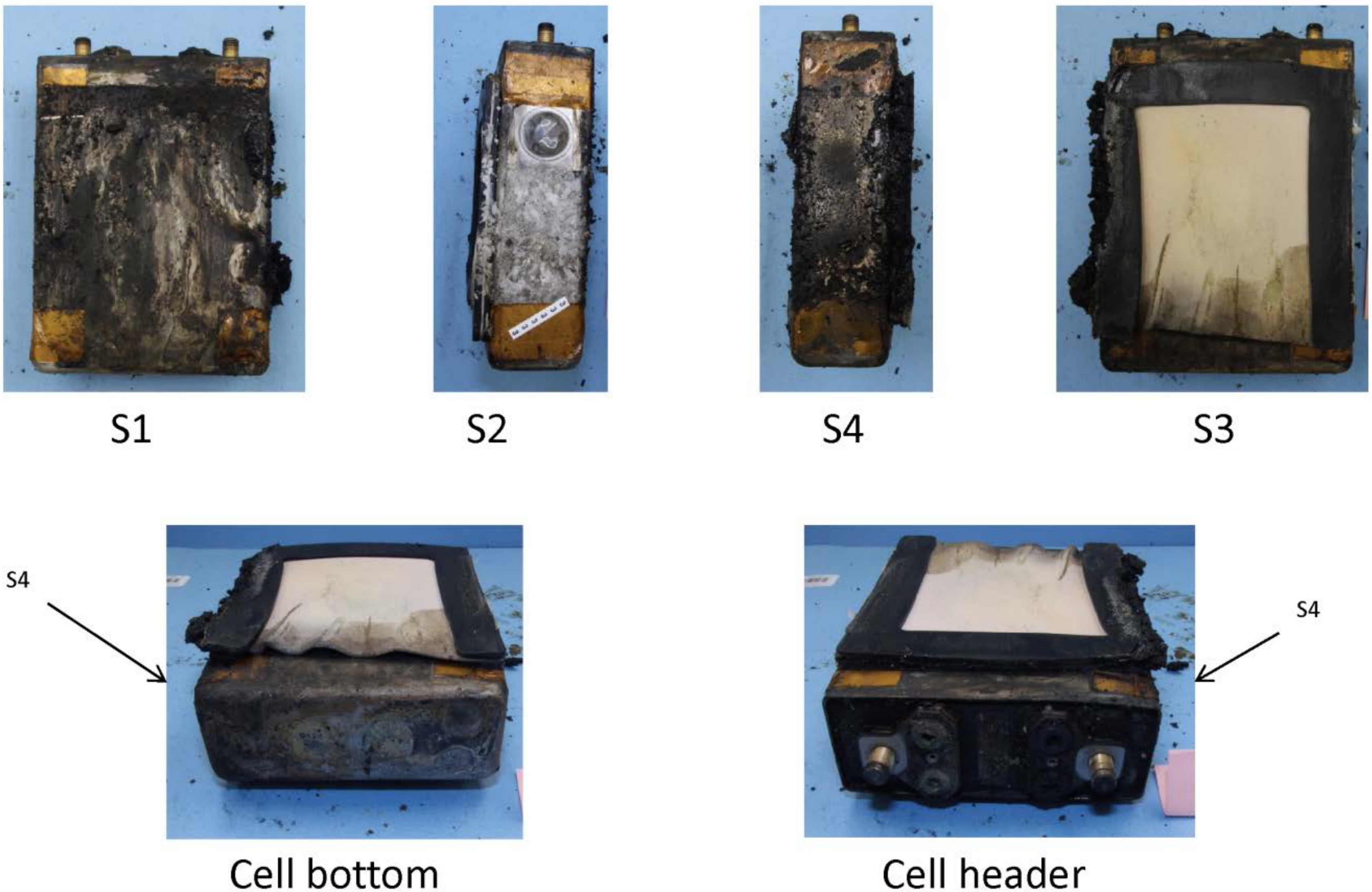

Figure 108. C3 (as removed).

Figure 109. C3 (with insulation removed).

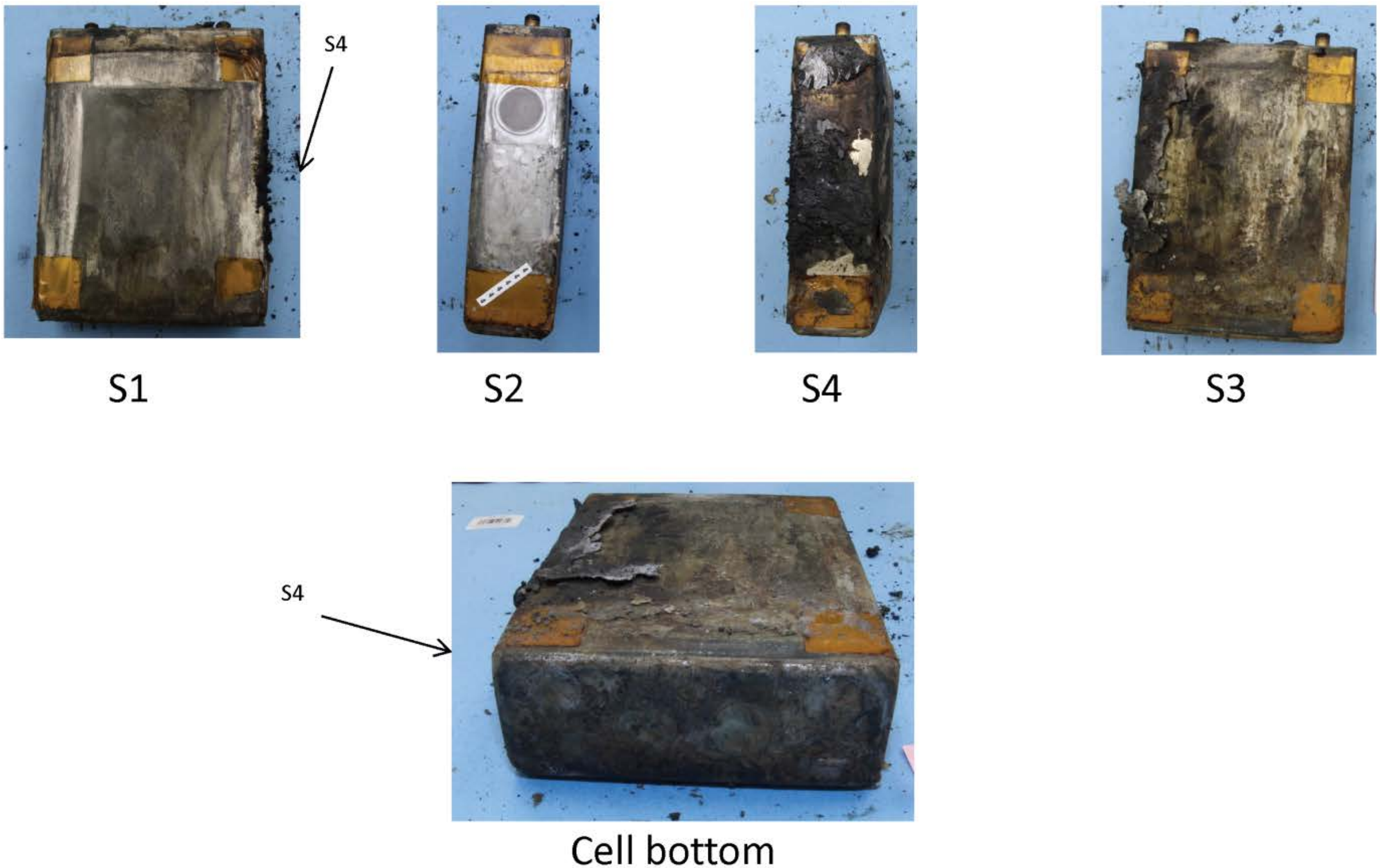

Figure 110. C4 (as removed).

Figure 111. C5 (as removed).

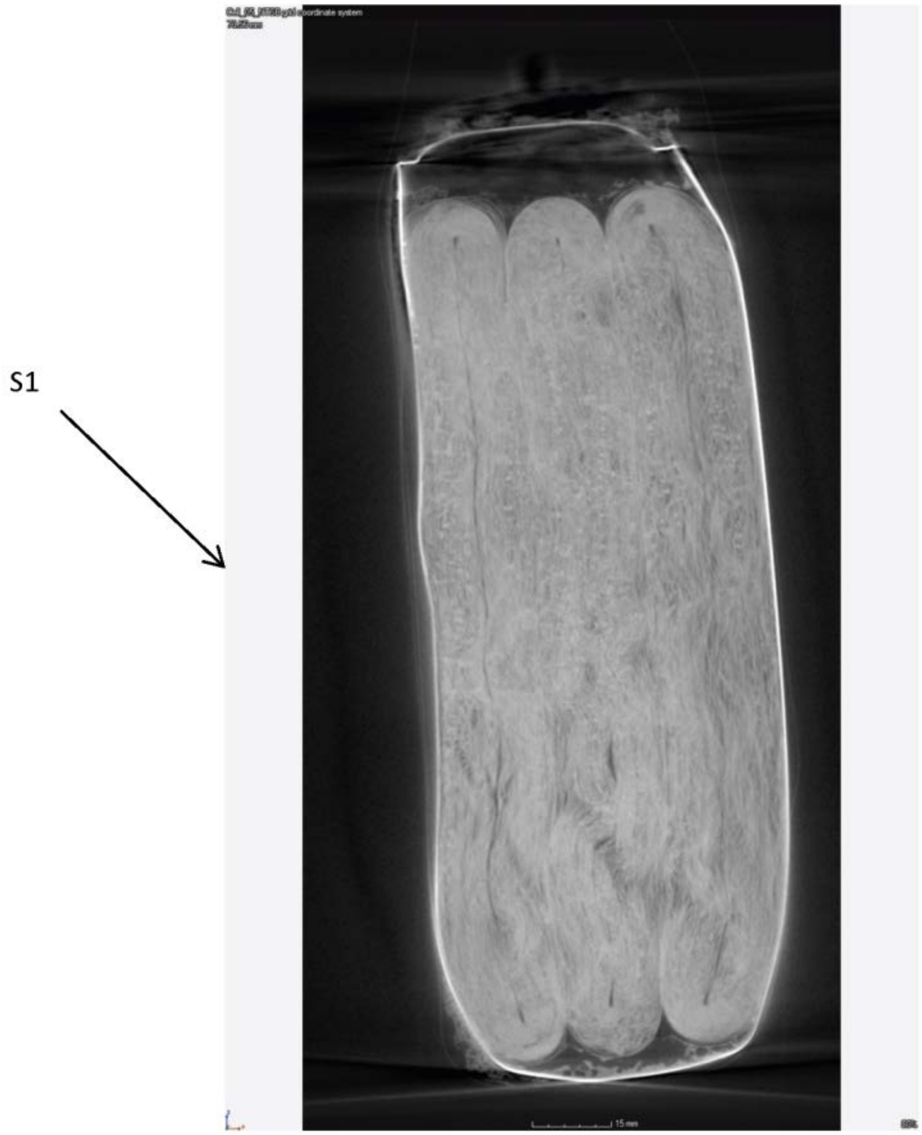

Figure 112. C5 CT scan image. The exemplar CT scan was taken on a plane about midway between the terminals.

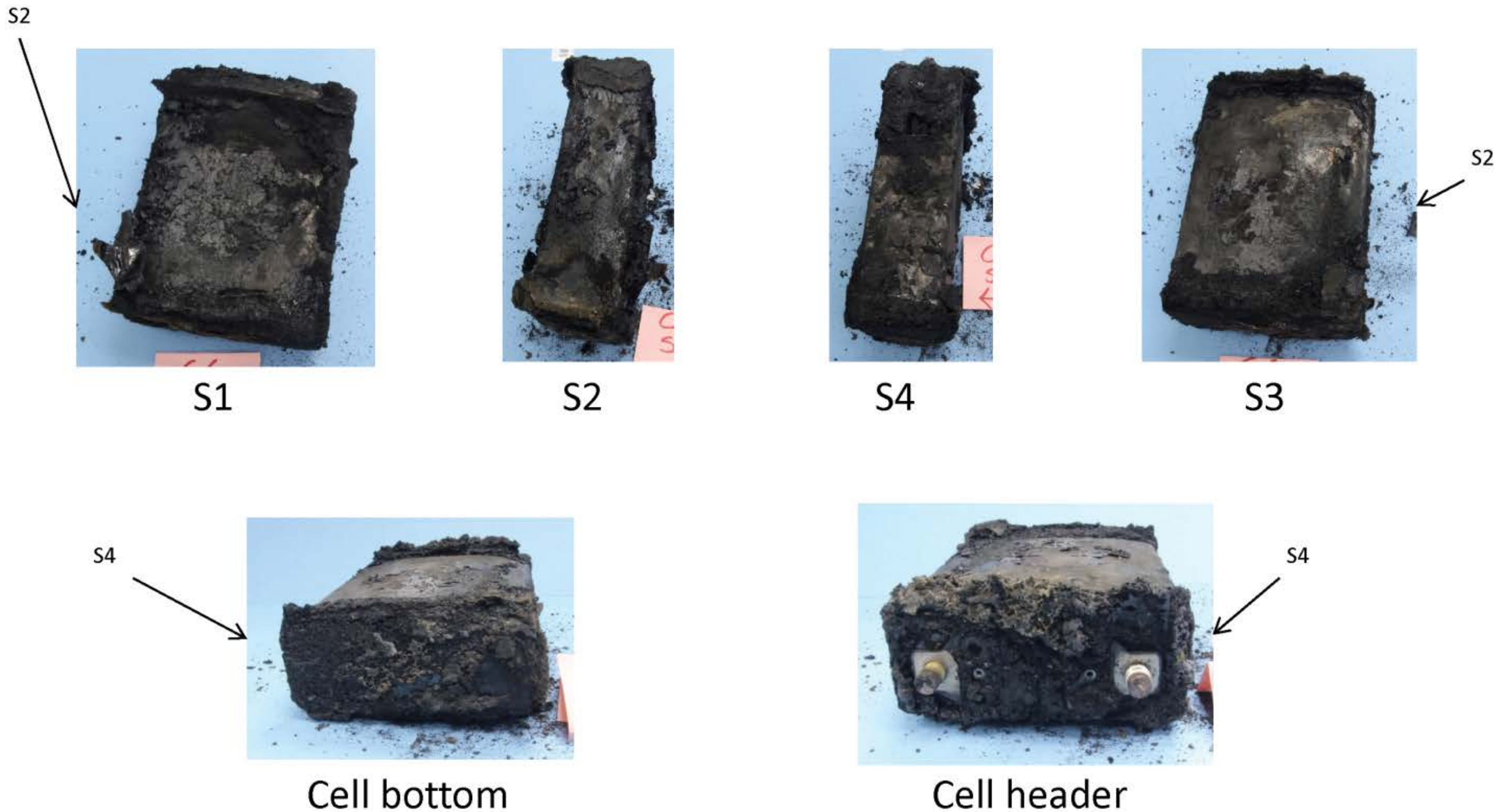

Figure 113. C6 (as removed).

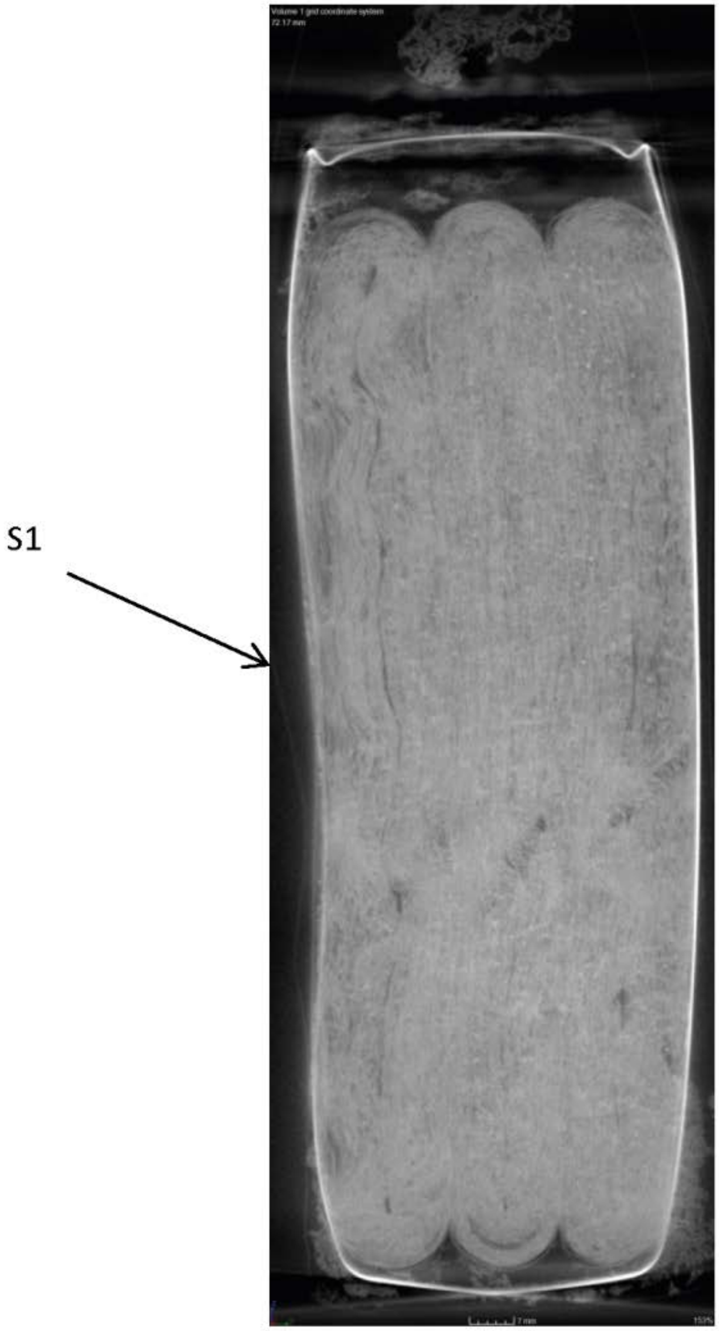

Figure 114. C6 CT scan image. The exemplar CT scan was taken on a plane about midway between the terminals.

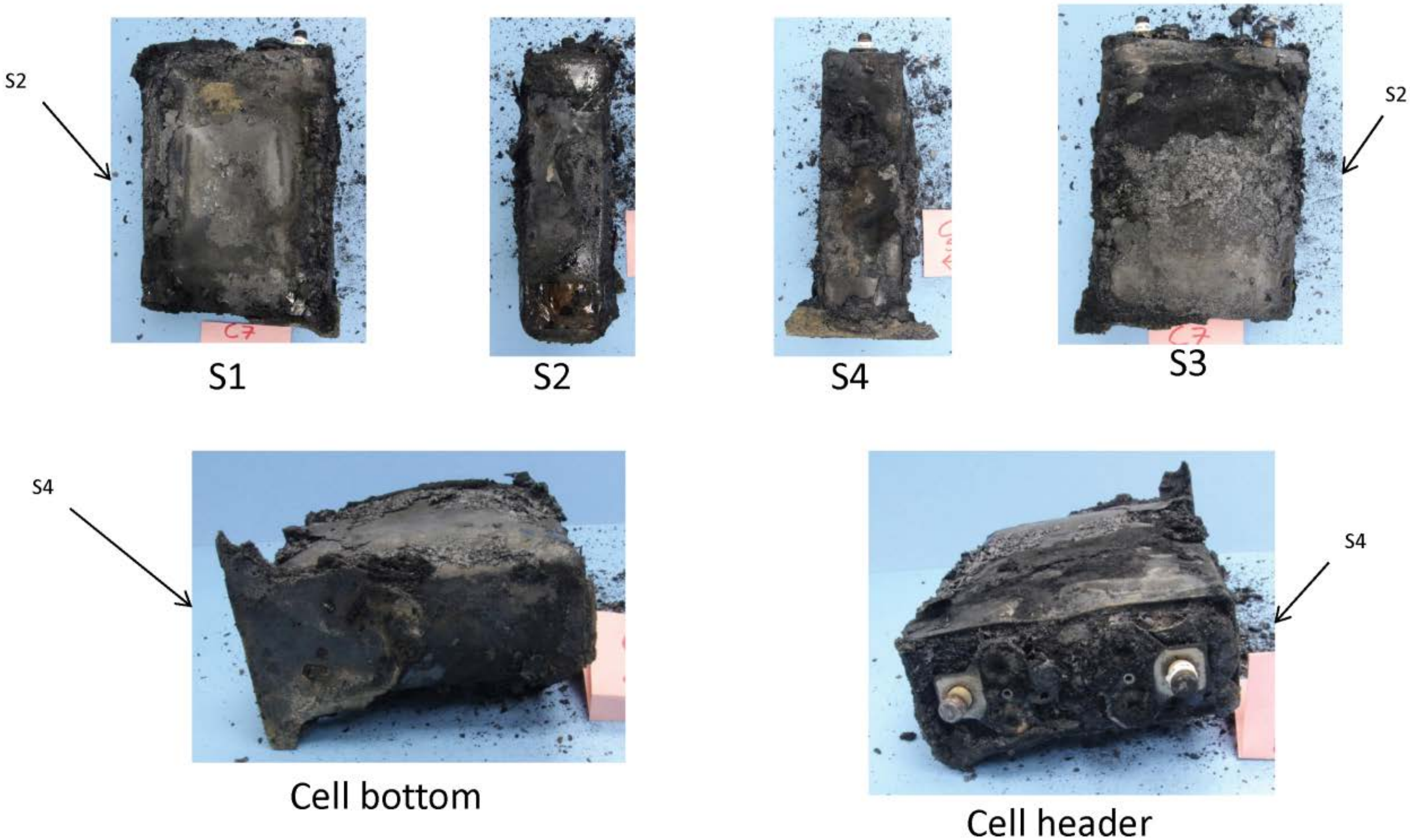

Figure 115. C7 (as removed).

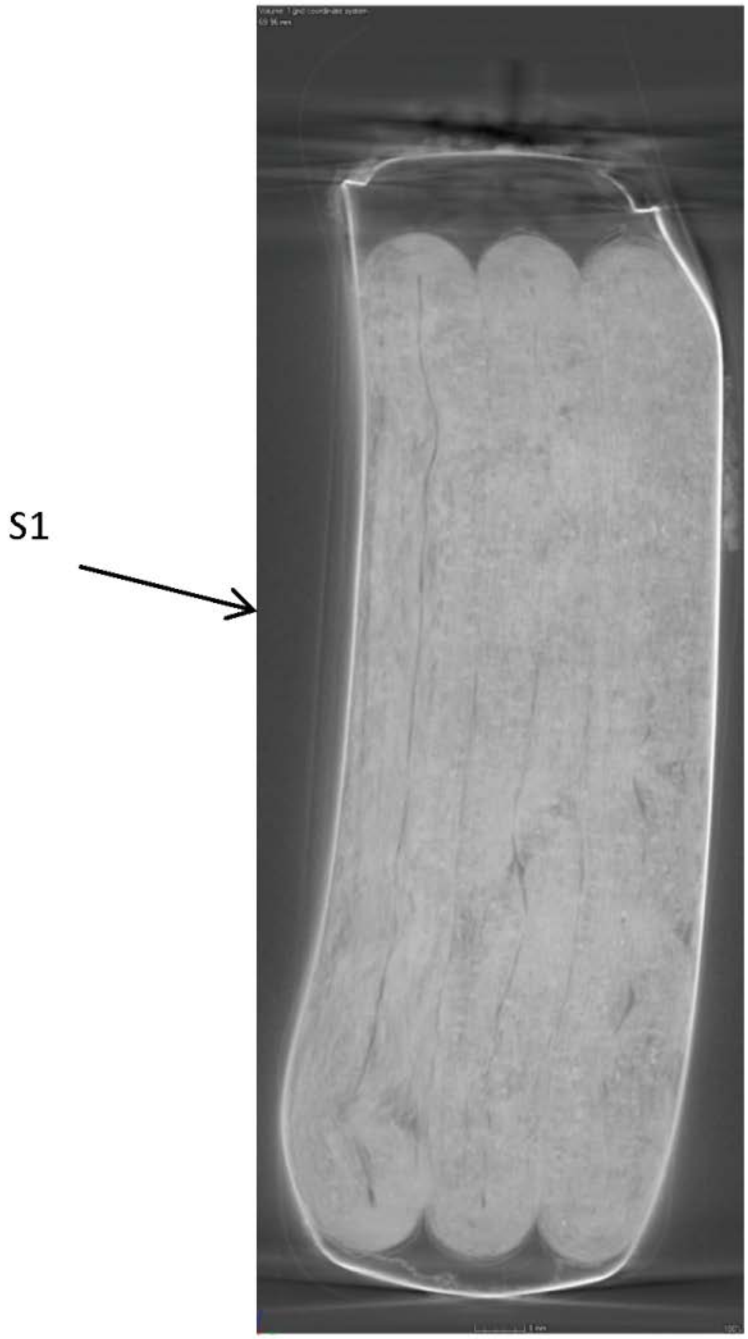

Figure 116. C7 CT scan image. The exemplar CT scan was taken on a plane about midway between the terminals.

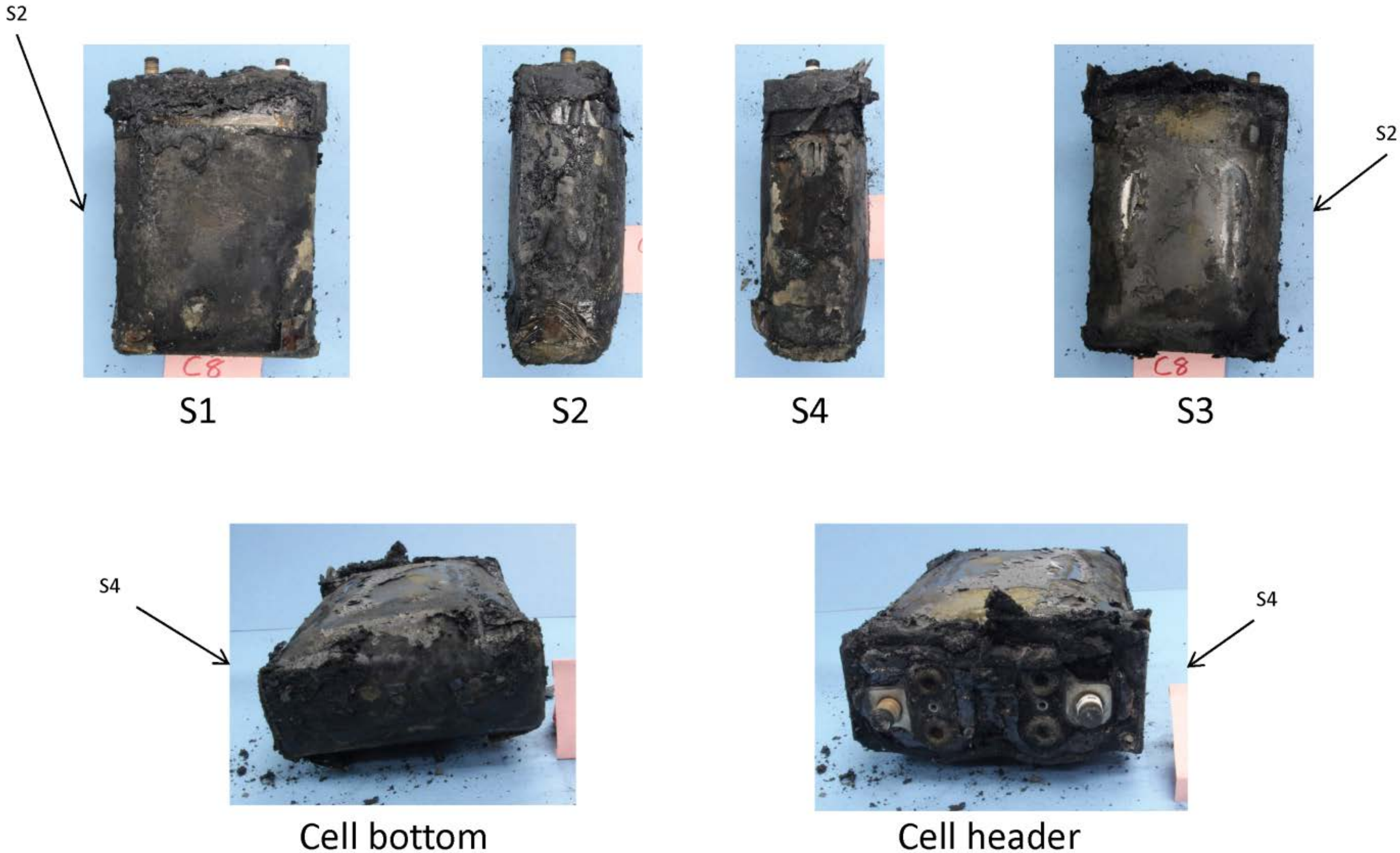

Figure 117. C8 (as removed).